MONTHLY NOTICES

OF THE

ROYAL ASTRONOMICAL SOCIETY

Volume 121 No. 6 1960

Published and Sold by the

ROYAL ASTRONOMICAL SOCIETY
BURLINGTON HOUSE
LONDON, W.1

Price £1 4*s.* 0*d.*; *in U.S.A.* $3.50

Subscription for volume £3 ; *in U.S.A.* $9

NOTICE

The Council has pleasure in announcing publication, early in 1961, of an extra volume of the *Geophysical Journal* (Volume 4), in honour of the seventieth birthday of

Sir Harold Jeffreys

The Geophysical Editors have obtained the co-operation of many of Sir Harold's distinguished colleagues and pupils, and believe that the contents of this special volume will represent the most advanced work in a number of fields in which Sir Harold has long been interested.

CONTRIBUTORS INCLUDE

S. Alterman	El Sayad M. Hassan	I. Lehmann
M. Bath	K. Hidaka	A. Marussi
F. Birch	U. Hochstrasser	R. H. Merson
E. C. Bullard	J. E. Jackson	W. H. Munk
K. E. Bullen	J. A. Jacobs	C. L. Pekeris
P. Caloi	H. Jarosch	F. Press
A. H. Cook	N. Jobert	R. Stoneley
A. Day	D. G. King-Hele	H. Takeuchi
F. F. Evison	L. Knopoff	C. Tsuboi
F. Gassman	R. L. Kovach	J. Verhoogen
A. L. Hales	E. R. Lapwood	P. L. Willmore

The complete volume, suitably bound in cloth boards, will also be available as a special publication.

Price £4 (US $ 12)

Orders, with remittance, should be sent to:

Assistant Secretary, Royal Astronomical Society, Burlington House, London, W.1

SPECIAL NOTICE TO FELLOWS

Fellows of the Society may obtain this bound volume of the *Geophysical Journal* at a specially reduced price of £1 10s. 0d. (US $ 4.50). It is particularly requested that Fellows wishing to receive a copy should send their orders, with remittance, as soon as possible to:

Assistant Secretary, Royal Astronomical Society, Burlington House, London, W.1

NOTICE TO AUTHORS

Presentation of Papers at Meeting

At some meetings of the Society the background and conclusions of selected papers are presented and then discussed. In order to assist the Secretaries in the selection of papers for such meetings, authors are asked to let the Society know, when submitting papers, whether they would be willing to give an account of their paper, if requested.

The attention of authors resident abroad is drawn to the fact that the Society welcomes information about their work. The Secretaries would be happy to consider having such work described at a meeting, in accordance with the author's wishes, either by a Secretary or other Fellow.

Publication of Papers

1. *General.*—It is the aim of the Society to be of the greatest possible service in disseminating astronomical results and ideas to the scientific community with the utmost possible speed. Contributors are accordingly urged to give the most careful consideration to the presentation of their work, for attention to detail will normally result in a substantial saving of time.

It is the practice of the Society to seek a referee's opinion on nearly every paper submitted for publication in *Monthly Notices*; experience has shown that frequently the comments of referees have enabled authors to improve the presentation of their work and so increase its scientific value.

2. *Communication.*—Papers must be communicated to the Society by a Fellow. They should be accompanied by a summary at the *beginning* of the paper stating briefly the content of the paper, and drawing attention to important new information and to the main conclusions. The summary should be intelligible in itself without reference to the paper, to a reader with some knowledge of the subject; it should not normally exceed 200 words in length. Authors are requested to submit MSS. in duplicate. These should be typed using double spacing and leaving a margin of not less than one inch on the left-hand side. Corrections to the MSS. should be made in the text and not in the margin. By Council decision, MSS. of accepted papers are retained by the Society for one year after publication; unless their return is then requested by the author they are destroyed.

3. *Presentation.*—Authors are allowed considerable latitude, but they are requested to follow the general style and arrangement of *Monthly Notices*. References to literature should be given either in the traditional form of a numbered list at the end of the paper, or as prescribed in *Notes on the Preparation of Papers to be Communicated to the Royal Society*.

4. *Notation.*—For technical astronomical terms, authors should [illegible] in the recommendations of Commission 3 of the International Astronomical Union (*Trans. I.A.U.*; Vol. VI, p. 345, 1938). Council has decided to adopt the I.A.U. 3-letter abbreviations for constellations where contraction is desirable (Vol. IV, pp. 221, 229). In general matters, authors should follow the recommendations in *Symbols, Signs and Abbreviations* (London: Royal Society, 1951) except where these conflict with I.A.U. practice.

5. *Diagrams.*—These should be designed to appear upright on the page, drawn about twice the size required in print and prepared for direct photographic reproduction except for the lettering, which should be inserted in pencil. Legends should be given in the manuscript indicating where in the text the figure should appear. Blocks are retained by the Society for 10 years; unless the author requires them before the end of this period they are then destroyed. Duplicate prints or prints of the diagrams should accompany each manuscript.

6. *Tables.*—These should be arranged so that they can be printed [illegible] on the page.

7. *Proofs.*—Authors are liable for costs of alteration [illegible] composition. It is therefore in their own and the Society's [illegible] maximum conciseness and simplification of symbols and equations [illegible]

CONTENTS

PAGE

P. J. Treanor, S. J., Stellar rotation in galactic open clusters 503

A. D. Petford, Micrometer measurement of high dispersion spectra 519

S. Aarseth, The rotation of a barred galaxy under gravitational forces 525

Bart J. and Priscilla F. Bok, Four standard sequences in the southern hemisphere 531

D. S. Mathewson, M. I. Large and C. G. T. Haslam, Radio emission from the Cygnus Loop 543

R. A. Lyttleton, Dynamical calculations relating to the origin of the solar system 551

Harold Jeffreys and Stuart Crampin, Rock creep: a correction 571

Errata 578

Printed in London by Taylor & Francis, Ltd., 1961 January

MONTHLY NOTICES
OF THE
ROYAL ASTRONOMICAL SOCIETY
Vol. 121 No. 6

STELLAR ROTATION IN GALACTIC OPEN CLUSTERS*

P. J. Treanor, S. J.

(Received 1960 August 2)

Summary

A survey of existing determinations of stellar rotational velocities reveals severe limitations on the use of this material due to the inhomogeneities in the methods of measurement and in the selection of the objects that have been measured. To secure information concerning a more homogeneous population, measurements of rotation have been made for 58 members of the Hyades cluster, 63 members of Praesepe, and for 10 members of the ζ-Persei association. A number of stars measured by Slettebak were included and good scale agreement is found with these. The results for the Hyades stars are systematically higher than those found by Struve.

The small rotational velocities of the 16 metallic line stars in Hyades and Praesepe confirm previous measures on stars of this type.

The variation of rotational velocity in the main sequence is investigated by a new analysis of the measures of Herbig and Spalding, of Slettebak, and of Slettebak and Howard, together with the present material. This analysis, based on a colour *vs.* rotational velocity diagram of equal groups of stars, reveals a sudden fall in rotation near F6 in the results of Herbig and Spalding. The other results are not inconsistent with this finding. The early-type stars show a large scatter. The rotations of the Hyades and Praesepe stars are in mutual agreement and tend to be somewhat larger than those of the general field in the neighbourhood of spectral type Fo.

Introduction.—A method of determining the line-of-sight component of stellar rotation from profile measurements of rotationally broadened lines was originally proposed by Shajn and Struve (1929), and was applied by them with success to spectroscopic binaries. Since the inclination of the axis of rotation to the line of sight is normally unknown, total rotational velocities cannot be determined for individual stars. However, the method provides a statistical metric which, when applied to large homogeneous samples of stars, may be used to derive the mean value and the distribution function of rotational velocities in particular groups of stars (Chandrasekhar and Münch 1950, Böhm 1952).

The earliest measures (Struve and Elvey 1931) already revealed a strong dependence of rotation on spectral type. The more detailed surveys of Herbig and Spalding and of Slettebak have revealed a complicated dependence on luminosity class within each spectral type (Herbig and Spalding 1955, Slettebak 1955). The data for investigating the possible dependence of rotation on population-types are not yet available, but such a dependence cannot be excluded. Although these facts combine to suggest that stellar rotation may prove to be a highly significant parameter in the study of stellar evolution, they greatly increase the observational requirements. Not only must the stars to be examined have accurate spectral classifications and belong to assignable population types, but a

* Contributions from the Lick Observatory, Series II, No. 111.

CONTENTS

P. J. Treanor, S. J., Stellar rotation in galactic star clusters 299

A. D. Penford, Micrometer measurement of high dispersion spectra 319

S. Aarseth, The rotation of a barred galaxy under gravitational forces 327

Peter J. and Priscilla P. Bok, Faint standard sequences in the southern Milky Way ... 341

D. S. Mathewson, M. F. Large and C. G. T. Haslam, Radio emission from the Cygnus Loop 345

R. A. Lyttleton, Dynamical calculations relating to the origin of the solar system ... 351

Harold Jeffreys and Stuart Crampin, Deep focus earthquakes 377

Errata 384

Printed in Great Britain by Taylor & Francis, Ltd., London

MONTHLY NOTICES
OF THE
ROYAL ASTRONOMICAL SOCIETY
Vol. 121 No. 6

STELLAR ROTATION IN GALACTIC OPEN CLUSTERS*

P. J. Treanor, S. J.

(Received 1960 August 2)

Summary

A survey of existing determinations of stellar rotational velocities reveals severe limitations on the use of this material due to the inhomogeneities in the methods of measurement and in the selection of the objects that have been measured. To secure information concerning a more homogeneous population, measurements of rotation have been made for 58 members of the Hyades cluster, 63 members of Praesepe, and for 10 members of the ζ-Persei association. A number of stars measured by Slettebak were included and good scale agreement is found with these. The results for the Hyades stars are systematically higher than those found by Struve.

The small rotational velocities of the 16 metallic line stars in Hyades and Praesepe confirm previous measures on stars of this type.

The variation of rotational velocity in the main sequence is investigated by a new analysis of the measures of Herbig and Spalding, of Slettebak, and of Slettebak and Howard, together with the present material. This analysis, based on a colour *vs.* rotational velocity diagram of equal groups of stars, reveals a sudden fall in rotation near F6 in the results of Herbig and Spalding. The other results are not inconsistent with this finding. The early-type stars show a large scatter. The rotations of the Hyades and Praesepe stars are in mutual agreement and tend to be somewhat larger than those of the general field in the neighbourhood of spectral type Fo.

Introduction.—A method of determining the line-of-sight component of stellar rotation from profile measurements of rotationally broadened lines was originally proposed by Shajn and Struve (1929), and was applied by them with success to spectroscopic binaries. Since the inclination of the axis of rotation to the line of sight is normally unknown, total rotational velocities cannot be determined for individual stars. However, the method provides a statistical metric which, when applied to large homogeneous samples of stars, may be used to derive the mean value and the distribution function of rotational velocities in particular groups of stars (Chandrasekhar and Münch 1950, Böhm 1952).

The earliest measures (Struve and Elvey 1931) already revealed a strong dependence of rotation on spectral type. The more detailed surveys of Herbig and Spalding and of Slettebak have revealed a complicated dependence on luminosity class within each spectral type (Herbig and Spalding 1955, Slettebak 1955). The data for investigating the possible dependence of rotation on population-types are not yet available, but such a dependence cannot be excluded. Although these facts combine to suggest that stellar rotation may prove to be a highly significant parameter in the study of stellar evolution, they greatly increase the observational requirements. Not only must the stars to be examined have accurate spectral classifications and belong to assignable population types, but a

* Contributions from the Lick Observatory, Series II, No. 111.

sufficiently large sample of stars must be available in each sub-group for statistically significant results to be obtained, while the method of measurement should guarantee accuracy and uniformity in the results.

A number of fairly massive attacks have now been made on the problem of securing statistically useful measurements of different kinds of stars, and these are summarized in Table 1. A comprehensive analysis of this material has been published by Boiarchuk and Kopylov (1958). Though impressive in aggregate, close inspection of the table reveals the inadequacy of the available data in relation to the requirements specified above. With the exception of the exploratory measurements of Struve on the Pleiades and the Hyades clusters (Struve 1945), and the measures by van Dien on the Pleiades (van Dien 1948) and of Deutsch (1955) on IC 4665, the stars have been chosen indiscriminately from the general field, from clusters and associations, the main criterion being spectral type, with or without luminosity classification, and apparent magnitude. The spectrographic dispersion, on which the probable error and the lowest detectable velocity depend, has varied considerably. An even greater source of error, both accidental and systematic, lies in the diversity of means employed in determining the rotations; these vary from accurate profile determinations, and careful spectrocomparator comparison of high dispersion material with photometrically calibrated standard stars, to subjective eye estimates, and measurements of line widths by micrometer wire settings. Intercomparisons that appear frequently in the quoted literature do, in fact, reveal quite large systematic errors associated with the cruder methods, as well as their large random errors.

Rotation in galactic open clusters.—The extensive determinations of rotation of stars with well-defined spectral and luminosity classifications in the general field made by Herbig and Spalding and by Slettebak, shed much light on the rotational characteristics of the stars, but emphasize the need for very much larger samples, particularly in certain sub-groups. The value of a sample of a given size depends on the intrinsic homogeneity of the population from which it is selected, and on the fraction of the population that it represents. The galactic open clusters provide well-defined limited aggregates of stars, with a common and often fairly well-established origin, age, and evolutionary history. The physical and dynamical characteristics of the members of the nearer clusters have been intensively studied. They constitute pure samples of well-studied population types, from which we may select sub-samples in which the relative smallness of the numbers is compensated in some degree by the homogeneity of the total material, of which they form a considerable fraction. Moreover, a comparison of the rotational velocities found in galactic clusters with stars in the general field should provide a measure of the dependence of rotation on population type.

In view of the very small amount of observational data available on the rotational properties of cluster stars, some new measures have now been undertaken and a preliminary comparison has been made with the results so far available for the general field.

Observational material.—In the autumn and winter of 1956 a series of spectra of the brighter Hyades was obtained with the Lick 36-inch refractor and the 2-prism spectrograph with 12-inch camera. The spectra were taken by Herbig and U. Steinlin on Kodak IIa-O plates, with a dispersion of 40 A/mm at Hγ. Single spectra of 58 Hyades members from Van Bueren's list were included (van

TABLE I

Investigations of stellar rotational velocities

Source	Date	No. of Stars	Lines	Disp. A/mm	Method	Class	Notes
Shajn and Struve	1929	83	4472, 4481	30	Estimated line widths	B, A	(Spectroscopic binaries)
Elvey	1930	59	4481	10	Profiles		
Struve and Elvey	1931	31	4481	10	Visual comp. with stand.	F0–K0	
Westgate	1933	275	4472, 4481	30	Comparator measures	O–B9	
Westgate	1933	112	4215	30	Comparator measures	F0–F8	
Smith and Struve	1944	69	...	55	Estimates	B2–K5	
Struve	1945	56	...	40, 75	Estimates	B5–K2	Pleiades
Struve	1945	27	...	40, 75	Estimates	A3–G0	Hyades
van Dien	1948	93	4481	30, 51	Profiles and comp.	B6–G0	Pleiades
Slettebak	1949	123	4026	40	Profiles	O, Be, B2–B5	
Schwarzschild	1950	9	4448, 4548 4603, 4625	10	Profiles	F5–F6	
Huang	1953	1550	4472, 4481	12	Micrometer line widths	O–G	
Deutsch	1953	19	4472, 4026		Visual comp. with stand.	B5–A2	IC 4665
Slettebak	1954	179	4481	28	Profiles	B8–A2	
Oke and Greenstein	1954	34	4476	2–20	Profiles	A, F, G	(Giants)
Slettebak	1955	185	4026, 3371	28	Profiles	B2–B5	
Herbig and Spalding	1955	638	4473, 4405	11	Visual comp. with stand.	F0–K5	
Slettebak	1955	653	4072, 4481	28	Profiles	A3–G0	
Slettebak	1956	43	4026, 4471	10	Profiles	O5–B2	
Abt	1957	10	4508	8·5	Profiles	A, F II	(Bright giants)
Abt	1958	15	4508	8·5	Profiles	A, F Ib	(Supergiants)
Kraft	1959	10	4508	4·5, 10	Profiles and comparisons	Cepheids	

Bueren 1952). A few supplementary plates were obtained by Herbig and the author in 1960 January. In addition, several spectra had been secured of stars for which Slettebak had determined velocities. These were used as a check on accidental and systematic errors. Ten spectra of early type stars in the ζ-Persei association, taken uniformly with the Hyades plates, were also available. All these plates were calibrated with a tube sensitometer. Dr Herbig kindly placed this material at the writer's disposal.

In addition, Dr W. P. Bidelman made available 63 spectra of stars in Praesepe, taken by him with the $f/2$ Schmidt camera spectrograph on the McDonald 82-inch reflector, and which he had used for his classifications of Praesepe stars (Bidelman 1956). These spectra, taken on film, included stars to photographic magnitude 10, and one fainter star. They were not calibrated, and had a dispersion of only 76 A/mm at Hγ. However, Bidelman had noticed that many of the stars appeared to be rotationally broadened. A preliminary inspection of the Praesepe plates, and a comparison of tracings made with a modified Moll photometer of Praesepe and Hyades plates, showed that the former were of very good quality, the instrumental pattern, in angstroms, being only 30 per cent broader than that of the Lick spectrograph.

On account of the well-known resemblance of Praesepe to the Hyades in age, spectral distribution and space motion, it was considered worth while to attempt to obtain some quantitative estimates of rotational velocity from this material.

Reduction.—The rotationally broadened profile of an intrinsically narrow line, prior to instrumental distortion, is given (Unsöld 1938) by

$$A(x) = \frac{2/\pi\sqrt{(1-x^2)} + \beta/2(1-x^2)}{1+2/3\beta}$$

where $x = \dfrac{c\Delta\lambda}{\lambda v \sin i}$, i is the inclination of the axis of rotation to the sight line, λ is the wavelength and $\Delta\lambda$ the wavelength distance from the line centre, c the velocity of light, and β an approximate limb-darkening coefficient. The observed profile will differ from this computed one on account of the finite line width and the instrumental distortion. If the observed profile in a line of a non-rotating star is $I(\lambda)$, the observed profile in the same line of a similar but rotating star will be

$$I'(\lambda) = \int_{-1}^{+1} I(\lambda_1)A(x)\,dx$$

where $x = (\lambda-\lambda_1)/\lambda = v/c$. The determination of a rotational velocity involves in principle the solution of this integral equation, or an equivalent one, for which various procedures have been proposed (see for example Unsöld 1938). For spectra of low dispersion, the instrumental pattern will be broadened only slightly by the intrinsic line width in a non-rotating star, and if attention is confined to lines not greatly broadened by saturation or by Stark effect, the mean profile of weaker metallic lines in a non-rotating star may be used as an approximation to $I(\lambda_1)$ in the integral equation. It is then possible to evaluate the integral for a number of spaced values of v, and to determine the rotations by comparison of the observed profiles with the computed forms. It is important to note that the approximations so introduced are expected to fail at low velocities of a few km/sec, but such low velocities are in any case quite indeterminate at the dispersion used;

the lowest velocity detectable by visual comparison in km/sec is numerically comparable with the dispersion in A/mm, while that which can be reliably detected on tracings or profiles is not much smaller. It was found in practice that reduced profiles and half-widths of metallic lines in the Ko III star ϵ Tau, (which, in common with other Ko III giants, has been found to have negligible velocity by Herbig and Spalding, and by Struve) were in satisfactory agreement, and that they also agreed with the profile of the $\lambda 4481$ line in the A2 star 68 Tau, which Struve and Slettebak both record as a star of negligible rotational velocity. With this measure of control, the expected profiles for $I'(\lambda)$ were computed. The reduction for the Hyades plates was then made as follows. Tracings were obtained on a modified Moll microphotometer, with a plate-to-paper magnification of 84, and a projected slit width of 10 microns over the whole range of useful density and good focus, from 4200 to 4500 A. Profiles of Mg II $\lambda 4481$ were obtained for stars to type Fo; for later types, Fe I $\lambda 4272$ was used. The former line is blended in the later types; the same is true to a lesser extent of $\lambda 4272$, but the interfering lines are farther from the line centre. It is not easy to find lines completely suitable for accurate photometry at this low dispersion. By means of their individual calibration curves, the line profile widths were determined at five selective intensity levels and the velocities obtained by interpolation in the computed $I'(\lambda)$ profiles.

Although the determination of rotational velocity so made is in principle more reliable than one obtained by more qualitative procedures, it was realized that the measurement of a single line in one or at most two spectra and at low dispersion must involve rather large sources of error, especially that due to local grain irregularities. In most of the spectra, especially in types Fo and later, and in the metallic line A stars, an abundance of metallic lines are available. As an exploratory check on the representative character of the profile measure, a second estimate of profiles for each star was obtained in the following way. Lines were chosen weak enough for their complete extent on the tracing to be contained within a nearly linear range of the plate characteristic, and the corresponding tracing half-width used as an index to the true half-width of the profile. The agreement of the mean of such values with the profile determination was unexpectedly good, except in a few isolated cases where the profile was already suspect. The values that appear in this paper are the mean of the two determinations.

Interagreement between various lines indicated probable errors of the order of ± 20 km/sec; a better estimate may be obtained by the comparison of our measures with those of Slettebak and with the measures of Huang, reduced to rotational velocities by the procedure described in his paper (Huang 1953). From Fig. 1 (*a*) and (*b*), it can be seen that there is no indication of any considerable systematic error, and that the scatter between Slettebak and the present measures is considerably less than the scatter between the latter and Huang. The standard deviation of a single star from the mean is 17 km/sec for Slettebak and the present values, and 24 km/sec for the latter and Huang. The scale difference between the results of Herbig and Spalding and those of Huang does not appear here, since the stars represented, which include a few non-Hyades stars, are earlier than F1. The scale error in Huang's results is a line-strength effect, probably enhanced by the blend that develops in Mg II $\lambda 4481$ for stars of later type. The agreement is reassuring. We have considered that the probable

error of our measures may be estimated realistically as ±20 km/sec. Nominal measured velocities below the limit of certain detection are denoted by <30, and for statistical purposes are assigned a value of 15 km/sec. The same values apply to the similar material for ζ-Persei.

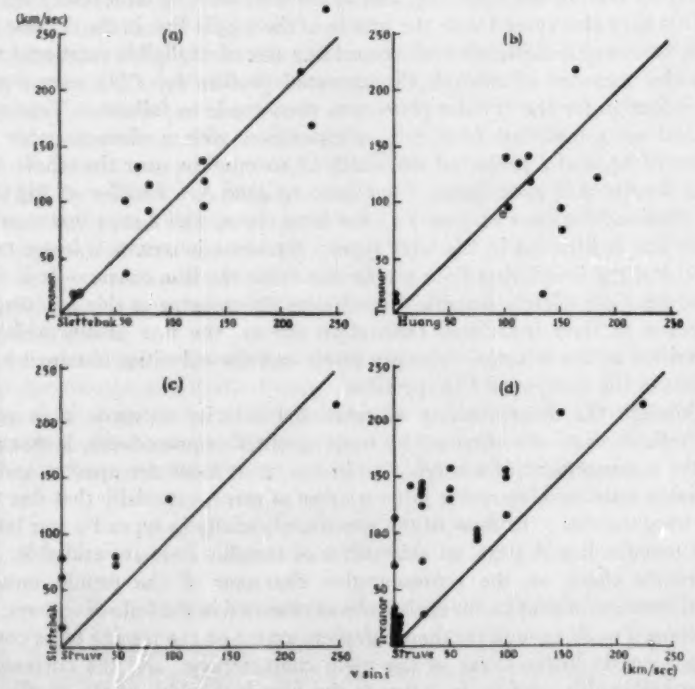

FIG. 1.

The only other results with which we can compare the Hyades measures are those of Struve (1945). It has been recognized that the scale of these early measures is subject to systematic errors. Fig. 1 (*c*) and (*d*), compares these with the results of Slettebak and with the present values. The results of Struve are systematically lower in both cases; a very similar scale difference exists between the measures of van Dien and Struve for the Pleiades (van Dien 1948). This effect illustrates the limited value of eye-estimates, made without adequate standards of comparison, in estimating moderately low velocities from spectra of low dispersion.

The success of the half-width measurements from the tracings of the Hyades suggested a method for dealing with the uncalibrated spectra of Praesepe. Microphotometer tracings were accordingly obtained with a magnification of 168, and the rotational measures were based on tracing half-widths of fairly weak metal lines, the half-width of the profile in a non-rotating star being equated to that of the star 39 Cnc (Ko III). The probable error has here been estimated at ±30 km/sec; velocities below the limit of certain detection have been denoted

< 45, and assigned half this value for statistical purposes. In many individual cases, and notably for the later type and metallic line stars the interagreement of measures from different lines indicates a rather smaller probable error.

Results and discussion.—Table II gives the values of $v \sin i$ for the Hyades, ζ-Persei and Praesepe. The spectral types for the Hyades stars are either published types, or in the cases in parentheses from unpublished provisional determinations on the MKK system, made by Bidelman about 1950. Stars that were then considered as of luminosity class IV are listed in the table as class IV–V, the alterations being made to put the classification more closely on the new or MK system. The classifications for Praesepe are also by Bidelman (1956). The spectral types of the ζ-Persei stars are from Harris (1956) and Crawford (1958). Remaining classifications are from various sources. The identifications of the ζ-Persei association members was made from the list by Blaauw (1952). The photometric data of Johnson for Praesepe (Johnson 1952) and for the Hyades (Johnson and Knuckles 1955), together with positional and other data not here reproduced, may be found conveniently in other sources (van Bueren 1952, Bidelman 1956).

With the exception of the few late-type giants in the Hyades and Praesepe clusters, most of our stars are main-sequence objects. These include however nine metallic line stars in Praesepe, and seven in Hyades, which we treat separately, on account of their known rotational peculiarity. To obtain a first impression of the comparative data now available, we analyse in Table III the data of Table II

TABLE II

Stellar rotational velocities (km/sec) in the Hyades, ζ-Persei association, and Praesepe

Name	HD	Sp	$v \sin i$	Notes
		Hyades		
68 Tau	27962	A2IV	<30	D
90	29388	A5V	115	SB1
92	29488	A5V	160	
65 κ	27934	A7V	90	
67	27946	A7	210	
64	27819	A7V	35	
78 θ^2	28319	A7 III	130	SB1
79	28355	A7	140	
HR 1427	28527	A7 V	100	
102 ι	32301	A7 V	115	
51	27176	A8	125	
60	27628	ML	<30	SB1
63	27749	ML	<30	SB1
HR 1403	28226	ML	130	
81	28546	ML	<30	
HR 1519	30210	ML	<30	SB1 ?
HR 1670	33204	(ML)	<30	
16 Ori	33254	ML	<30	
45 Tau	26462	(Fo)	<30	
57	27397	(Fo)	100	SB1
58	27459	Fo	35	SB1
80	28485	Fo	150	D
69 υ Tau	28024	Fo III–IV	215	SB1

TABLE II (*continued*)

Name	HD	Sp	$v \sin i$	Notes
71 Tau	28052	Fo V	170	
76	28294	(Fo)	135	
83	28556	(Fo)	140	
86	28910	Fo V	95	
89 ρ	29375	(Fo)	155	
HR 1507	30034	Fo	75	
97	30780	Fo	155	
HR 1238	25202	(F1)	(160)	SB2
HR 1480	29499	(F1)	70	
45	26462	(Fo)	< 30	
48	26911	(F2 IV–V)	< 30	
HR 1385	27901	(F2 IV–V)	110	
85	28677	(F2 V)	100	SB1 ?
	26345	(F2 V)	< 30	
	26737	(F5 IV–V)	60	
	26784	(F5)	< 30	
	27524	(F5 IV–V)	110	
	27561	(F5 IV–V)	< 30	
	27534	(F6 IV–V)	40	
	28406	(F6 V)	< 30	
	29225	(F6 IV–V)	45	
55	27383	(F8 V)	< 30	D
	27848	F8	< 30	
70	27991	(F8 V)	< 30	D
	28363	(F8 V)	< 30	SB1
	30810	(F8 V)	< 30	D
	27691	Go	< 30	SB1, D
77 θ'	28307	G8 III	< 30	SB1 ?
54 γ	27371	Ko III	< 30	SB1
61 δ	27697	Ko III	< 30	
74 ϵ Tau	28305	Ko III		
		ζ-Persei association		
HR 1074	21856	B1 V	150	
40 Per	22951	Bo·5V	130	
38 o Per	23180	B1 III	150	D
	23478	B3 IV	180	
HR 1163	23625	B2 V	170	D
HR 1191	24131	B1 V	140	
X Per	24534	Ope	150	
HR 1215	24640	B2 V	140	
ζ Per	24398	B1 Ib	(270)	D
	25539	B3	120	
		Praesepe		
	73598	Ko III	< 45	
39 Cnc	73665	Ko III	o	assumed
HR 3428	73710	Ko III	< 45	
	73974	Ko III	< 45	
35 Cnc	72779	Go III	95	
40 Cnc	73666	A1	< 45	
	72942	A4	< 45	
	72846	A5	140	
	73210	A5	< 45	
	73574	A5	60	
	73872	A5	75	

TABLE II (*continued*)

Name	HD	Sp	$v \sin i$	Notes
	73819	A6	100	
	73576	A7	245	
	73890	A7	60	SB(2)
	74028	A9	245	
	74050	A9	115	
	73430	A9	<45	
	73449	A9	(250)	uncertain
	73450	A9	110	
	73712	A9	(200)	
	73763	A9	130	
42 Cnc	73785	A9 III	195	SB
	73161	F0	155	
	73175	F0	100	
	73345	F0	90	
38 Cnc	73575	F0 III	185	
	73746	F0	<45	
	73798	F0	135	
	73616	F2	150	
+20° 2161		F2	90	
	73729	F2	(250)	SB2
	73993	F2	(150)	
	74058	F3	80	
	73397	F4	120	
	73937	F4	95	
	73429	F5	130	
	73617	F5	150	
	73854	F5	<45	
	73994	F5	50	
+19° 2054		F6	<45	
	73081	F6	<45	
+19° 2050		F6	<45	
KW 155		F6	<45	
	73597	F6	<45	
	73641	F6	<45	
	73640	F6	<45	
+20° 2170		F6	<45	
+19° 2074		F6	<45	
+21° 1891		F6	<45	
+20° 2183		F6	<45	
+20° 2193		F6	<45	
+20° 2140		F7	<45	
	74186	F8	<45	
	73045	ML	<45	A4–F5 III
	73174	ML	60	A4–F0 III
	73618	ML	70	A4–F0 III D
	73619	ML	(140)	A4–F2 III SB2
	73711	ML	<45	A3–F0 III
	73709	ML	<45	A3–F2 III
	73730	ML	<45	A3–F2 III
41 ε Cnc	73731	ML	<45	A5–F0 III SB2
	73818	ML	80	A7–F2 III
+20° 2157			120	

Note.—Single- and double-line spectroscopic binaries are denoted by SB_1, SB_2 respectively; double stars are indicated by D. Values enclosed in parentheses are uncertain. Metallic-line stars are denoted by ML.

in ranges of spectral type. For comparative purposes, the main-sequence data of Herbig and Spalding (1955) and Slettebak (1955) have been included, and also the rotational velocities of 12 Pleiades stars of luminosity class V measured by van Dien (1948). It is immediately evident that rotations in the Hyades and in Praesepe stars at the same spectral type are very similar; their combined value has been entered in the last column of Table III and they will be considered jointly in what follows.

TABLE III

Stellar rotational velocities in bright main-sequence field stars and in clusters
$v \sin i$ (km/sec)

	Slettebak	Herbig	Pleiades	Per II	Hyades	Praesepe	H+P
B1–B3	157 (67)	...	...	138 (5)	...	...	...
B5–B7	202 (35)	...	...	...	...	...	...
B8–A2	139 (87)	...	...	...	...	...	...
B5–A2	170 (122)	...	164 (12)	...	...	...	...
A3–A9	136 (37)	...	...	...	121 (9)	112 (13)	116 (22)
F0–F2	68 (15)	60 (6)	...	...	100 (15)	115 (8)	111 (23)
F3–F6	24 (14)	33 (33)	...	...	33 (8)	46 (21)	42 (29)
F7–G0	<25 (20)	<25 (35)	...	...	<30 (6)	<45 (2)	<35 (8)
Metallic	45 (20)	...	...	...	32 (7)	40 (8)	36 (15)

The figure in parentheses gives the number of stars concerned.

The metallic line stars.—The present results confirm the characteristic low rotational velocity assigned to the metallic line stars by Slettebak and others. The true character of these stars is still uncertain (see Jaschek and Jaschek 1957, 1959), although Babcock (1958) has suggested that the peculiar predominantly magnetic A-type stars show their characteristic spectrum when viewed pole on. It is interesting to consider an analogous possibility in connection with the metallic-line stars. They are relatively far too numerous in both Hyades and Praesepe to form the natural tail of the rotational velocity distribution of A stars, or to be the statistical fraction of normal A stars viewed pole-on. Their velocity of rotation, and their relative frequency indicate that they are over-luminous F stars. It is perhaps just conceivable that the over-luminosity may be a pole effect due to a real temperature difference between pole and equator, such as that considered by Baldwin (1944). It would be interesting in this connection to be able to identify former metallic-line stars that have evolved from the main sequence. Not enough of these giant stars have been classified and measured for a distinction based on rotation to be established. Any explanation of the metallic line or peculiar A-type stars based on temperature differences between pole and equator must raise the question of dual classification in stars of earlier spectral type. Individual examples of such spectra have been suspected to exist (Bidelman 1960).

Rotation of stars along the main sequence.—Oke and Greenstein (1954) and Sandage (1955) have shown that the existing determinations of the rotational properties of stars in the giant and subgiant region of the H–R diagram can be explained by the conservation of angular momentum in the course of evolution from the main sequence. Whether or not this explanation proves to be universally true, it is clear that the initial distribution of angular momentum in the main sequence is of basic importance in the study of stellar rotation and evolution.

The situation is complicated, in the case of field stars, by the initial ascent from the main sequence that stars make before the break-off point is reached. This process must give rise to a mixture of rotational characteristics in stars of the same spectral type in a collection of main-sequence objects of varying age. No such effect would be expected in a cluster.

The general picture of the variation of stellar rotation along the main sequence has not changed greatly since the pioneering work of Struve. After reaching a maximum in the B stars, the rotational velocity is considered to fall off steadily through spectral types A and F. It has long been strongly suspected, at least, that this decrease becomes rapid, producing almost a discontinuity in the region of type F6. The evolutionary significance of such a jump has been discussed by Struve (e.g. 1954b). The establishment of the exact form of the variation, and in particular the variation in the F stars, has not yet been achieved. Huang (1953) published a form for this curve based on a very large collection of spectra. These are without luminosity classifications however, and his method of measurement resulted in a scale error that is a somewhat uncertain function of spectral type. Both Slettebak and Herbig and Spalding have compared rotational velocities for different groups of spectral classes. One disadvantage of this treatment as the latter authors point out, is that the sparseness and irregular distribution of the data result in an unequal representation of the different spectral classes, and the distribution within any arbitrarily chosen range differs from one collection of measures to another. Such a coarse analysis, while presenting a fair overall picture, may conceal some significant irregularities.

In order to compare the cluster measurements with the measures of main-sequence field stars by Herbig and Spalding, and by Slettebak, the three sets of measures were re-analysed by a method designed to overcome these limitations. The rotational velocity was studied as a function of colour index in preference to spectral type. In the case of the Hyades and the Praesepe stars, which have accurately determined colour indices and are known to be unreddened, the individual $B-V$ values were used. In view of the absence of accurate luminosity classifications for the Praesepe stars, and of the uncertainty attached to the Hyades stars classed IV–V, only those cluster stars were excluded from the analysis for which the photometric data indicated that they were clearly brighter (by about half a magnitude) than the general run of main-sequence stars in the cluster. An unreddened colour index was assigned to all the non-cluster stars on the basis of the relation established by Johnson and Morgan (1953) between $B-V$ and spectral classification for stars of luminosity class V.

The stars in each set of measurements were assembled in order of increasing colour index and divided into equal groups. The choice of the number in each group is a matter of some moment, since if too few are chosen, statistical fluctuations predominate, and if too many, an unduly large range of colour index is included in each group. Selection was first made in groups of 16 stars. Subsequently, in a separate analysis, the stars of later type were sub-divided into groups of eight, in order to obtain a finer interval between points. The mean value of $v \sin i$ and the mean colour index were derived for each such group, with the individual values for all the main-sequence stars listed in the three relevant papers of Slettebak, in the table in Herbig and Spalding's paper, and for the cluster material. Known and suspected double-line binary systems were excluded as far as possible.

Chandrasekhar and Münch (1950) have derived formulae relating the mean observed velocities $y=\overline{v\sin i}$ together with the mean square and mean cube velocities, with the mean total velocity $\bar{v}$, the mean square deviation $\overline{(v-\bar{v})^2}$ which measures the breadth of the distribution pattern, and the mean cube deviation, which is a metric of the skewness of the distribution. The relations are

$$\bar{v}=\frac{4}{\pi}y; \quad \overline{(v-\bar{v})^2}=1{\cdot}5\overline{y^2}-\frac{16}{\pi^2}\bar{y}^2;$$

$$\overline{(v-\bar{v})^3}=\frac{16}{3\pi}\overline{y^3}-\frac{18}{\pi}\overline{y^2}\,\bar{y}+\frac{128}{\pi^3}\bar{y}^3.$$

In Table IV we give the values of the true mean velocities, corrected for the inclination effect, and the measures of the mean square deviations for all the groups of 16 stars measured. In the case of the slowly rotating stars, the distribution pattern is badly distorted by errors of measurement, and in these cases only the mean velocity is given. The groups were too small for the measurement of skewness to be applied significantly. It will be noticed that the distribution pattern appears to increase in width with the increasing rotational velocity. While this effect is perhaps to be expected, it must be remembered that it may well reflect the increasing errors in measurement as the lines become more diffuse. However, the number of stars in each group is sufficient, taken with the broad measure of agreement in the distribution metric, to enable an estimate of the breadth of the distribution function to be made for the main-sequence stars.

TABLE IV

Colour-rotational velocity relation of main sequence stars (Groups of 16 stars)

Slettebak			Herbig and Spalding		
$B-V$	$\bar{v}$	$\overline{(v-\bar{v})^2}$	$B-V$	$\bar{v}$	$\overline{(v-\bar{v})^2}$
−0·240	199*	135	+0·390	64	44
0·220	142	93	0·457	22	...
0·200	195	137	0·490	11	...
0·181	257	80	0·560	9	...
0·155	277	74	0·612	9	...
0·121	243	111	+0·744	9	...
0·080	206	118			
−0·025	246	83	Hyades and Praesepe		
+0·020	142	107			
0·055	133	78	+0·156	126	52
0·075	162	83	0·231	141	61
0·118	167	70	0·290	156	56
0·176	148	54	0·395	69	50
0·325	90	62	0·461	36	...
0·460	26	13	+0·540	21	...
+0·558	15	...			

* Unit is km/sec.

The variation in velocity may be examined more effectively with the help of Fig. 2 (*a*) and (*b*). In Fig. 2 (*a*) the values of v are now plotted as a function of $B-V$. In Fig. 2 (*b*) the results of the finer analysis by groups of eight stars is given for the later type part of the main sequence. It will be noticed that this finer analysis reveals the existence of the sharp quasi-discontinuity in the results of Herbig and Spalding near the value $B-V=+0{\cdot}46$, corresponding to MK spectral

type F5·5 V. Points that correspond to nominal mean velocities below the limits of measurement for each observer have been underlined. It will be seen that the results of Slettebak and those for the clusters do not show this discontinuity, which occurs in the region where their measures are sparse and inaccurate; whereas the higher dispersion and larger number of stars in the Herbig and Spalding results lend support to the reality of the discontinuity.

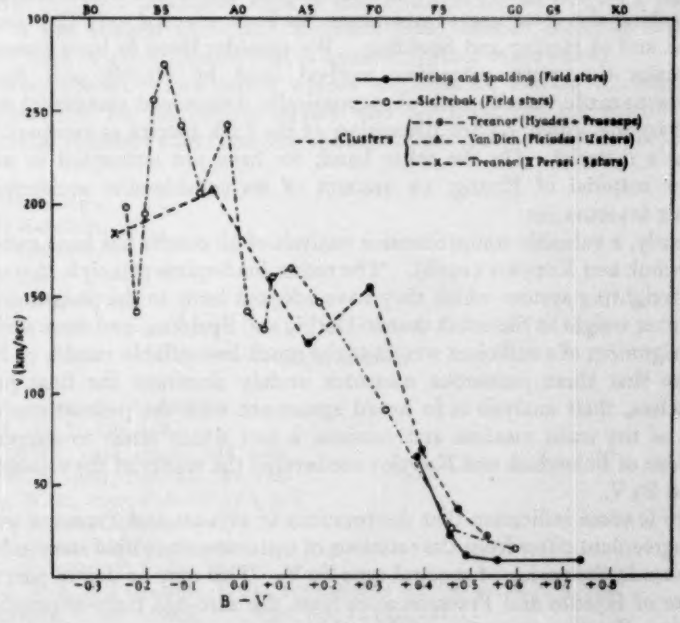

(*a*)

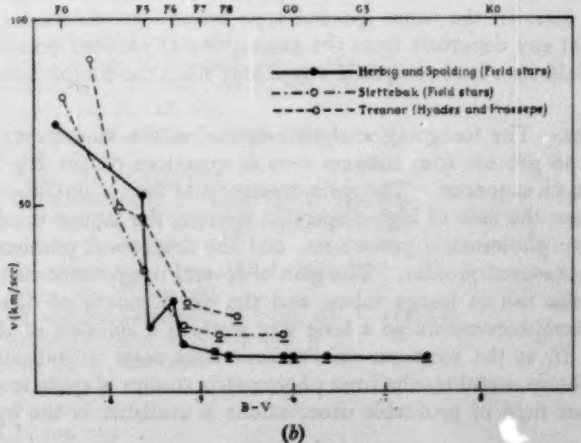

(*b*)

FIG. 2.

In Fig. 2 (*a*) the larger group membership obliterates the sudden fall by its averaging effect. While the general trend of the main-sequence rotations follows

the expected lines to a fair extent, the figure reveals the very large fluctuations in the observed results of Slettebak for earlier types. Though doubtless the figure illustrates the extent of the statistical fluctuations, and also the accidental errors, the individual points have sufficient weight to make the extent of the deviations a little surprising, and to suggest that other effects than rotation may affect line broadening, or that the true distribution of stellar rotation with spectral type is only crudely represented by the hitherto accepted qualitative relationship.

In making the foregoing comparisons, we have selected only the results of Slettebak and of Herbig and Spalding. We consider these to have comparable value, since the more subjective method used by Herbig and Spalding (comparisons made visually with photometrically determined standards) is compensated by the much higher dispersion of the Lick spectra as compared with Slettebak's material. On the other hand, we have not attempted to use the abundant material of Huang, on account of its considerable accidental and systematic inaccuracies.

Recently, a valuable comprehensive analysis of all results has been published by Boiarchuk and Kopylov (1958). The rather inadequate principle that underlies the weighting system which they have adopted leads to the assignment of a much higher weight to Slettebak than to Herbig and Spalding, and more seriously, to the assignment of a sufficient weight to the much less reliable results of Huang to ensure that these numerous measures unduly dominate the final picture. Nevertheless, their analysis is in broad agreement with the present one in the position of the main maxima and minima, a fact which tends to support the conclusions of Boiarchuk and Kopylov concerning the reality of the minima near A2 V and B3 V.

There is some indication that the rotations of Hyades and Praesepe while in mutual agreement differ from the rotations of main-sequence field stars in having a maximum in the region of spectral type F0 V. This may be due in part to the departure of Hyades and Praesepe stars from the zero-age main-sequence near this point. Further evaluation of this effect must await a more critical spectral classification. The existence of real systematic difference in the measured rotations of stars in the same spectral type cannot be excluded. It may be remarked that any departure from the assumption of random orientation in the cluster and field stars here compared would only affect the comparison by a small-scale factor.

Conclusion.—The foregoing analysis emphasizes the inadequacy of existing observations to provide firm answers even to questions concerning rotations of stars in the main sequence. The main deterrents to the accumulation of reliable data have been the lack of high-dispersion spectra, the labour involved in the more accurate photometric procedures, and the theoretical problems of interpreting the measured profiles. The gain of several magnitudes currently being realized by the use of image tubes, and the development of direct-intensity recording microphotometers go a long way towards a solution of the first two difficulties. If, as the measures on Praesepe stars seem to indicate, it is also possible to obtain useful results from photometric studies of quite low dispersion spectra, a vast field of profitable observations is available in the open galactic clusters.

The problem of the interpretation of broadened profiles remains a serious limiting factor especially in two extreme cases. Slettebak (1956) has shown that

turbulent broadening is comparable with the rotation effect in very early-type stars, and in these stars the available lines may be Stark-broadened. The second case concerns rotations of less than 20 km/sec. The measurement of profiles then requires high dispersion and a correction based on an accurately determined instrumental pattern. The interpretation in this case also requires an accurate knowledge of the unbroadened stellar profiles, and of the broadening mechanism of other processes, such as macroturbulence, as well as a rigorous solution of the integral equation. Between these difficult extremes there lies however a field of great interest that is open to further observation.

Acknowledgments.—The author wishes to thank Dr Herbig for suggesting this problem and for his helpful advice, and Dr Bidelman for providing the spectra of the Praesepe stars, and unpublished spectroscopic data on the Hyades.

Lick Observatory,
Mt Hamilton,
California:
1960 *June.*

References

Abt, H. A., 1957, *Ap. J.*, **126**, 503.
—— 1958, *Ap. J.*, **127**, 658.
Babcock, H. W., 1958, *Ap. J.*, **128**, 228.
Baldwin, R. B., 1944, *Pop. Ast.*, **52**, 134.
Bidelman, W. P., 1956, *P.A.S.P.*, **68**, 318.
—— 1960, *P.A.S.P.*, **72**, 24.
Blaauw, A., 1952, *B.A.N.*, **11**, 405.
Bohm, K. H., 1952, *Z. f. Ap.*, **30**, 117.
Boiarchuk, A. A. and Kopylov, I. M., 1958, *Soviet Astronomy, A.J*, **2**, 752.
Chandrasekhar, S. and Münch, G., 1950, *Ap. J.*, **111**, 142.
Crawford, D. L., 1958, *Ap. J.*, **128**, 185.
Deutsch, A. J., 1955, *Principes Fondamentaux de Classification Stellaire*, p. 25 (Paris).
Elvey, C. T., 1930, *Ap. J.*, **71**, 221.
Harris, D. L. III, 1956, *Ap. J.*, **123**, 371.
Heckmann, O., and Johnson, H. L., 1956, *Ap. J.*, **124**, 477.
Herbig, G. and Spalding, J. F., 1955, *Ap. J.*, **121**, 391.
Huang, Su-Shu, 1953, *Ap. J.*, **118**, 285.
Jaschek, C. and Jaschek, M., 1957, *A. J.*, **62**, 343.
—— 1959, *Z. f. Ap.*, **47**, 29.
Johnson, H. L., 1952, *Ap. J.*, **116**, 640.
Johnson, H. L. and Knuckles, C. F., 1955, *Ap. J.*, **122**, 209.
Johnson, H. L. and Morgan, W. W., 1953, *Ap. J.*, **117**, 313.
Kraft, R. P., 1959, *Ap. J.*, **129**, 50.
Oke, J. B. and Greenstein, J. L., 1954, *Ap. J.*, **120**, 384.
Sandage, A. R., 1955, *Ap. J.*, **122**, 263.
Schwarzschild, M. and Schwarzschild, B., 1950, *Ap. J.*, **112**, 248.
Shajn, C. and Struve, O., 1929, *M.N.*, **89**, 222.
Slettebak, A., 1949, *Ap. J.*, **110**, 498.
—— 1954, *Ap. J.*, **119**, 146.
—— 1955, *Ap. J.*, **121**, 653.
—— 1956, *Ap. J.*, **124**, 173.
Slettebak, A. and Howard, R. F., 1955, *Ap. J.*, **121**, 102.
Smith, B. and Struve, O., 1944, *Ap. J.*, **100**, 360.
Struve, O., 1945, *Pop. Ast.*, **53**, 201 and 259.

Struve, O., 1945 b, *Ap. J.*, **102**, 265.
Struve, O. and Elvey, C. T., 1931, *M.N.*, **91**, 663.
Unsöld, A., 1938, *Physik der Sternatmosphären*, p. 316 (Berlin).
Westgate, C., 1933, *Ap. J.*, **77**, 141; **78**, 46.
—— 1934, *Ap. J.*, **79**, 357.
van Bueren, H. G., 1952, *B.A.N.*, **11**, 385.
van Dien, E., 1948, *J.R.A.S. Can.*, **42**, 249.

MICROMETER MEASUREMENT OF HIGH DISPERSION SPECTRA

A. D. Petford

(Communicated by the Director, University Observatory, Oxford)

(Received 1960 August 3)

Summary

A position-sensitive germanium photocell has been used as the basis of a setting device for measuring spectra, and has given a great reduction in the time of measurement, and some increase in precision, compared with visual measurement.

---

1. *Introduction.*—The traditional way of measuring photographed spectra is by setting the cross wire of a measuring microscope on the spectrum lines. This can be done to within a few microns with narrow lines, but when the lines are a millimetre or so wide, as in the case of solar spectra with dispersion of several millimetres per Angstrom, or of stellar spectra with extremely broad lines—for example those of the eclipsing variable Y Cygni—setting by eye becomes very much less accurate as well as slow and tiring. Several devices have been described for replacing this operation by a simpler one, for example the bringing of two oscilloscope traces to coincidence (**1**, **2**), but these are all fairly complicated, depending on a repetitive scan of part of the spectrum.

The present device was suggested by the availability of a position-sensitive germanium photocell of high linearity and stable zero. This has been described by Baker (**3**) and consists of a single germanium wafer, about 2·5 mm square and 0·2 mm thick, having a rectifying junction in the centre of one face. The opposite face is the active area, and has ohmic contacts towards the centres of its edges. An opposite pair of these will give a photovoltage when the face is asymmetrically illuminated, for example by the image of a spectral line, and as the image is moved across the face the voltage will fall to zero and then increase with the opposite polarity. In the zero position the 'centre of gravity' of the line will be on the centre of the cell.

2. *Design.*—The device is attached to a Hilger measuring microscope, in which the spectrum is traversed past the microscope by the measuring screw. Backlash has been reduced by biasing the plate carriage against the nut with a weight. The plate is illuminated by a 20 v 10 w projector lamp and a simple condensing system, and the light is chopped at 800 cps by a 16-bladed shutter driven by a 3000 rpm shaded-pole motor.

The eyepiece of the microscope is replaced by a fitting having an unsilvered beam-splitting plate sending an image to a crosswire and eyepiece, the majority of the light passing the beam-splitter and forming an image on the photocell. This image is restricted in size perpendicular to the dispersion by a slit in a silvered glass plate, so that only a height of 0·14 mm of the spectrum can contribute to the cell illumination. At a magnification of $\times 2$ the whole width of the cell parallel to the dispersion is covered by the line image.

In principle a galvanometer could be used to indicate the symmetrical position. The arrangement used is more complicated than this because a sufficiently sensitive galvanometer has too long a period for convenience, and is also more expensive.

The cell output is fed to the transistorized amplifier and detector shown in Fig. 1. The 1KΩ potentiometer serves to balance the cell to zero output when uniformly illuminated. The amplifier is that described by Avery and Bowes (4) but having the capacities changed to give peak gain at 800 cps. A gain of 12 v/μamp is obtained, and the noise figure with 500 Ω source impedance is less than 6 db. using a selected input transistor.

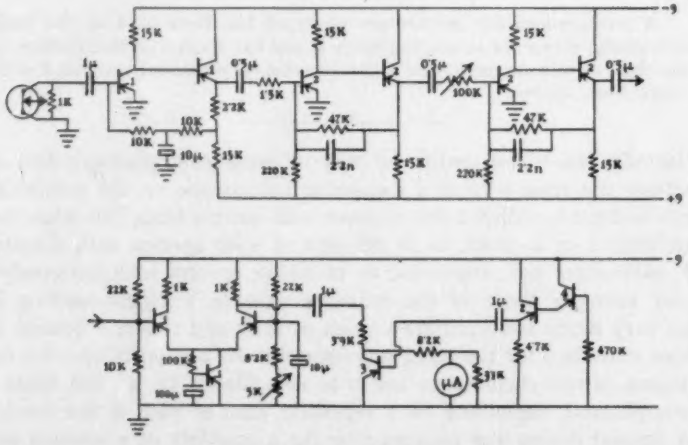

FIG. 1.—*Amplifier and detector circuit. The transistors are:* 1, *V* 10/50 *A*; 2, *V* 10/30 *A*; 3, *OC* 71; 4, *OCP* 71.

The final stage is a limiting amplifier which serves to prevent the meter deflection from going beyond full scale, and is linear between the output limits ± 3 v and saturated beyond that. The synchronous detector uses the OC71 as a switch to earth the meter input on alternate half-cycles of the cell illumination. A reference waveform is derived from the OCP71 placed in the edge of the lightbeam between chopper and microscope, and amplified to 5 v peak-to-peak. The meter, a centre zero instrument, has a sensitivity of 12·5 μamps full scale each way, and is used slightly underdamped.

When the light is 'on', the polarity of the cell output depends on the direction in which the line image is offset from the cell centre, and the synchronous detector connects the meter to the amplifier only at this time, when the amplifier output also has this polarity. Thus the direction of the meter deflection depends on the direction of offset and its magnitude on the distance of offset when this is less than the full-scale deflection.

The power is supplied by three 9 v batteries, giving complete decoupling between the amplifier and the reference generator. These give 3–4 m amps each.

3. *Performance.*—For use in the measurement of solar absorption spectra the normal visual procedure would generally be followed, the unit being used to set on both solar lines and telluric lines of oxygen or water vapour, and the differences between these settings yielding a measure of the shift of the solar line relative to

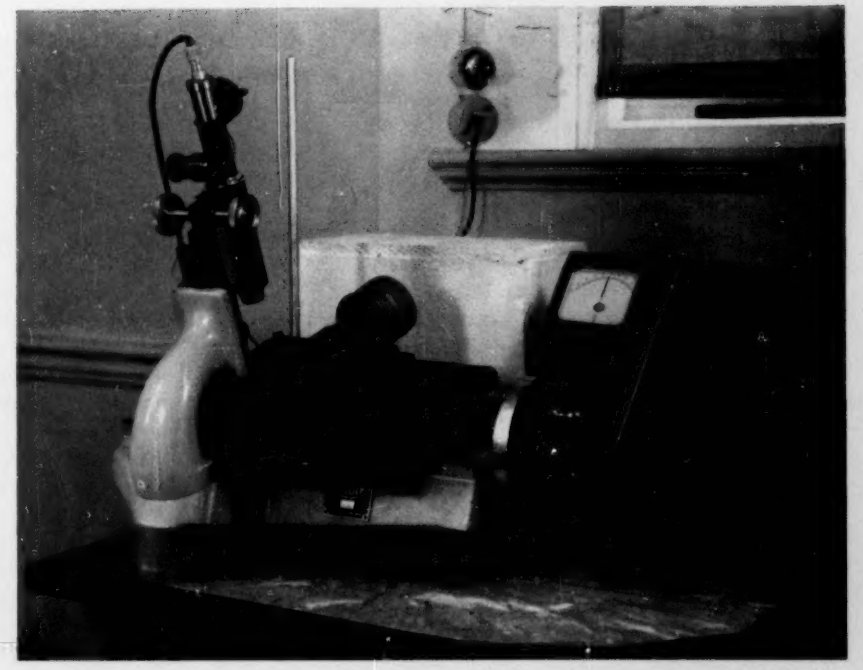

General view of measuring position, showing Hilger machine with eyepiece adaptor, meter mounted on amplifier and battery box, and softboard sound-screen over chopper disc and lamp.

a standard position. This procedure eliminates from measures across a spectrum the effect of slit tilt and curvature, uneven collimator illumination, and effects due to the cross-spectrum plate motion on the measuring machine not being straight or perpendicular to the measuring motion along the spectrum.

However, this ideal procedure can only be used in the vicinity of the few good telluric lines, all to the red of λ5900 A. To test the performance the unit has been used to measure velocity shifts of the non-Zeeman line λ5576·1 A in the spectrum of a sunspot and the adjacent photosphere taken with the Oxford 35 m telescope and the 5th order Babcock grating. The dispersion was 6 mm/A. (This was used because these were the only available spectra of this very high dispersion, for which the method is especially advantageous, which had been extensively measured by the normal visual method.) Since there are no telluric lines in this region, spectra were also taken with an absorption tube of iodine vapour in front of the spectroscope slit. The iodine spectrum has a very large number of lines in this region, so that several fell on the solar line being measured, and hence these comparison spectra had to be distinct from those on which the solar line was measured. A compact group of iodine lines at λ5575·25 A was used as the standard to eliminate slit curvature. This was done by cutting across the plates 1 cm to the blue of the solar line and 1 cm to the red of the iodine group and mounting these two sections of plate on the measuring machine as if they formed a continuous run of spectrum. Setting on the solar line and then on the iodine group, the difference in the readings of the Hilger drum is a direct measure of the velocity shift, with an unknown constant added. For the present differential measures the latter was unimportant. The meter scale near zero was about 1 division/micron.

The Hilger machine has had a cross-slide fitted, with a micrometer head, so that the spectrum can be traversed by, typically, tenths of a millimetre in a direction perpendicular to the dispersion.

The measures are recorded on an Olivetti 'Elettrosumma' adding machine, using the left hand. This machine has a keyboard with serial rather than parallel entry, easily operated by touch, and a touch on another key then prints the number entered. Up to eight digits can be entered at once: these are; horizontal plate carriage position in millimetres, two digits; vertical position in millimetres and tenths, three digits; and drum reading in microns, three digits. Another drum setting at the same plate position requires only the last three digits to be entered. This has been found a great improvement over hand written readings, and is far less expensive than the ideal method of direct digital printout.

The curves in Fig. 2 show the mean of four traverses across the spectrum of a small spot by visual measurement, made with great care by Miss J. Holmes, and a single traverse with the photodiode device. The spread among the visual measures, each of which comprised five settings on the line, is estimated to be 0·15 km/sec.

The curves in Fig. 3 show single photodiode measures by two observers, one of whom, Miss M. G. Adam, had not previously used the device, though experienced in visual measurement. The curves suggest a reproducibility between observers of ±0·03 km/sec, or ±3 microns, and the time of measurement was also less by a factor of ten than that for the set of visual measures giving comparable accuracy.

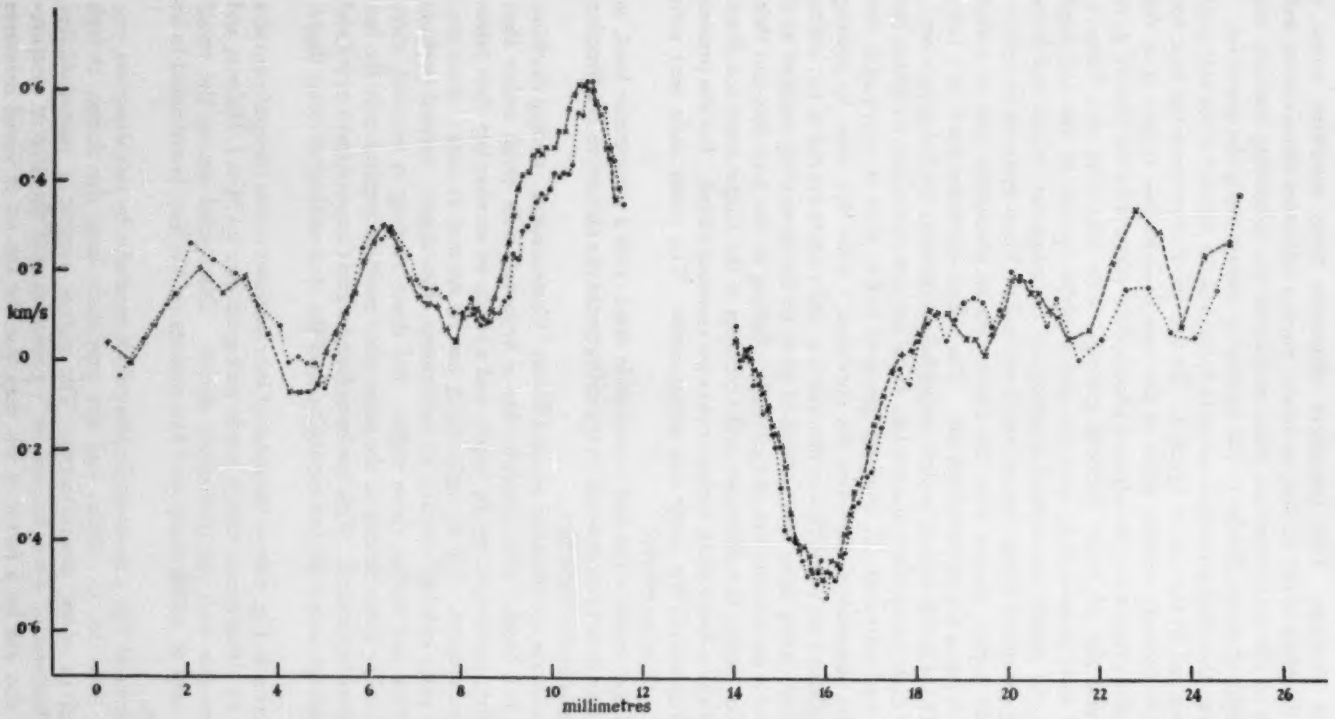

FIG. 2.—*Comparison of measures made visually (filled circles: mean of 20 settings at each point) and with the photodiode (crosses: single settings).*

The spectrum was taken with the slit across the diameter of a sunspot, and the velocities are derived from measures of the Doppler shift of the non-Zeeman line 5576·1 A. The velocity variations in the regions 0–8 mm and 18–25 mm are due to photospheric velocity fields, and 8–11·5 mm and 14–18 mm, in the penumbra of the spot, to the Evershed effect.

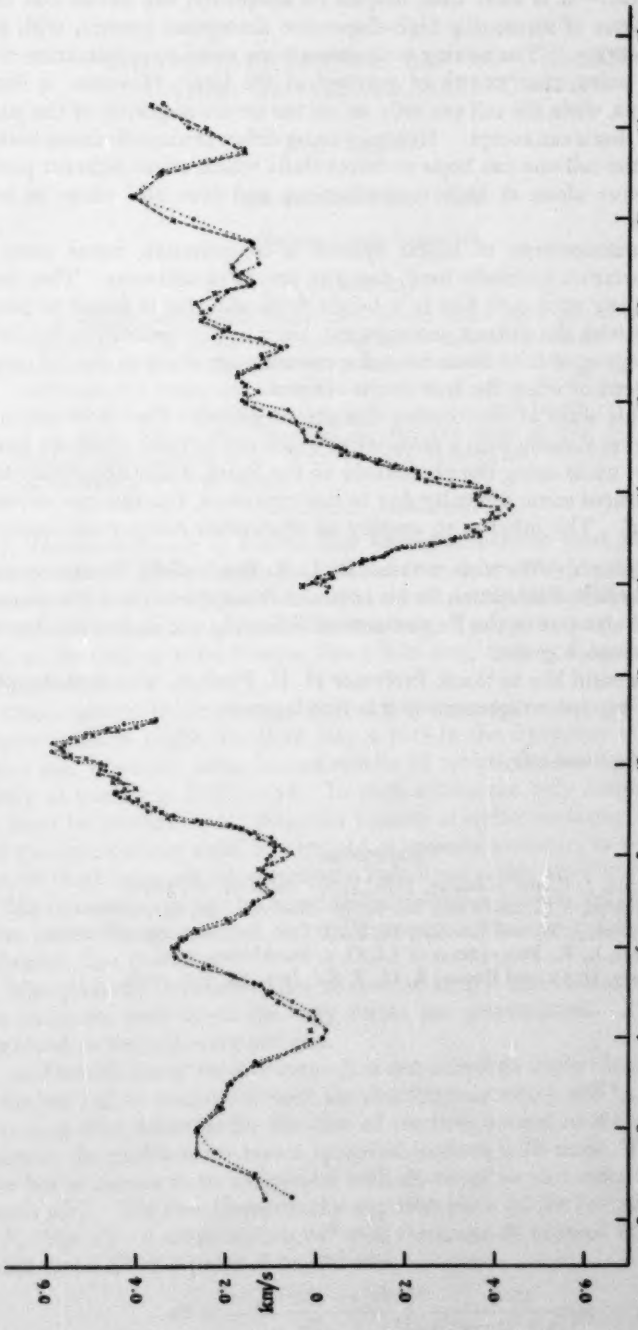

FIG. 3.—*Comparison of photodiode measures (single settings) on the same plate and line as Fig. 2 by two observers. (Filled circles: ADP; crosses: MGA.)*

4. *Conclusion.*—It is clear that, despite its simplicity, the device can much reduce the labour of measuring high-dispersion absorption spectra, with some increase in accuracy. The setting is apparently on some approximation to the visual setting point, the 'centre of gravity' of the line. However, a further possibility exists, since the cell can only set on the centre of gravity of the part of the line profile that it can accept. Hence by using different magnifications between the plate and the cell one can hope to detect shifts which affect different parts of the profile; core alone at high magnifications and core and wings at lower magnifications.

For the measurement of stellar spectra a complication arises since the comparison spectrum normally used, the iron arc, is in emission. This means that one is setting on a dark line in a bright field, and this is found to present some difficulty with the present arrangement, since any irregularity in the bright field, due to fogging or faint lines, has a disproportionate effect on the cell output, as it is asymmetrical when the true line is centred.

Two possible ways of overcoming this are suggested. One is to set on the iron arc spectrum visually with a cross-wire, which can be done relatively quickly and accurately, while using the photodiode on the broad stellar absorption lines. This would present some difficulty due to line curvature, but this can obviously be surmounted. The other is to employ an absorption comparison spectrum.

Acknowledgments.—We wish to thank Dr L. R. Baker of the British Scientific Instrument Research Association for his advice on this application of his photocell.

Thanks are also due to the Department of Scientific and Industrial Research for a special research grant.

Finally, I should like to thank Professor H. H. Plaskett, who took the plates measured, for his encouragement of this development.

The University Observatory
Oxford:
1960 *August.*

References

(1) Rymer, J. B. and Halliday, J. S., *J. Sci. Inst.*, **27**, 50, 1950.
(2) Tomkins, F. S. and Fred, M., *J. Opt. Soc. Am.*, **41**, 641, 1951.
Bennett, J. M. and Koehler, W. F., *J. Opt. Soc. Am.*, **49**, 466, 1959.
(3) Baker, L. R., Proceedings of I.C.O. 5, Stockholm, 1959.
(4) Avery, D. G. and Bowes, R. C., *J. Sci. Inst.*, **35**, 212, 1958.

THE ROTATION OF A BARRED GALAXY UNDER GRAVITATIONAL FORCES

S. Aarseth

(Communicated by F. Hoyle)

(Received 1960 August 16)

Summary

A simple geometrical model of a barred spiral with central nucleus is considered. The problem of rotation about an axis normal to the bar axis is discussed, and it is found that a certain density distribution in the bar will make the system remain stable for a time of order 3×10^9 years. When the ratio of the diameter of the nucleus to the total length of the bar is 1 : 3, as in Fig. 2, this situation requires the ratio of total bar mass to central mass to equal 0·54. If the latter is taken to be $5 \times 10^{10} \odot$ the period of rotation is $1{\cdot}5 \times 10^8$ years.

1. *Introduction.*—It is known that barred structures exist in a number of spiral galaxies. These are in the form of two symmetrical bars emerging from opposite sides of a nucleus. Usually at a sufficiently large distance the straight bar structure vanishes quite discontinuously, leaving trailing arms. In some systems the trailing arms develop into a thin ring, making a configuration rather like the letter θ.

Observational evidence suggests that gas is present in many of these galaxies. Magnetic forces might therefore play a part in the dynamics of such systems. There are, however, some barred spirals in which the bar appears to consist mostly of stars, e.g. NGC 1398. In such a case the only forces acting on the bar must be gravitational. Since for reasons of stellar evolution it seems certain that gas-free systems must be very old, it appears necessary to suppose that the bars in these cases are comparatively long-lived rather than transient features. In this connection it may be noted that although it has not yet been proved that these barred systems rotate, the trailing arms at the ends of the bar is a good indication that this is so.

The problem therefore arises as to how long a barred structure in rotation can maintain itself when the only forces are gravitational. This question is examined in the following sections.

2. *Formulation of the problem.*—It is our object to study the density function in the bar and to examine if there are distributions which will be secularly stable over long time intervals for the case of rotation normal to the major axis. To examine the problem we take a spherical nucleus with mass M and radius R_1. The bar is chosen to be cylindrical with diameter $2a$ and mass density per unit length $\rho(r)$. The two diametrically opposite parts of the bar run from $\pm R_1$ to $\pm R_2$ (Fig. 1). A cross-section πa^2 with thickness dr situated at r gives rise to a radial force dF at a point P on the axis,

$$dF = \frac{2G\rho(r)(r_P - r)\,dr}{a^2} \int_0^a \frac{y\,dy}{[(r_P - r)^2 + y^2]^{3/2}}. \qquad (1)$$

If we take inward forces to be positive, the total radial force on unit mass at P is

$$F(r_P)=\frac{GM}{r_P^2}+\frac{2G}{a^2}\left[\int_{R_1}^{r_P}\rho(r)\left\{1-\frac{r_P-r}{[(r_P-r)^2+a^2]^{1/2}}\right\}dr\right.$$
$$\left.-\int_{r_P}^{R_2}\rho(r)\left\{1+\frac{r_P-r}{[(r_P-r)^2+a^2]^{1/2}}\right\}dr+\int_{-R_2}^{-R_1}\rho(|r|)\left\{1-\frac{r_P-r}{[(r_P-r)^2+a^2]^{1/2}}\right\}dr\right]. \quad (2)$$

It is our aim to examine if any function $\rho(r)$ can satisfy the requirement of rigid body rotation. Thus if all parts of the bar move with uniform angular velocity Ω the centrifugal force at P is $r_P\Omega^2$, where r_P is the central distance of P. For circular motion, which is implied here, this must be compensated by the inward gravitational force $F(r_P)$. That is, $F(r_P)=r_P\Omega^2$.

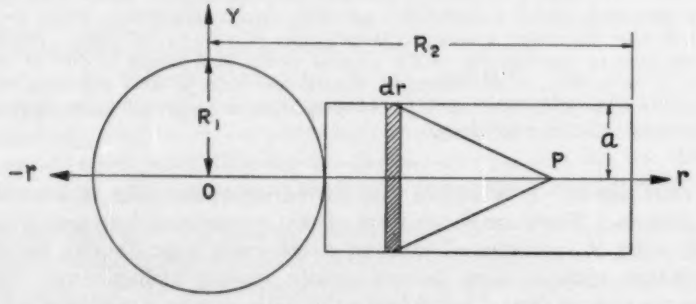

FIG. 1.—*Drawing of half of the bar and nucleus. (Not drawn to scale.)*

Dividing equation (2) by $2GM$ and using the scaled density $\rho'(r)=\rho(r)/M$, this requirement becomes:

$$r_P\alpha=\frac{1}{2r_P^2}+\frac{1}{a^2}\left[\int_{R_1}^{r_P}\rho'(r)\left\{1-\frac{r_P-r}{[(r_P-r)^2+a^2]^{1/2}}\right\}dr\right.$$
$$\left.-\int_{r_P}^{R_2}\rho'(r)\left\{1+\frac{r_P-r}{[(r_P-r)^2+a^2]^{1/2}}\right\}dr+\int_{-R_2}^{-R_1}\rho'(|r|)\left\{1-\frac{r_P-r}{[(r_P-r)^2+a^2]^{1/2}}\right\}dr\right]. \quad (3)$$

Here $\alpha=\Omega^2/2GM$ is a constant parameter.

This is an implicit integral equation for the function $\rho'(r)$. Differentiation with respect to r_P reduces (3) to an integral equation of the second kind, but during this operation a constant part of the force is lost so that this procedure is unfortunately not useful. To solve the equation we have therefore taken $\rho'(r)$ to be a well-behaved function, requiring that it be expandable in a power series; viz.

$$\rho'(|r|)=\sum_n A_n|r|^n. \quad (4)$$

The task is then to determine the coefficients A_n so that (3) is satisfied.

3. *Numerical work.*—As a simplification the bar is taken to have constant cross-section. This does not seem to be in serious conflict with observation. One numerical model is dealt with here, namely $R_2=3R_1$, $a=\frac{1}{3}R_1$, and $R_1=3$ kpc, as shown in Fig. 2.

To determine the coefficients A_n the power series (4) has been restricted to terms with $n=0, \pm 1, \pm 2$. We need five fitting points to introduce the condition of uniform rotation, and these are taken to be $r_P=3$, 4, 5, 6 and 7 kpc. It turns out that solutions for $\rho'(r)$ are available for a sequence of values of the parameter α. Only one of these solutions satisfies the additional requirement of uniform rotation at the ends of the bar, however. This is the solution shown in Fig. 3.

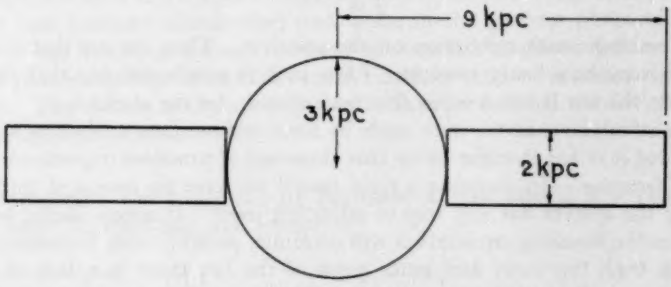

FIG. 2.—*Model of bar and nucleus used in the calculations.*

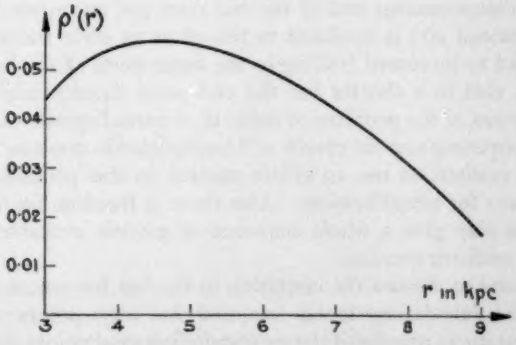

FIG. 3.—*Graph of the scaled density distribution in the bar satisfying the requirement of uniform angular velocity.*

To determine whether the condition of constant Ω is satisfied at intermediate points it is convenient to use Simpson's formula for approximate integration of equation (3). It is found that between 7 and 9 kpc the maximum deviation from the required force for rigid body rotation is ≈ 1 per cent. Between 3 and 4 kpc the maximum deviation is ≈ 2 per cent, and in both cases there is a lack of force. For the middle part of the bar the agreement is very good at all intermediate points. Now from the definition of α, $T^2=2\pi^2/GM\alpha$, where T is the period of rotation. Accordingly after n rotations the deviation in time will be

$$dT=-\frac{nT}{2}\frac{d\alpha}{\alpha}\approx-\frac{nT}{2}\frac{d(r_P\alpha)}{r_P\alpha}=-\frac{nT}{2}\frac{dF}{F}, \tag{5}$$

since changes in r_P can be neglected here. If we define break-up of the outer bar when dT has accumulated to $0{\cdot}1T$, then $n=20$, since $dF/F\cong 0{\cdot}01$.

According to this definition the system will therefore remain stable for about 20 rotations. With the value of α obtained in the above solution and with $M = 5 \times 10^{10}\odot$, $T = 1{\cdot}5 \times 10^{8}$ years. Hence the system remains stable for a time interval of order 3×10^{9} years. The total bar mass M_b is found from integration of $\rho'(r)$:

$$M_b = 2M \int_{R_1}^{R_2} \rho'(r)\, dr \approx 0{\cdot}54M. \tag{6}$$

This is an important restriction on the solution. Thus we see that "stable" rotation requires a heavy nucleus. Even so it is worth noticing that the mean density in the bar is $\approx 1{\cdot}6$ times the mean density for the nucleus.

The calculations above were made by hand and are thus subject to numerical errors, but it is not thought likely that these are of practical importance.

4. *Discussion.*—In choosing a rigid model we have no means of finding out whether the system has any way of adjusting itself. It seems likely, however, that once the breaking-up starts it will continue, possibly with increasing speed. Since in both the inner and outer parts of the bar there is a lack of inward gravitational pull, the breaking-up may well lead to trailing arms, near the nucleus as well at the ends of the bar. Indeed, the prediction of trailing arms also in the inner part of the bar is supported by photographic evidence.

Clearly the discontinuous end of the bar does not correspond to a physical situation. If instead $\rho(r)$ is modified to fall off as an error function at the end points it will lead to increased trailing in the outer parts of the bar. It is quite likely, however, that in a shorter bar the end-point density might go down to zero. Further cases of the problem of rotation of barred spirals will be examined by automatic computing and the results will be reported in due course. Obviously it will be more realistic to use an oblate nucleus in this problem, but this has been omitted here for simplification. Also there is freedom for other values of R_1/R_2 and these may give a whole sequence of models available to satisfy the requirement of uniform rotation.

It now remains to discuss the condition in the bar for points not on the bar axis. During the calculations it was assumed that mass points not on the axis took part in the uniform rotation if the corresponding axial points did so. The force acting on stars not situated on the bar axis differs in second order in its radial component from the force on the bar axis. This second-order variation would affect the situation, if at all, only after a comparatively large number of rotations of the system. More important, a star that is off the axis will be subject to a transverse component of force directed towards the axis. In a frame of reference rotating with the bar, this component of force must cause such a star to move in an orbit about the bar axis. It is of course the kinetic energy of motion of the stars in these orbits that maintains the thickness of the bar. The bar thickness would be expected to vary with the central distance r, rather than to maintain the constant value used in the above calculation. Such a variation would change somewhat the mass function $\rho(r)$ required to give approximate rigid body rotation.

Given the present particular model, there are two restrictions necessary for rigid body rotation: a correct value of M_b/M and a correct value of α. If M is given, this implies that T is determined uniquely. These restrictions will presumably be weakened when other values of R_1/R_2 are included. Even so

the class of mass distributions permitting rigid body rotation would seem to be so narrow that one wonders how so many galaxies as are actually observed could come to fall into this particular group. Some systematic process whereby the mass distribution can be adjusted to meet the necessary conditions seems to be implied.

Since no such process appears to be available once the initial gas has condensed into stars, it is suggested that any redistribution of mass from an initially more or less arbitrary distribution took place in the gaseous phase of the life history of the barred galaxies. A strong diametrical magnetic field with lines of force pinned through a nucleus would certainly tend to produce rigid body rotation. The details of the operation of such a process fall outside the scope of the present paper, however.

This problem was suggested by Professor Hoyle, and it is a pleasure to acknowledge his kind help and advice.

Fitzwilliam House,
Cambridge :
1960 *August* 13.

FOUR STANDARD SEQUENCES IN THE SOUTHERN HEMISPHERE

Bart J. and Priscilla F. Bok

(Received 1960 August 29)

Summary

The four photo-electric sequences are in Tables V to IX for the stars shown in Plates I to IV. The centres are for Selected Areas 141, 193 and 158 and for the van Wijk Sequence in the Large Magellanic Cloud. The basic material is from Boyden Station (1950–51) and from Mount Stromlo Observatory (1957–59). All results are reduced to the Johnson-Morgan *UBV* system.

---

1. *Introduction.*—During 1950–51 the authors established at Boyden Station several sequences of standard photo-electric magnitudes in the range of apparent magnitude 8 to 15. The blue filter used in this work—Corning No. 5551—was not very satisfactory, since it transmits too much light in the violet; the "yellow" magnitudes, observed with Corning Filter No. 3385, should be close to the Johnson–Morgan *UBV* System (**1**, **2**). The Boyden observations were made with a photo-electric photometer built by A. P. Linnell and I. R. King, attached to the 60-inch Rockefeller reflector of Boyden Station (silvered mirror).

These same sequences have been re-measured at Mount Stromlo Observatory, with the three filters used by A. R. Hogg:

U = Corning 9863,
B = Chance OB1, 1 mm + GG 15, 2 mm,
V = Chance OY4, 2 mm.

The photo-electric photometer was attached to the 74-inch Mount Stromlo reflector and used in the manner described by Hogg in his paper "Photometric observations of 244 bright stars" (**3**).

The four sequences are for the following centres:

(i) *Selected Area* 141 (centred at $\alpha = 1^h 05^m$, $\delta = -29° 33'$, 1950 position). It lies close to the South Galactic Pole and was chosen to serve as a standard for an extensive photographic programme of colours and magnitudes in a part of the sky that holds much interest for the student of galactic structure. Work on spectral classification for this same section of the sky is now under way at the Uppsala Observatory in Sweden. Since the majority of the sequence stars are main-sequence stars of spectral class A and later, a comparison between the Boyden and Stromlo results is of considerable interest for relating the two photo-electric systems.

(ii) *Selected Area* 193 (centred at $\alpha = 11^h 30^m$, $\delta = -60° 20'$, 1950 position). This is in one of the richest parts of the southern Milky Way, a region relatively free from overlying interstellar obscuration and with many early B and A stars; it obviously holds a key position in studies of the spiral structure of our Galaxy (**4**, **5**, **6**). The photo-electric sequence is serving as a standard for the measurement of photographic and photovisual magnitudes of stars in this section of the southern Milky Way. A spectral survey for this part of the sky is under way from objective prism spectra (B. E. Westerlund) and from slit spectra for selected stars (W. Buscombe and P. M. Morris).

(iii) *Selected Area* 158 (centred at $\alpha = 18^h\ 26^m$, $\delta = -29°\ 55'$, 1950 position). It is one of the least-obscured sections at low galactic latitudes ($b^I = -10°$, $b^{II} = -8°$) close to the galactic centre, where it is obviously important (**4**, **5**) to obtain a reliable curve relating interstellar absorption with distance. The sequence is serving also as a standard reference sequence for a photographic-spectroscopic survey for a fairly large section of the sky at these latitudes and longitudes. Space density gradients, adequately corrected for interstellar absorption effects, and for separate spectral and colour subdivisions, are of special interest for a region so close to the galactic centre and it is one of the principal aims of the present programme to provide these. Since the work was begun at Boyden Station in 1950–51, the region has assumed added importance, for near it ($\alpha = 18^h\ 27^m$, $\delta = -33°\ 05'$, 1950 position) is the field selected by the International Astronomical Union (**7**) for the study of variable stars in a section of the sky at low galactic latitudes and near the galactic centre.

(iv) *van Wijk sequence in the Large Magellanic Cloud* (centred at $\alpha = 05^h\ 19^m$, $\delta = -68°\ 32'$, 1950 position). During 1950–51, van Wijk (**8**) established at Boyden Station a sequence of photo-electric magnitudes with the aid of the photometer and filters used also by the present authors. Because of the obvious urgent need for standard sequences in the Large Magellanic Cloud, we decided to re-measure this sequence together with the others. The sequence is currently serving as a basic standard for work in Nail and Shapley's Constellation III (**9**, **10**). We note that the van Wijk Sequence is located in a not very dense section of the Large Cloud—which makes it seem likely that the majority of the sequence stars are foreground stars. In fact, the region of the van Wijk Sequence possibly represents a loose association of stars seen superposed on the Large Cloud.

2. *The photometric system.*—The following stars, all but one in the lists of Johnson and Morgan (**1**, **2**), were used as basic standards for the establishment of the zero-point of our visual (V) magnitudes, and the definition of our colour system, $B-V$ and $U-B$:

τ Cet, α Hyi, ξ^2 Cet, κ Cet, ϵ Eri, π^4 Ori, HD 36395,
τ C Ma, β Aql A, α Del, ϵ Aqr, ξ Peg, ρ Peg, 55 Peg.

On several nights standard stars of a wide range of colours were observed, the measurements corrected for effects of atmospheric extinction, and the results compared with the standard *UBV* magnitudes. There is no suggestion of a difference in colour system between our (A. R. Hogg's) system and the standard *UBV* system of V magnitudes. If we relate our system numerically to the *UBV* system, then we find:

$$V_J = V_{Bok} + \alpha(B-V)_J,$$

where $\alpha = 0{\cdot}00 \pm 0{\cdot}03$ (p.e.). For convenience, all magnitudes and colours on the standard *UBV* system carry the suffix J for Johnson.

For the $(B-V)$ colours, the following relation was found to hold:

$$(B-V)_J/(B-V)_{Bok} = 1{\cdot}35 \pm 0{\cdot}02 \text{ (p.e.)} \qquad (1)$$

in good agreement with Hogg's value of 1·37 for the conversion factor.

Our limited data for the transformation of our $(U-B)$ Natural Colours to the standard *UBV* system confirm the rather complex relations found by Hogg.

We quote the following excerpt from Hogg's provisional paper (3):

....."it became apparent that the filter system employed could not be linearly related to the JM system in this colour particularly for spectral types A–F. An average empirical curve was then determined relating the natural system to the colours on the standard *UBV* system. This curve, traced on transparent paper, was superposed on the natural *U–B* graph for the standard stars and was moved along the natural axis to a position of best fit. The curve can be very approximately described by three straight lines, viz:

(i) For $U-B<-0{\cdot}02$, the gradient is $U-B/\text{natural}=1{\cdot}26$.

(ii) For $-0{\cdot}02<U-B<+0{\cdot}04$, the gradient is $U-B/\text{natural}=0{\cdot}22$.

(iii) For $U-B>+0{\cdot}04$, the gradient is $U-B/\text{natural}=0{\cdot}94$.

It will be seen that the natural curve greatly opens out the scale for colours between $-0{\cdot}02$ and $+0{\cdot}04$."

A graphical representation of Hogg's curve is shown in Fig. 1.

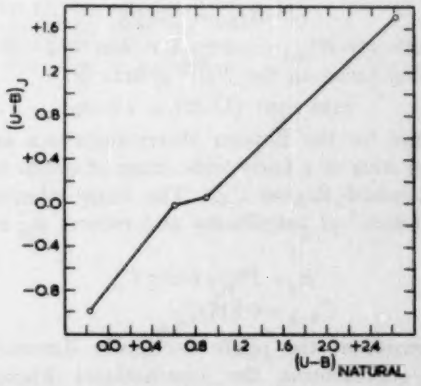

FIG. 1.—*A. R. Hogg's curve relating* $(U-B)$ *colours on his Natural System to* $(U-B)_J$.

For most nights we used the following average extinction coefficients, A, expressed in magnitudes and wholly derived from our material:

$$\text{in } V: A=0{\cdot}25$$
$$\text{in } B: A=0{\cdot}38$$
$$\text{in } U: A=0{\cdot}60.$$

On the few nights for which our extinction curve was notably different from the average, individual night corrections were derived and applied. We made every possible effort to keep under 0·30 the difference in *sec z* between the Johnson–Morgan standards and our zero-point standard stars, but on a few occasions larger differences had to be tolerated. No attempt was made to apply extinction corrections dependent on colour. This procedure seemed justified since we did not use any red stars for purposes of zero-point comparison. All observed photometer deflections, reduced to logarithmic scale of apparent magnitudes, were corrected to outside the atmosphere.

The procedure for the reduction of our measurements to the *UBV* system can be illustrated best by an example. On the night of 1957 September 28/29, Star 139 of SA 141 was compared with the Johnson–Morgan standard κ Cet. For κ Cet we have from Johnson and Morgan (1):

$$V=4{\cdot}82 \quad B-V=+0{\cdot}68 \quad U-B=+0{\cdot}18.$$

After corrections for extinction are applied, the observed differences between Star 139 and κ Cet are:

$$\Delta V = 4{\cdot}43, \quad \Delta(B-V) = -0{\cdot}19, \quad \Delta(U-B) = -0{\cdot}30.$$

We derive the visual magnitudes of Star 139:

$$V = 4{\cdot}82 + 4{\cdot}43 = 9{\cdot}25.$$

The observed difference $\Delta(B-V)$ in our Natural System amounts, for these same two stars, to $-0{\cdot}19$ and hence:

$$\Delta(B-V)_J = 1{\cdot}35 \times -0{\cdot}19 = -0{\cdot}26.$$

We then find for Star 139:

$$(B-V)_J = +0{\cdot}68 - 0{\cdot}26 = +0{\cdot}42.$$

To derive $(U-B)_J$ for Star 139, we proceed as follows:
To $(U-B)_J = +0{\cdot}18$ for κ Cet in the Johnson–Morgan list, there corresponds, according to Fig 1, a value $(U-B)_{Nat} = +1{\cdot}03$. The observed difference is:

$$(U-B)_{Nat} = -0{\cdot}30,$$

which yields the value $(U-B)_{Nat} = +0{\cdot}73$ for Star 139. From Fig. 1 we find that the corresponding value on the *UBV* system is:

$$\text{Star 139: } (U-B)_J = +0{\cdot}02.$$

The colour system for the Boyden observations was established with the assistance of selected stars of a fairly wide range of colour in Selected Area 68 and in Harvard Standard Region C4. The basic relations for the Boyden Station 'Natural System' of magnitudes and colours m_y and C_{b-y} are given by the formulae:

$$m_y = Pv_p + 0{\cdot}205\, C_p$$
$$C_{b-y} = 0{\cdot}834\, C_p$$

where Pv_p = IPV represent the photo-electrically determined magnitude as nearly as possible representing the International Photovisual System of magnitudes, and where C_p is the equivalent of the International Colour Index. The above equations indicate sufficiently for our purpose the characteristics of the colour system employed at Boyden Station. Since we shall reduce the Boyden Station results to the *UBV* system of magnitudes and colours, it seems unnecessary to enter here into full details concerning the reductions of the observations made in 1950.

For sequence stars which are neither very blue nor very red, and which are not markedly reddened by interstellar absorption, we may expect a rather simple relation to exist between the Mount Stromlo colours reduced to $(B-V)_J$ by (1) and the Boyden Station colour indices, C_p. The basic material for all four sequences is shown graphically in Fig. 2. The two colour systems cannot be related to each other by a single linear formula—which is understandable in view of the above-mentioned characteristics of the Boyden Station blue filter. Because of the scatter in the diagram, no use will be made of the Boyden Station measurements for the stars with $(B-V)_J < +0{\cdot}20$ and the stars with $(B-V)_J > +1{\cdot}10$ will similarly be omitted. Table I shows numerically the relation used for the reduction of C_p to $(B-V)_J$.

Between $C_p = +0{\cdot}20$ and $C_p = +1{\cdot}00$ the tabulated values are related to each other by the formula:

$$(B-V)_J = +0{\cdot}29 + 0{\cdot}81\, C_p \qquad (2)$$

whereas for $0{\cdot}00 < C_p < +0{\cdot}20$ the formula:

$$(B-V)_J = +0{\cdot}23 + 1{\cdot}10\,C_p \qquad (3)$$

holds.

We may in a similar manner derive relations between V_J (Stromlo) and IPV (Boyden). For the four sequences under consideration we find that the Boyden and Mount Stromlo visual magnitude systems are related to each other by the formula:

$$V_J = \mathrm{IPV} + 0{\cdot}18 \times (B-V)_J + \text{constant}. \qquad (4)$$

Since we are reducing all Boyden values to the standard *UBV* system, only the slope of the relation as shown in (4) is of interest at this point.

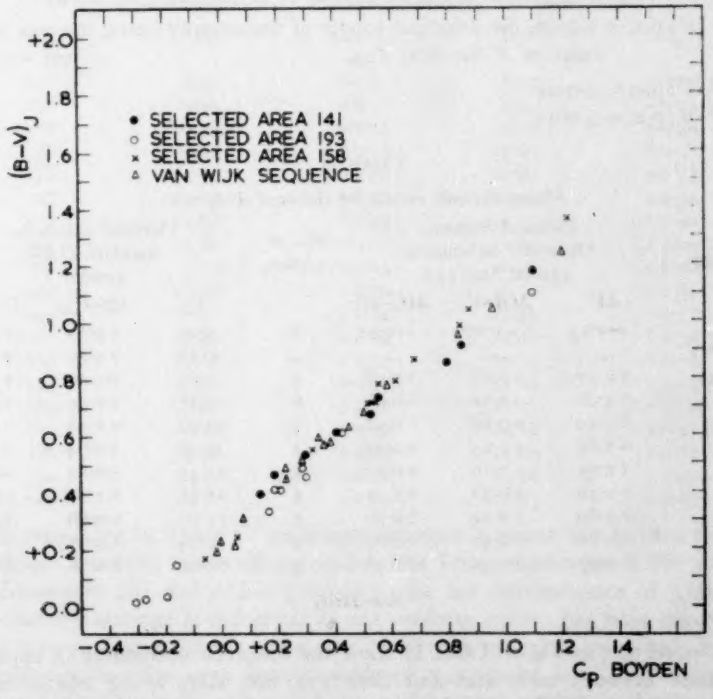

FIG. 2.—*Reduced values of* $(B-V)_J$ *measured at Mount Stromlo compared with Boyden Station colour indices* C_p.

TABLE I

Reduction of C_p*(Boyden) to* $(B-V)_J$*Stromlo*

C_p	$(B-V)_J$
0·00	+0·23
+0·10	+0·34
+0·20	+0·45
+0·30	+0·53
+0·40	+0·61
+0·50	+0·69
+0·60	+0·78
+0·70	+0·86
+0·80	+0·94
+0·90	+1·02
+1·00	+1·10

3. *The sequence for Selected Area* 141.—At Mount Stromlo Observatory, the zero-point star, No. 139, was compared with the listed Johnson–Morgan standards on ten nights. The final derived mean values and their probable errors are:

$$V_J = 9{\cdot}28 \pm 0{\cdot}02 \text{ (p.e.)}$$
$$(B-V)_J = +0{\cdot}40 \pm 0{\cdot}01 \text{ (p.e.)}$$
$$(U-B)_J = +0{\cdot}01 \pm 0{\cdot}01 \text{ (p.e.)}$$

Table II contains the resulting magnitudes and colours from the Stromlo 74-inch observations for the eleven stars in the sequence for which reliable results are available. For a mean derived from observations on at least four nights, the following probable errors, expressed in magnitudes, hold:

V: p.e. = $\pm 0{\cdot}02$, the principal source of uncertainty being the p.e. of the value of V for Star 139.

$B-V$: p.e. = $\pm 0{\cdot}01$.

$U-B$: p.e. = $\pm 0{\cdot}02$.

TABLE II

Mount Stromlo results for Selected Area 141

Star (*HA* 102)	(Natural System) Observed differences against Star 139			No. of nights	Derived values on standard *UBV* system		
	ΔV	$\Delta(B-V)$	$\Delta(U-B)$		V_J	$(B-V)_J$	$(U-B)_J$
21	−0·23	−0·07	−0·01	6	9·05	+0·31	+0·01
139*	...	...	...	...	9·28	+0·40	+0·01
HD 6339	+0·57	+0·07	+0·08	3	9·85	+0·49	+0·03
177	+1·08	+0·10	+0·03	6	10·36	+0·54	+0·02
98	+1·49	+0·06	−0·12	4	10·77	+0·48	−0·02
158	+1·62	+0·25	+0·41	5	10·90	+0·74	+0·29
172	+2·05	+0·16	+0·20	5	11·33	+0·62	+0·10
205	+2·39	+0·58	+1·14	4	11·67	+1·18	+0·98
173	+2·69	+0·21	+0·36	3	11·97	+0·68	+0·24
144	+2·76	+0·39	+0·85	4	12·04	+0·93	+0·71
186	+4·93	+0·34	+0·58	5	14·21	+0·86	+0·46

* Standard.

Columns 2, 3 and 4 of Table II show the observed differences in apparent magnitude between each star and Star 139, the stars being numbered in accordance with the listing for Selected Area 141 in *Harvard Annals* **102**. These differences are the means derived from at least three comparisons and they are on the Natural System of the Hogg photo-electric photometer and filters on the 74-inch reflector. The final three columns contain the derived values of V_J, $(B-V)_J$ and $(U-B)_J$ for each star on the standard *UBV* system. The procedure for obtaining these reduced values has been outlined in the preceding section.

We now present the Boyden Station results. Two stars in the sequence of Selected Area 141 were used as primary standards for zero-point comparisons. They are numbers 139 and 61 of the list in *Harvard Annals* **102**. They were compared on numerous occasions with standard stars in Selected Area 68 measured by Stebbins, Whitford and Johnson (**11**) and stars in Harvard Standard Region C4 measured by O. J. Eggen, who kindly communicated his

results in advance of publication. Since in the present paper we endeavour to reduce our final results to the *UBV* system, we shall not concern ourselves here with the zero-point difficulties that existed in 1950.

Table III lists the Boyden values. The magnitudes, m_y, and colours, C_{b-y}, are on the "Natural System" of Boyden Station and the reduced values IPV (identical with Pv_p) and C_p are shown in the last two columns. For stars with IPV < 14·0, the probable error in IPV equals ±0·01, that of C_p ±0·015. For fainter stars the respective probable errors are ±0·02 and ±0·03. All stars are identified by their serial numbers in *Harvard Annals* **102**.

TABLE III

Selected Area 141: *Boyden station results of* 1950

Star (*HA* 102)	m_y	C_{b-y}	IPV	C_p
223	8·27	+0·21	8·22	+0·25
139	9·45	+0·11	9·42	+0·13
177	10·55	+0·24	10·49	+0·29
98	10·96	+0·14	10·93	+0·17
158	11·09	+0·46	10·98	+0·55
27	11·19	+0·27	11·13	+0·32
172	11·55	+0·33	11·47	+0·40
205	11·91	+0·91	11·69	+1·09
173	12·18	+0·43	12·07	+0·52
144	12·27	+0·70	12·10	+0·84
193	12·31	+0·64	12·15	+0·77
61	12·56	+0·29	12·49	+0·35
125	12·62	+0·32	12·54	+0·38
214	13·58	+0·37	13·49	+0·44
182	13·61	+0·58	13·47	+0·70
213	14·28	+0·39	14·18	+0·47
186	14·42	+0·66	14·26	+0·79
141	14·45	+0·76	14·26	+0·91
142	14·70	+0·69	14·53	+0·83

We reproduce in Table IV an intercomparison between the Boyden Station and Mount Stromlo values all reduced to the Johnson–Morgan *UBV* system. The differences ΔV and $\Delta(B-V)$ listed in the last two columns of Table IV show that the attempt at reduction to one uniform system has been successful. There is no indication of any systematic trend with apparent magnitude. This demonstrates that the 1950 Boyden scale of magnitudes is identical with the 1957–59 Mount Stromlo scale over a range of five magnitudes, a pleasing result in view of the very different instrumentation and calibration techniques used for the two series.

The average differences found from Table IV are:

$$\overline{|\Delta V|} = 0{\cdot}012; \quad \overline{|\Delta(B-V)|} = 0{\cdot}027.$$

and

$$\overline{\Delta V} = +0{\cdot}003 \quad \overline{\Delta(B-V)} = -0{\cdot}002.$$

From the internal agreement between the 1950 and the 1957–59 series, we deduce that the probable error of the mean of a 1950 and of a 1957–59 reduced V magnitude equals:

$$\pm 0{\cdot}005$$

and that of a mean reduced value of $B-V$ equals:

$$\pm 0{\cdot}012.$$

We noted earlier that the principal source of error in the listed V magnitude arises because of the uncertainties in the zero-point comparisons and this uncertainty is not included in the above estimate.

The finally derived standard sequence for Selected Area 141 is given in Table V. The spectral classes of the sequence stars have recently been determined by B. Ljunggren and T. Oja at Uppsala (**12**) and these are shown in the second column. All magnitudes and colours listed in Table V are on the standard *UBV* system and the estimated probable errors are:

$$\text{in } V: \pm 0.02$$
$$\text{in } (B-V): \pm 0.01$$
$$\text{in } (U-B): \pm 0.02.$$

TABLE IV

Selected Area 141: Boyden and Mount Stromlo results, UBV system

Star (*HA* 102)	Boyden Station values		Mount Stromlo values		Differences	
	V_J	$(B-V)_J$	V_J	$(B-V)_J$	ΔV	$\Delta(B-V)$
139	9·26	+0·37	9·28	+0·40	−0·02	−0·03
177	10·36	+0·53	10·36	+0·54	0·00	−0·01
98	10·79	+0·42	10·77	+0·48	+0·02	−0·06
158	10·89	+0·73	10·90	+0·74	−0·01	−0·01
172	11·35	+0·61	11·33	+0·62	+0·02	−0·01
205	11·69	+1·17	11·67	+1·18	+0·02	−0·01
173	11·97	+0·70	11·97	+0·68	0·00	+0·02
144	12·05	+0·97	12·04	+0·92	+0·01	+0·05
186	14·20	+0·93	14·21	+0·86	−0·01	+0·07

TABLE V

Standard sequence for Selected Area 141

Star (*HA* 102)	Sp.	V_J	$(B-V)_J$	$(U-B)_J$
223	F5	8·09	+0·49	...
21	A5	9·04	+0·31	+0·01
139	F2	9·28	+0·38	+0·01
HD 6339	F5	9·85	+0·49	+0·03
177	dGo	10·37	+0·53	+0·02
98	F5	10·78	+0·45	−0·02
158	dKo	10·90	+0·74	+0·29
27	F8	11·00	+0·54	+0·02
172	dG8	11·34	+0·62	+0·10
205	gKo:	11·68	+1·18	+0·98
173	dG8	11·98	+0·70	+0·24
144	dK2	12·04	+0·94	+0·71
193	dK2	12·10	+0·90	+0·60
61	dGo	12·38	+0·58	+0·02
125	dGo	12·43	+0·59	...
214	...	13·39	+0·64	...
182	dK	13·40	+0·86	...
213	...	14·08	+0·67	...
186	dK	14·21	+0·90	+0·46
141	:dK	14·23	+1·03	...
142	...	14·50	+0·96	...

The photographic work by Mrs J. M. Basinski required photo-electric magnitudes for a few additional stars; these were needed for purposes of checking on errors caused by unevenness of sensitivity in photographic emulsions. Eight additional stars were measured on at least three nights for the surroundings of Selected Area 141. These stars are not all in *Harvard Annals* **102** and they are shown in Plate I as stars *a* to *h*. Their *UBV* magnitudes and colours, all measured at Mount Stromlo Observatory, are given in Table VI.

4. *The sequences for Selected Areas* 193 *and* 158 *and the van Wijk Sequence.*— Tables VII, VIII and IX contain the adopted standard sequences on the *UBV* system for Selected Areas 193 and 158 and for the van Wijk Sequence in the Large Magellanic Cloud. The arrangement of each table is rather similar. The first columns contain the identification numbers of each star, the HD or HDE spectral types and the number of nights on which the star was observed with the 74-inch reflector at Mount Stromlo Observatory. Then follow the Mount Stromlo values of V_J, $(B-V)_J$ and $(U-B)_J$ and the Boyden Station values for the same stars, reduced according to formulae (2), (3) and (4). The adopted values of V_J and $(B-V)_J$ are shown in the last two columns: no $(U-B)$ values are available from Boyden Station and the values $(U-B)_J$ listed in the sixth column are the final ones.

TABLE VI

Additional stars near Selected Area 141

(See Plate I for identification)

Symbol of Star (Plate I)	*HA* 102	V_J	$(B-V)_J$	$(U-B)_J$
a	...	9·77	+0·25	0·00
b	...	10·79	+0·67	+0·10
c	52	10·93	+1·03	+0·61
d	...	11·34	+0·40	−0·01
e	276	12·31	+0·64	−0·02
f	...	12·40	+0·62	+0·04
g	253	13·64	+0·99	+0·35
h	34	14·32	+0·80	+0·21

TABLE VII

Standard sequence for Selected Area 193

Star (*HA* 103)	Sp. (*HA* 112)	No. of obs.	Mount Stromlo V_J	Mount Stromlo $(B-V)_J$	Mount Stromlo $(U-B)_J$	Boyden V_J	Boyden $(B-V)_J$	Adopted V_J	Adopted $(B-V)_J$
2622	Ao	6	7·93	+0·04	−0·03	...	...	7·93	+0·04
2509	B2	5	8·38	+0·21	−0·75	...	...	8·38	+0·21
313	A2	4	8·66	+0·21	+0·04	...	...	8·66	+0·21
3074	Ko	7	9·31	+1·11	+1·01	9·31	+1·18	9·31	+1·14
940	B9	5	9·60	0·00	−0·23	...	...	9·60	0·00
875	B8	std	9·89	+0·03	−0·34	9·87	0·00	9·88	+0·02
4584	Ao	5	9·94	−0·01	−0·15	...	...	9·94	−0·01
4709	Fo	6	10·27	+0·41	+0·02	10·28	+0·43	10·28	+0·42
4082	B9	5	10·36	+0·03	−0·51	...	...	10·36	+0·03
4879	Ao	5	10·82	+0·04	−0·12	10·79	+0·05	10·80	+0·04
3056	...	3	11·33	+0·02	−0·51	11·30	−0·02	11·32	0·00
2796	...	4	11·54	+0·15	−0·18	11·56	+0·08	11·55	+0·12
2676	...	4	11·67	+0·29	+0·03	...	...	11·67	+0·29
3137	...	3	12·00	+0·34	+0·04	11·98	+0·39	11·99	+0·36
3143	...	3	12·19	+0·41	+0·07	12·27	+0·45	12·23	+0·43
2669	...	4	12·25	+0·62	+0·02	12·26	+0·63	12·26	+0·62
2739	...	3	12·40	+0·49	+0·04	12·40	+0·51	12·40	+0·50
2520	...	3	13·19	+0·46	+0·01	13·19	+0·52	13·19	+0·49

TABLE VIII

Standard sequence for selected area 158

Star (*HA* 102)	Sp. (*HD*)	No. of obs.	Mount Stromlo V_J	Mount Stromlo $(B-V)_J$	Mount Stromlo $(U-B)_J$	Boyden V_J	Boyden $(B-V)_J$	Adopted V_J	Adopted $(B-V)_J$
3291	G5	9	8·42	+0·72	+0·14	8·40	+0·71	8·41	+0·72
3557	G5	7	8·91	+1·05	+0·54	8·91	+1·00	8·91	+1·02
667	...	std.	10·31	+0·25	+0·03	10·29	+0·28	10·30	+0·26
1241	...	9	10·33	+0·72	+0·15	10·32	+0·72	10·32	+0·72
3800	...	8	10·63	+0·56	+0·02	10·63	+0·55	10·63	+0·56
4379	...	5	10·76	+0·78	+0·36	...	...	10·76	+0·78
503	...	3	10·98	+0·80	+0·22	11·01	+0·79	11·00	+0·80
1231	...	5	11·12	+0·17	−0·01	11·11	+0·19	11·12	+0·18
4579	...	6	11·22	+1·38	+0·92	11·31	+1·26	11·26	+1·32
4291	...	4	11·57	+0·35	+0·04	...	...	11·57	+0·35
3188	...	3	11·68	+0·79	+0·11	11·71	+0·74	11·70	+0·76
3163	...	3	11·78	+1·82	+1·15	...	...	11·78	+1·82
3149	...	4	12·78	+2·01	+1·44	...	...	12·78	+2·01
3178	...	4	13·15	+0·99	+0·40	13·21	+0·96	13·18	+0·98
3206	...	6	13·75	+0·87	+0·20	13·70	+0·84	13·72	+0·86
3234	...	5	14·12	+0·72	+0·02	(13·82)	+0·72	14·12	+0·72

TABLE IX

Van Wijk Sequence in Large Magellanic Cloud

Star (Plate IV)	*HA* 100 No.	*HA* 100 Sp.	No. of obs.	Mount Stromlo V_J	Mount Stromlo $(B-V)_J$	Mount Stromlo $(U-B)_J$	Boyden V_J	Boyden $(B-V)_J$	Adopted V_J	Adopted $(B-V)_J$
2	...	...	7	9·39	+1·27	+1·21	9·40	+1·25	9·40	+1·26
1	269319	A5	std	10·24	+0·22	+0·02	10·23	+0·20	10·24	+0·21
3	269310	A7	5	10·47	+0·26	+0·02	10·47	+0·22	10·47	+0·24
4	269301	F2	6	10·89	+0·34	+0·01	10·91	+0·31	10·90	+0·32
5	269373	F5	4	11·26	+0·48	+0·01	11·26	+0·47	11·26	+0·48
17	...	...	3	11·56	+0·30	−0·80	...	...	11·56	+0·30
6	269324	G5	6	11·57	+0·52	+0·02	11·58	+0·47	11·58	+0·50
7	269384	G5	4	11·86	+0·60	+0·02	11·85	+0·57	11·86	+0·58
9	269377	K7	3	11·87	+0·99	+0·61	11·87	+0·96	11·87	+0·98
18	...	...	4	12·00	+1·12	+0·68	...	...	12·00	+1·12
19	269463	B	4	12·04	−0·02	−0·90	...	...	12·04	−0·02
21	...	...	3	12·26	+2·39	+1·70	...	...	12·26	+2·39
8	...	...	7	12·28	+0·54	+0·02	12·28	+0·51	12·28	+0·52
20	...	...	4	12·36	+0·65	+0·16	...	...	12·36	+0·65
13	...	...	4	12·36	+1·08	+0·75	12·38	+1·06	12·37	+1·07
10	...	...	4	12·53	+0·65	+0·08	12·43	+0·64	12·48	+0·64
11	...	...	3	12·59	+0·71	+0·20	12·56	+0·69	12·58	+0·70
12	...	...	4	12·75	+0·61	+0·03	12·75	+0·59	12·75	+0·60
14	...	...	3	13·44	+0·26	+0·02	13·41	+0·26	13·42	+0·26
15	...	...	2	13·63	+0·62	0·00	13·67	+0·56	13·65	+0·59
22	...	...	2	13·66	+0·84	+0·70	...	...	13·66	+0·84
16	...	...	3	14·07	+0·81	+0·26	14·03	+0·76	14·05	+0·78

In the case of the van Wijk Sequence, the Boyden values are of course based entirely on van Wijk's observations. We decided not to list the identifications from the Potsdam Spektral Durchmusterung (**13**), but identification is a simple and straightforward matter with the assistance of Plates I, II and III. The most discordant value of V_J, Mount Stromlo *versus* Boyden, is No. 3234 in Selected Area 158. Since we had several checks on the Stromlo determination, we have given zero weight to the discordant Boyden value for this star.

It was necessary to measure certain additional stars to assist in the checking of the photographic work for Selected Area 193. Most of these extra stars were measured at the Mount Bingar Field Station (26-inch reflector) and their magnitudes and colours will be published separately.

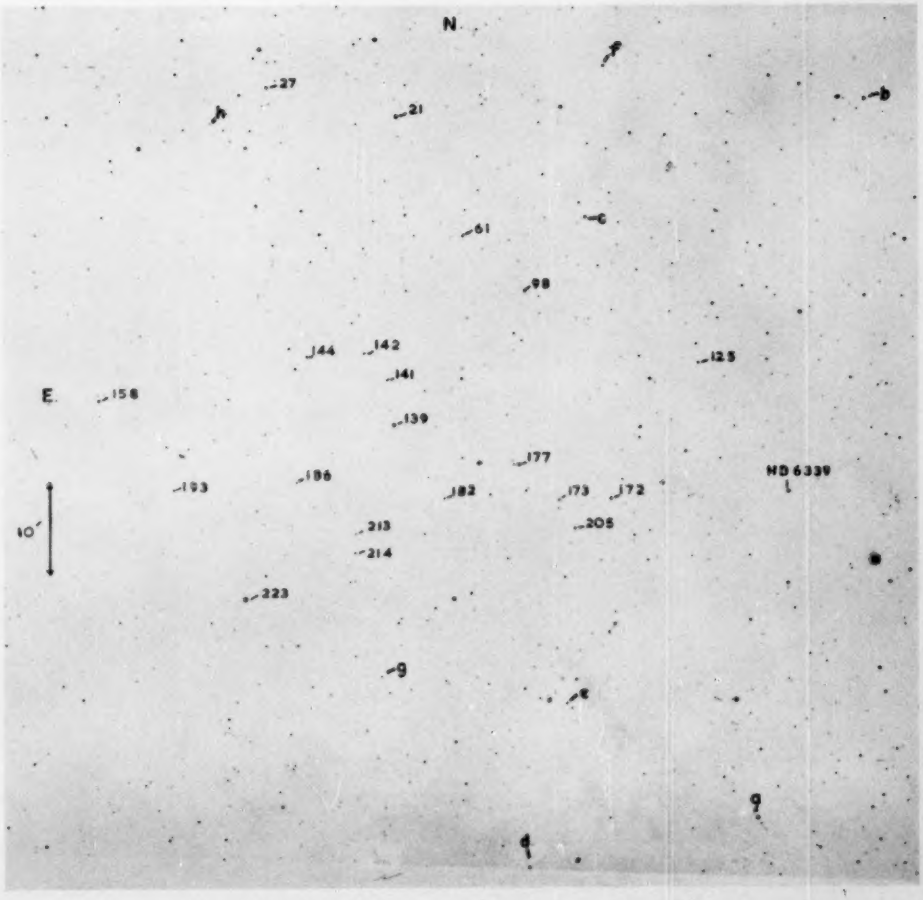

The sequence stars for Selected Area 141.

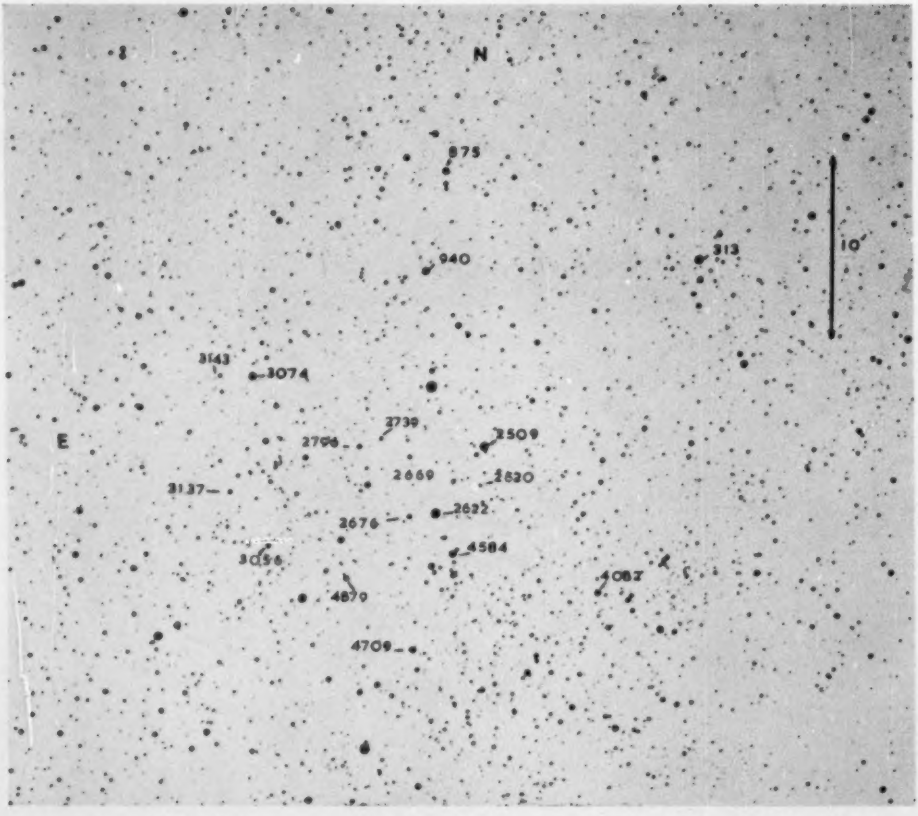

The sequence stars for Selected Area 193.

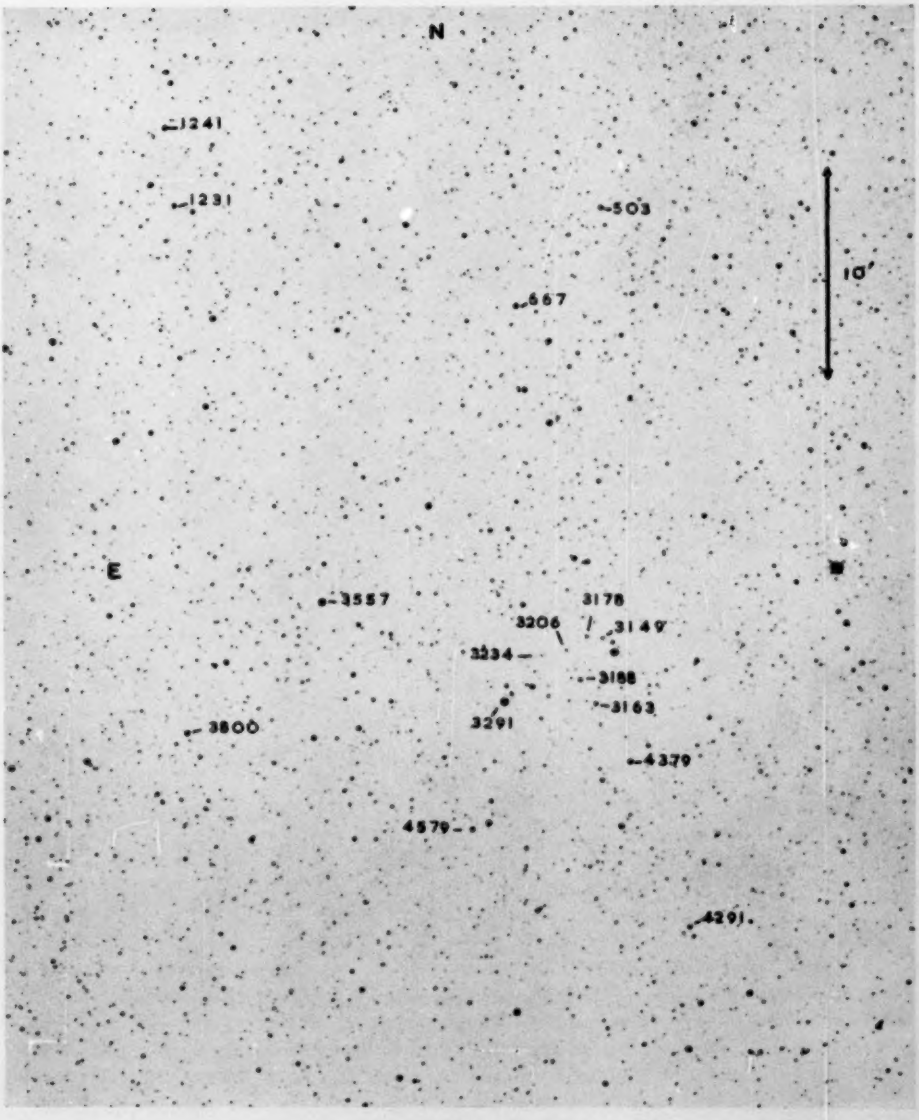

The sequence stars for Selected Area 158.

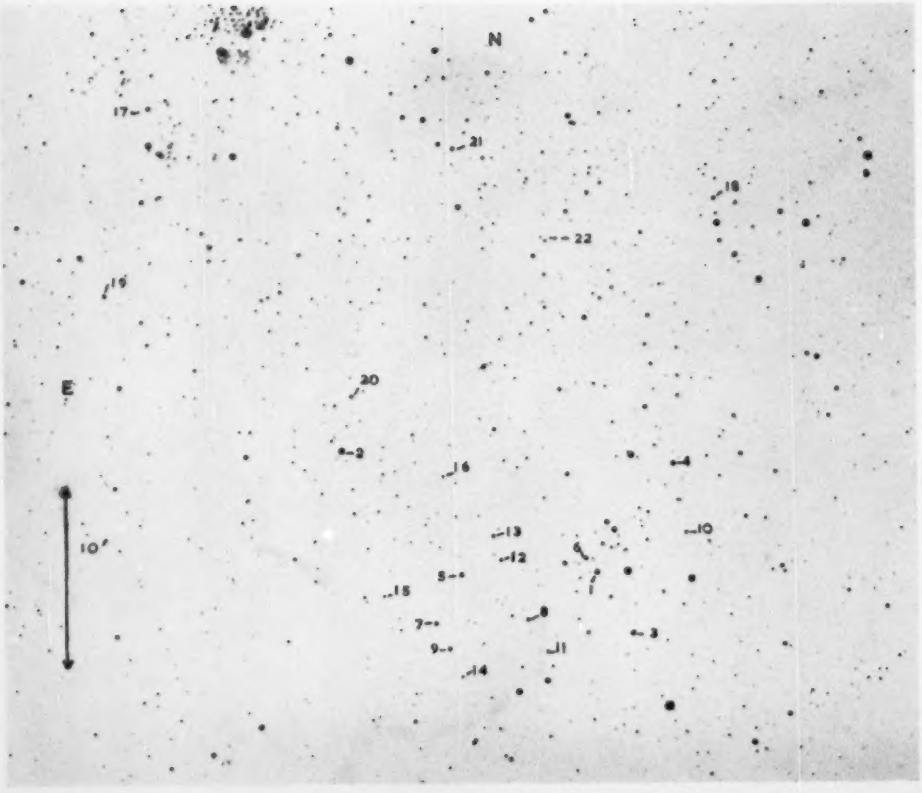

The extended van Wijk sequence for the Large Magellanic Cloud.

All stars are marked on Plates II (Selected Area 193), III (Selected Area 158) and IV (van Wijk Sequence). For the van Wijk Sequence in the Large Magellanic Cloud, the original numbering system has been retained, but extra stars have been added, in this case to provide a somewhat more comprehensive distribution of colour indices than in the original sequence.

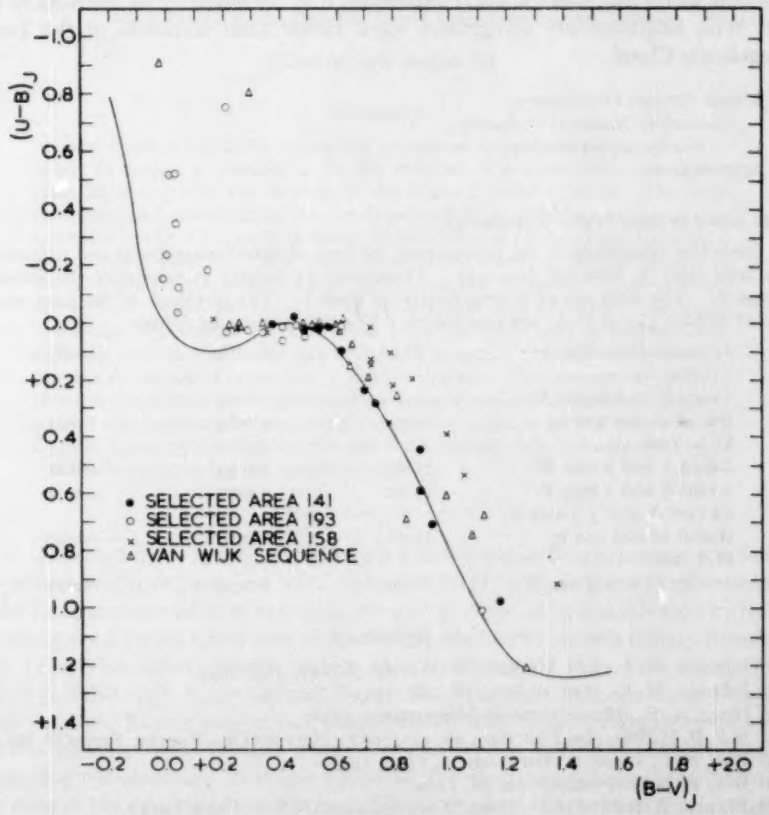

FIG. 3.—*Reduced values of* $(U-B)_J$ *plotted versus reduced values of* $(B-V)_J$*; Mount Stromlo results only.*

5. *Relations between* $(U-B)_J$ *and* $(B-V)_J$.—For the stars measured at Mount Stromlo Observatory we have $(U-B)_J$ as well as $(B-V)_J$. It is of interest to plot one quantity versus the other and compare the results (Fig. 3) with the curve for non-reddened stars shown in Fig. 7 of the Johnson–Morgan paper (1). The agreement is satisfactory for Selected Area 141, which is very near the South Galatic Pole and for which the majority of stars with $(U-B)$ colours measured at Mount Stromlo are probably main sequence stars. Fig. 3 is basically little more than a proof that we have succeeded in reducing our magnitudes and colours to the standard *UBV* system. We have also drawn in Fig. 3 the points for Selected Areas 158 and 193 and for the van Wijk Sequence. There is proof of reddening among the bluest stars of Selected Area 193, but

it would be premature to attempt to draw any conclusions from Fig. 3, since extensive photo-electric and photographic studies aimed specifically at the study of space reddening in this area are already well on the way toward completion. There is a suggestion of a reddening effect in Selected Area 158 and only two stars in the van Wijk Sequence show clear reddening effects. We note again that there is every indication that the majority of the stars in the van Wijk Sequence are foreground stars, rather than members of the Large Magellanic Cloud.

Mount Stromlo Observatory,
Australian National University,
Canberra, Australia:
1960 *August.*

Note added in proof (1960 *December* 9).

Since the submission of the manuscript, we have obtained magnitudes and colours for five faint stars in Selected Area 141. These may be helpful in extending the standard sequence. The stars are all shown faintly on Plate I. The positions of the stars are all related to Star 223 of H.A. **102** (see chart). The relevant results follow:

Distance from Star 223 (Plate I)	V_J	$(B-V)_J$	$(U-B)_J$
6 mm N and 6 mm W (listed as star 219 in H.A. **102**)	14·91	+0·64	+0·04
2 mm S and 2 mm W	15·97	+0·53	+0·01
3 mm S and 3 mm W	15·60	+0·70	+0·04
12 mm N and 3·5 mm E (listed as star 224 in H.A. **102**)	15·61	+0·77	+0·27
10 mm N and 5 mm E	16·24	+0·39	−0·10

References

(1) Johnson, H. L., and Morgan, W. W., *Ap. J.*, **117**, 313, 1953.
(2) Johnson, H. L., *Ann. d'Astr.*, **18**, 292, 1955.
(3) Hogg, A. R., Mount Stromlo Mimeogram, 1958.
(4) Bok, B. J., *Proc. Am. Phil. Soc.*, **96**, 540, 1952; Harvard Obs. Reprint, Series II, No. 42.
(5) Bok, B. J., *Vistas in Astronomy*, **2**, 1522, 1956.
(6) Bok, B. J., *Observatory*, **79**, 58, 1959.
(7) Blaauw, A. (ed.), *I.A.U. Symp.* No. 1, 5, Camb. Univ. Press, 1955.
(8) van Wijk, U., Harvard Bull. No. 921, 7, 1952.
(9) Nail, V. McK., and Shapley, H., *P.N.A.S.*, **39**, 358, 1953; Harvard Reprint No. 373.
(10) Buscombe, W., Gascoigne, S. C. B., and de Vaucouleurs, G., *Australian J. Sci.*, **17** Supplement to No. 3, December, 1954.
(11) Stebbins, J., Whitford, A. E., and Johnson, H. L., *Ap. J.*, **112**, 469, 1950.
(12) Ljunggren, B., and Oja, T., *Arkiv för Astr*, **2**, 391, 1959; Uppsala Medd. No. 125.
(13) *Potsdam Publications*, **27**, Nos. 1, 2 and 3; **28**, No. 1, 1929–1935.

RADIO EMISSION FROM THE CYGNUS LOOP

D. S. Mathewson, M. I. Large and C. G. T. Haslam

(Communicated by the Director, Jodrell Bank Experimental Station)

(Received 1960 August 31)

Summary

The Cygnus Loop, an expanding system of bright nebulosities about 3° of arc in extent, is thought to be the remnant of a supernova type II and probably represents the nearest of the Class I radio sources. The high resolution and sensitivity of the 250 ft paraboloid at 408 Mc/s made possible a detailed study of the radio emission within this type of object and its relation to the optical features. The radio emission was found to be most intense in the optically faint southern region, the position of maximum emission being $20^h\ 48^m\ 21^s$, +29° 40′ (1950). The radio source associated with the bright nebulosity NGC 6992–5 was resolved from the main body of emission and although very similar in size and shape to the optical feature it was displaced towards the centre of expansion by about 12′ of arc. An attempt was made to estimate the relative contributions of the thermal and non-thermal components of the radio emission by measuring the spectral index at several points in the Cygnus Loop by combining the 408 Mc/s survey with a lower resolution 158 Mc/s survey using the 250 ft paraboloid.

---

1. *Introduction.*—The Cygnus Loop is a slowly expanding filamentary nebulosity whose brightest parts are NGC 6960 and NGC 6992 (Plate I). The centre of the Loop is assumed to be at (1950) $20^h\ 49^m{\cdot}5$, +30° 48′·5 and it is seen by looking along the Cygnus spiral arm of the Galaxy about 770 parsecs distant from the Sun (1). Five other objects of this class are known. They are IC 443 (2), HB 9 (3), HB 21 (3), S 147 (4) and Puppis A. Together with the Crab Nebula, Tycho's nova, Kepler's nova and Cassiopeia A, they form the group of 10 non-thermal galactic radio sources which have now been definitely identified with expanding nebulosities. It is also probable that there are many other objects of this class in the galactic plane, but invisible due to dust obscuration, for example, the strong "γ-Cygni" source within the Cygnus X H II complex, which has been shown to be an extended non-thermal radio source (5).

Radio emission from the Cygnus Loop was first reported by Walsh and Hanbury Brown (6) at 92·5 Mc/s using the 218 ft transit paraboloid at Jodrell Bank. The large angular diameter of nearly 3° of the Cygnus Loop provided an excellent opportunity to study the relationship between the optical and the radio emission in this class of object, using the good resolving power of the 250 ft radio telescope at 408 Mc/s.

2. *Observations at 408 Mc/s using the 250 ft paraboloid at Jodrell Bank.*—These observations were carried out in May 1959. The antenna beam was elliptical, having half-power widths of 40 and 54 minutes of arc and the effective solid angle of the beam was 0·70 sq. degrees. The system was calibrated using the radio source 14N5A which was assumed to have a flux density of 47×10^{-26} watts m^{-2} $(c/s)^{-1}$ at 408 Mc/s (7).

Fig. 1 shows the 408 Mc/s radio isophotes drawn in intervals of 4°K brightness temperature. After removal of the background radiation, which was estimated by interpolation on the individual scans, the total flux density of the Loop was estimated to be $260 \pm 50 \times 10^{-26}$ watts m^{-2} $(c/s)^{-1}$.

3. *The relationship between optical and radio features.*—Fig. 2 shows the distribution of optical and radio emission from the Cygnus Loop. The relationship between the radio and optical features will now be discussed.

(*a*) The optical object (including the southern extension) measures approximately $2°{\cdot}8 \times 3°{\cdot}5$. The radio source is about $3° \times 4°$. Thus the radio source must be almost completely contained within the expanding nebulosity.

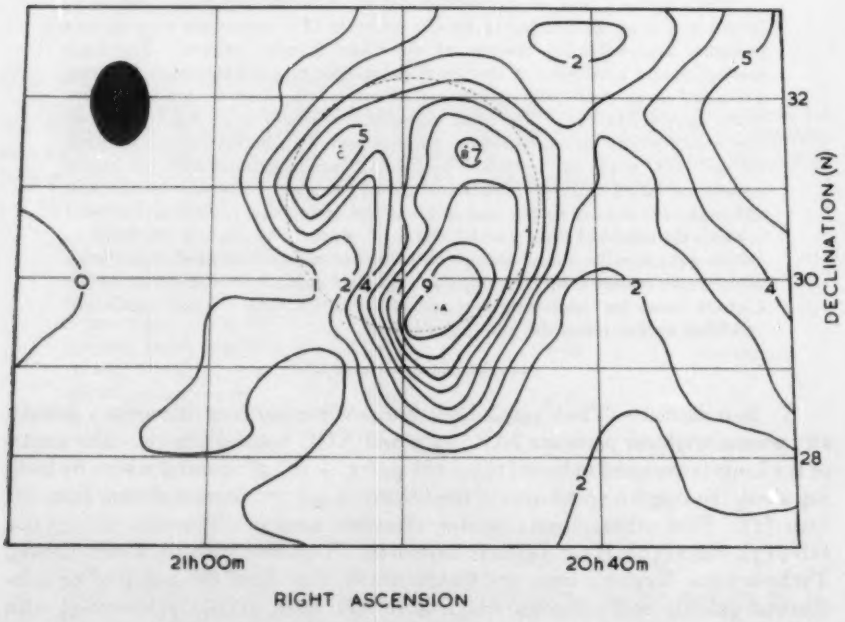

FIG. 1.—*408 Mc/s radio isophotes of the Cygnus Loop using the 250 ft paraboloid. They indicate the brightness temperature above a chosen reference region* ($21^h\,07^m$, $+30°$). *The contour brightness temperature unit is 4°K. The aerial beam to half-power points is shown in the top left-hand corner. The co-ordinates are for epoch 1950. The positions of the three radio peaks A, B and C and the 4th magnitude star 52 Cygni* ($20^h\,43^m\,35^s$, $+30°\,32'$) *are marked. The dotted circle represents the outer limits of the expanding shell.*

(*b*) There is a marked decrease in the radio emission in the SE quadrant of the Loop. This trough almost separates NGC 6992–5 from the main body of the shell and corresponds to a part of the nebula showing no optical emission. This is the only part of the Loop which is void of any optical emission over a region about the size of the aerial beam, and represents also the only section of the object from which very little radio emission is received. This establishes a correlation between the optical features of the Loop and the radio emission, and also shows that the shell is definitely incomplete.

(*c*) There are 3 peaks in the radio emission, the positions of which are marked A, B and C in Fig. 2. A, the most intense peak, lies just inside the southern rim

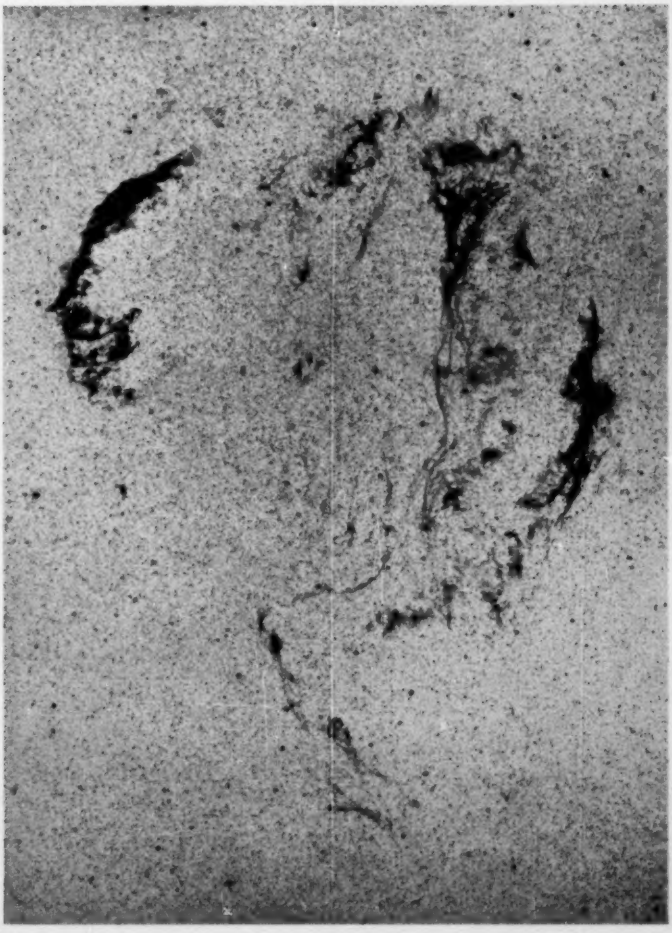

The Cygnus Loop

The Cygnus Loop, photographed in red light (wave-length 6400–6600 A) with the 48-inch Schmidt telescope on Mt Palomar. North is to the top and east to the left. The dense mass on the right-hand side is NGC 6960, in which is involved the 4th magnitude star 52 Cygni. At the top left-hand side is the bright nebulosity NGC 6992 whose more open lower end bears the label 6995.

Fig. 1 shows the 408 Mc/s radio isophotes drawn in intervals of 4 °K brightness temperature. After removal of the background radiation, which was estimated by interpolation on the individual scans, the total flux density of the Loop was estimated to be $260 \pm 50 \times 10^{-26}$ watts m^{-2} $(c/s)^{-1}$.

3. *The relationship between optical and radio features.*—Fig. 2 shows the distribution of optical and radio emission from the Cygnus Loop. The relationship between the radio and optical features will now be discussed.

(*a*) The optical object (including the southern extension) measures approximately $2°{\cdot}8 \times 3°{\cdot}5$. The radio source is about $3° \times 4°$. Thus the radio source must be almost completely contained within the expanding nebulosity.

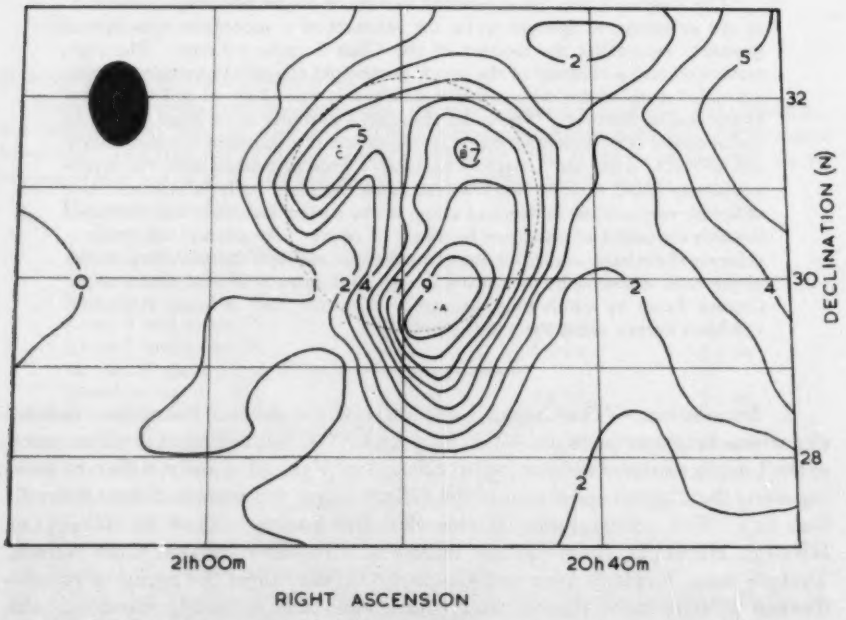

FIG. 1.—*408 Mc/s radio isophotes of the Cygnus Loop using the 250 ft paraboloid. They indicate the brightness temperature above a chosen reference region* ($21^h\ 07^m$, $+30°$). *The contour brightness temperature unit is 4 °K. The aerial beam to half-power points is shown in the top left-hand corner. The co-ordinates are for epoch 1950. The positions of the three radio peaks A, B and C and the 4th magnitude star 52 Cygni* ($20^h\ 43^m\ 35^s$, $+30°\ 32'$) *are marked. The dotted circle represents the outer limits of the expanding shell.*

(*b*) There is a marked decrease in the radio emission in the SE quadrant of the Loop. This trough almost separates NGC 6992–5 from the main body of the shell and corresponds to a part of the nebula showing no optical emission. This is the only part of the Loop which is void of any optical emission over a region about the size of the aerial beam, and represents also the only section of the object from which very little radio emission is received. This establishes a correlation between the optical features of the Loop and the radio emission, and also shows that the shell is definitely incomplete.

(*c*) There are 3 peaks in the radio emission, the positions of which are marked A, B and C in Fig. 2. A, the most intense peak, lies just inside the southern rim

The Cygnus Loop

The Cygnus Loop, photographed in red light (wave-length 6400–6600 A) with the 48-inch Schmidt telescope on Mt Palomar. North is to the top and east to the left. The dense mass on the right-hand side is NGC 6960, in which is involved the 4th magnitude star 52 Cygni. At the top left-hand side is the bright nebulosity NGC 6992 whose more open low-r end bears the label 6995.

of the Loop, in between two rather optically faint diffuse shells. B is associated with the carrot-shaped bright filamentary nebulosity towards the northern rim. C lies about 12 minutes of arc inside the very bright nebulosity NGC 6992–5.

(*d*) Peak C, the weakest of the three peaks, lies in the northern section of the "ridge" in the radio emission which runs almost parallel with NGC 6992, but with an inward displacement of about 12 minutes of arc. There seems to be a very good correspondence in size and shape of the radio source with the optical object, but the radio source is displaced towards the centre of expansion. The optical size is roughly $1^{\circ}{\cdot}2 \times 0^{\circ}{\cdot}2$, whilst the radio size is $1^{\circ}{\cdot}6 \times 0^{\circ}{\cdot}75$. The source does not broaden the aerial beam in the narrow dimension, indicating that the radio size in that dimension is equal to, or less than, about 35 minutes of arc.

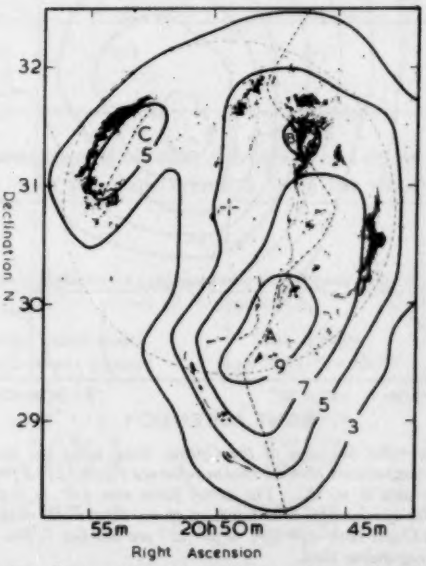

FIG. 2.—*The distribution of optical and 408 Mc/s radio emission from the Cygnus Loop. Only the 12°, 20°, 28° and 36 °K brightness temperature contours (Fig. 1) have been drawn for clarity. The contour brightness temperature unit is 4 °K. The positions of the three radio peaks (A, B and C) in the region are marked and the tops of the radio ridges are dotted in. The centre of expansion is marked by a cross, and a circle of diameter 170′ of arc is drawn to represent the outer boundary of the expanding shell, Minkowski* (1). *Parts of the optically faint southern region have been touched up (refer Plate I).*

(*e*) The long high intensity radio "fringe" running from N to S of the Loop contains both the A and B peaks of the radio emission. Commencing in the north, the ridge runs through the carrot-shaped, bright filamentary nebulosity which contains the peak B, then into a region with very diffuse optical features to a point about 20 minutes of arc E of NGC 6960. Then follows perhaps the most interesting feature: the ridge changes course, rises in intensity, and winds its way in an S-shaped fashion between two rather faint, slightly diffuse, systems of striated filaments having opposite curvatures (Fig. 2). The radio ridge then continues at reduced intensity outside the outer shell of the Loop, and along the trailing southern extension, but displaced about 14 minutes of arc westward of the optical feature.

In general there seems to be better correlation between the radio emission and the diffuse patches of nebulosity than with the very bright filaments. In the most intense region of the radio emission, the filaments have a marked striated pattern. In the projected plane, these filaments are separated by about one quarter of a parsec and they are about 5 pc long.

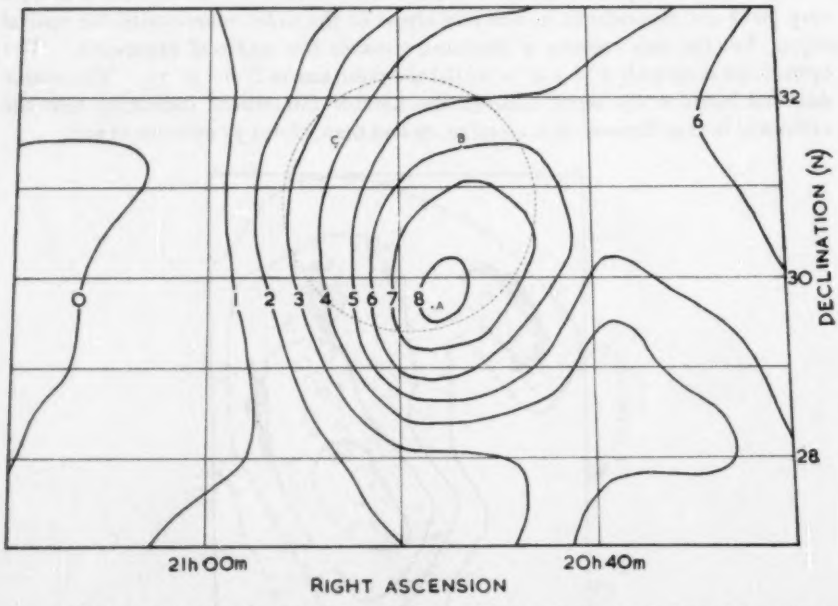

FIG. 3.—158 *Mc/s radio isophotes of the Cygnus Loop using the 250 ft paraboloid. They indicate the brightness temperature above a chosen reference region* ($21^h\ 07^m$, $+30°$). *The contour brightness temperature unit is 20 °K. The aerial beam was 1·6° to 2·2° to half-power units. The co-ordinates are for epoch 1950. The positions of the three radio peaks A, B and C and the 4th magnitude star 52 Cygni* ($20^h\ 43^m\ 35^s$, $+30°\ 32'$) *are marked. The dotted circle represents the outer limits of the expanding shell.*

4. *Spectral index measurements of the radio emission.*—It has been seen from comparison of the 408 Mc/s isophotes with the optical features that although the optically bright northern section is a radio emitter, it is the optically faint southern region which is the strongest radio source. In November 1959 the Cygnus Loop was surveyed at 158 Mc/s, using the 250 ft radio telescope, to investigate any variations in the spectral index over the Loop. The aerial beam was elliptical, having half-power widths of $1°{\cdot}6 \times 2°{\cdot}2$. The effective solid angle of the beam was 4·0 sq. degrees. The system was calibrated using the 14N5A source which at 158 Mc/s has a flux density of 75×10^{-26} watts $m^{-2}\,(c/s)^{-1}$ (8). The 158 Mc/s radio isophotes are shown in Fig. 3. After removal of the background radiation the total flux density of the Loop was measured to be $350 \pm 70 \times 10^{-26}$ watts $m^{-2}\,(c/s)^{-1}$. Comparing this with the flux density at 408 Mc/s, the overall spectral index (α) is $-0{\cdot}32$. The 408 Mc/s contour map was smoothed to produce contours similar to those that an aerial beam ($1°{\cdot}6 \times 2°{\cdot}2$) would produce and the spectral index was measured at the positions of the three peaks A, B and C by comparing their brightness temperature at the two frequencies, 158 Mc/s and

408 Mc/s. The results are given in Table I. The probable error of source position is 5 minutes of arc.

The general implication of the results shown in Table I, is that in the optically bright northern regions, a greater proportion of the emission is thermal than in the optically faint southern parts where the radiation is predominantly non-thermal.

TABLE I

Spectral index of the radio emission from positions A, B and C (see Fig. 2) using 408 Mc/s and 158 Mc/s Jodrell Bank observations.

	A	B	C
Position (1950)	$20^h\ 48^m\ 21^s$ $+29°\ 40'$	$20^h\ 46^m\ 45^s$ $+31°\ 28'$	$20^h\ 53^m\ 18^s$ $+31°\ 28'$
T_b °K (158 Mc/s)	154	107	67
T_b °K (408 Mc/s)	15·5	13	8
Spectral index (α)	−0·44	−0·23	−0·23

Flux density measurements of other workers over a range of frequencies from 38 Mc/s to 1390 Mc/s for the radio emission from the whole Loop are given in

TABLE II

Flux density measurements of the radio emission from the Cygnus Loop over a range of frequencies from 38 to 1390 Mc/s.

Frequency Mc/s	Aerial beam width (half-power points)	Flux density $wm^{-2}(c/s)^{-1} \times 10^{-26}$	Workers
38	0°·6 × 40°	750 ± 200	C. H. Costain (9)
81·5	2° × 15	470 ± 150	J. E. Baldwin (10)
158	1°·6 × 2°·2	350 ± 70	Jodrell Bank
178	0°·23 × 4°·6	430 ± 80	J. E. Baldwin and P. R. R. Leslie (9)
408	0°·67 × 0°·9	260 ± 50	Jodrell Bank
915	2°·2	100 ± 25	J. S. Eaton and J. D. Kraus (11)
1390	0°·57	90 ± 20	G. Westerhout (12)

Table II. Fig. 4 shows a plot of flux density against frequency. It is seen that from 38 Mc/s to 408 Mc/s the spectral index of the radio emission is −0·4, which indicates that at least part of the radio emission is non-thermal in origin.

However at about 500 Mc/s, the flux density decreases much more quickly with increase in frequency. This may be due to either a cut-off at about 500 Mc/s in the non-thermal mechanism, or because at the higher frequencies only the brightest parts of the Cygnus Loop are seen due to the low signal to noise ratio. The latter explanation is supported by the smaller radio size of the source of only 1°·5 measured at these higher frequencies in comparison with 3° at the lower frequencies.

5. *Thermal emission.*—At 408 Mc/s, assuming that the filaments in the Cygnus Loop have an electron temperature of 40 000 °K (13) the optical length is given by $2{\cdot}7 \times 10^{-7}$ EM, where EM is the emission measure (14). The emission measure is certainly less than 10^5 for NGC 6992–5 and NGC 6960, hence their optical depth is small and these nebulosities are "optically-thin" at 408 Mc/s and probably remain so even at 38 Mc/s. Therefore the flux density from the thermal

component of the radiation from the Cygnus Loop should remain constant from 38 Mc/s to 1390 Mc/s.

As NGC 6992–5 is isolated from the main body of the Loop it is possible to measure the flux density of the 408 Mc/s radio emission from the region around this nebulosity. This was found to be about 35×10^{-26} watts $m^{-2}(c/s)^{-1}$. The relative contributions to the radio emission from the region of NGC 6992–5 by the thermal and non-thermal components may be assessed using the value of the spectral index ($-0{\cdot}23$) found for this nebulosity from the 158 Mc/s and 408 Mc/s observations (Table I), and assuming a non-thermal spectral index of $-0{\cdot}5$. This is based on the spectral index ($-0{\cdot}44$) measured at point A in the optically weak southern section of the Cygnus Loop. The flux density of the thermal component was calculated to be 19×10^{-26} watts $m^{-2}(c/s)^{-1}$, and the emission measure derived from this value was 6000 cm^{-6} pc.

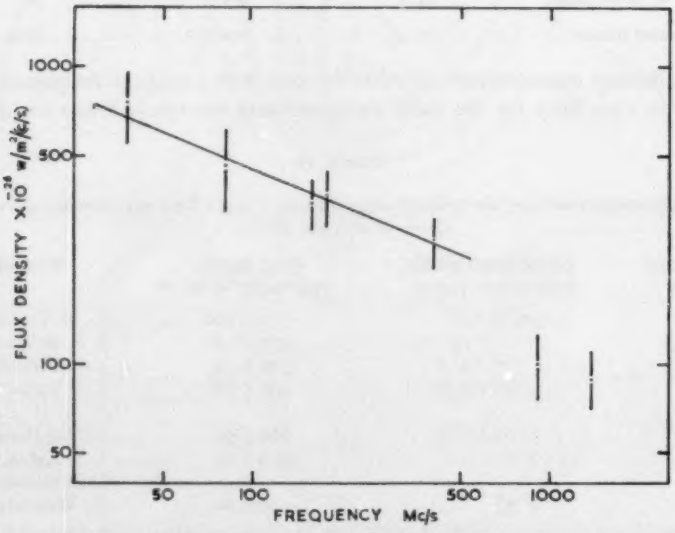

FIG. 4.—*The variation of the flux density of the radio emission from the Cygnus Loop over a range of frequencies from* 38 *Mc/s to* 1390 *Mc/s* (*Table II*).

At 178 Mc/s, Baldwin and Leslie (**9**) using an aerial beam with high resolution in right ascension (13′·5 of arc to half-power points) although poor in declination (4°·6), resolved the thermal component of the radio emission from NGC 6992–5. The intensity of this component was measured to be about 11×10^{-26} watts m^{-2} $(c/s)^{-1}$. If Baldwin and Leslie's result and the Jodrell Bank result are averaged, the thermal component from NGC 6992–5 is 15×10^{-26} watts $m^{-2}(c/s)^{-1}$ and EM = 5000. The average value of the electron density quoted by Osterbrock (**13**) is 200 cm^{-3} for a typical bright filament with a diameter of 7×10^{-3} parsec. The number of filaments in the line of sight would then be about 18. If the electron density is taken as 500 cm^{-3}, which is the maximum value found, then the number of filaments in the line of sight is two.

If the thermal radio emission is assumed to be constant over NGC 6992–5, brightness temperature contours, as shown in Fig. 5, would be produced when

this nebulosity was surveyed with a 47 minutes of arc aerial beam at 408 Mc/s. If these contours are subtracted from the overall brightness temperature contours of NGC 6992–5 (Fig. 1), the radio isophotes shown in Fig. 6, which now represent the non-thermal component of the radio emission from the region about NGC 6992–5, are obtained. The displacement of the centre of the non-thermal emission from the optical feature is now even more noticeable, amounting to about 18 minutes of arc.

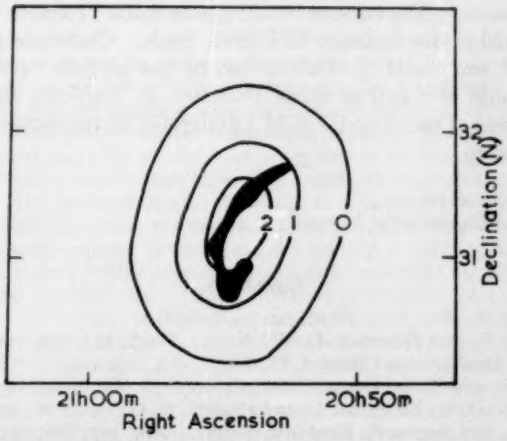

FIG. 5.—*Thermal emission from NGC 6992–5 at 408 Mc/s. The contour brightness temperature unit is 4 °K. The flux density from the thermal, optically-thin radiation from this nebulosity has been calculated to be* $15+10^{-26}$ *watts* m^{-2} $(c/s)^{-1}$ *and the contours have been derived for an aerial beam of 47′ of arc to half-power points, assuming uniform emission over NGC 6992–5. Co-ordinates are for 1950.*

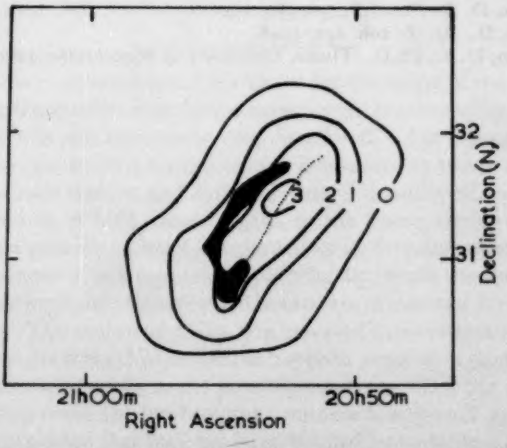

FIG. 6.—*408 Mc/s radio isophotes of the non-thermal component of the radio emission from NGC 6992–5. The contour brightness temperature unit is 4 °K. These have been obtained by subtracting the thermal radiation contribution (Fig. 5) from the total emission (Fig. 1). The inward displacement of the non-thermal radio source from the optical feature can clearly be seen. The co-ordinates are for 1950.*

In an attempt to gain a very rough estimate of the total thermal contribution to the radio emission from the Cygnus Loop, the area of the luminous regions was measured and, assuming $T_e = 40\,000$ °K and EM = 5000, the flux density of the thermal component amounted to 50×10^{-26} watts m^{-2} $(c/s)^{-1}$. This value probably represents an upper limit for the thermal emission.

An interpretation of these results from the 158 Mc/s and 408 Mc/s surveys of the Cygnus Loop has been attempted (**15**) and will be presented in a later paper.

Acknowledgments.—The authors would like to thank Professor A. C. B. Lovell for making available the facilities at Jodrell Bank. Gratitude is expressed to Professor Lovell and Dr H. P. Palmer for the use of their 158 Mc/s receivers. The authors would also like to thank Professor R. Hanbury Brown for many useful suggestions. One of us (D.S.M.) gratefully acknowledges a Leverhulme Research Fellowship.

University of Manchester,
Jodrell Bank Experimental Station:
1960 *July.*

References

(1) Minkowski, R., *Rev. Mod. Phys.*, **30**, 1048, 1958.
(2) Baldwin, J. E., and Dewhirst, D. W., *Nature, Lond.*, **173**, 164, 1954.
(3) Brown, R. Hanbury, and Hazard, C., *M.N.*, **113**, 123, 1953.
(4) Hase, V. F., and Shain, G. A., *Crimean Astrophys. Obs.*, **7**, 93, 1951.
(5) Mathewson, D. S., Large, M. I., and Haslam, C. G. T., *M.N.*, **120**, 242, 1960.
(6) Walsh, D., and Brown, R. Hanbury, *Nature, Lond.*, **175**, 808, 1955.
(7) Seeger, C. L., Westerhout, G., and Conway, R. G., *Ap. J.*, **126**, 585, 1957.
(8) Brown, R. Hanbury, and Hazard, C., *M.N.*, **119**, 297, 1959.
(9) Baldwin, J. E., and Leslie, P. R. R., *M.N.*, **120**, 72, 1960.
(10) Baldwin, J. E., *M.N.*, **115**, 690, 1955.
(11) Eaton, J. J., and Kraus, J. D., *Ap. J.*, **129**, 282, 1959.
(12) Westerhout, G., *B.A.N.*, **14**, 215, 1958.
(13) Osterbrock, D. E., *P.A.S.P.*, **70**, 180, 1958.
(14) Stromgren, B., *Ap. J.*, **108**, 242, 1948.
(15) Mathewson, D. S., Ph.D., Thesis, University of Manchester, 1960.

DYNAMICAL CALCULATIONS RELATING TO THE ORIGIN OF THE SOLAR SYSTEM

R. A. Lyttleton

(Received 1960 September 14)

Summary

The dynamical aspects of certain hypotheses for the formation of planets are shown to be capable of close representation by a restricted three-body system, and accurate machine integrations of the equations of motion have been carried out on such a basis to test the hypotheses. It is first shown that the collisional and tidal mechanisms as applied to the Sun could not result in any particles going into orbital motion outside the Sun at however small at distance. The calculations also show that in a two-body collision of stars only a negligible quantity of material is likely to escape from both stars and be available for capture by the Sun; the amount could rise to planetary order only if the relative speed of the colliding stars when widely separated were several hundred kms per sec. Rotational break-up of a companion star to the Sun might fulfil such a condition.

The rotational instability of a primitive planet growing gradually from a disk of material in motion round the Sun would probably result in disruption into two main pieces with high mass-ratio and separating with hyperbolic speed. The motion of small particles formed in the stream of material drawn out between the separating main masses can also be investigated by means of a restricted three-body analogy, and in this way it is shown that satellite orbits are possible as a result of the great elongation that the last Jacobi figure possesses together with the high relative velocity of the separating pieces. It is suggested that the rotational stability of the great planets has been reached in this way and by the same means their principal satellites produced. The smaller main pieces resulting from the break-up would have sufficient terminal speed to escape entirely from the solar system.

---

1. *Introduction.*—A number of hypotheses for the origin of the planets and the satellites involve the motion of two main masses with much smaller objects moving under their action in the immediate neighbourhood. For example, in the tidal and collision theories, so-called, a second star is assumed to sweep close to the Sun in slightly hyperbolic motion and draw off a small quantity of material from the surface of the Sun or of both stars. Again, in the fission theory of formation of satellites, a single primitive planet is regarded as undergoing rotational break-up into two main masses which separate hyperbolically, while the satellites result as droplets of almost negligible mass formed in a stream of material drawn out between the main pieces. The analytical difficulties involved in investigating such motions in any detail are so great that hitherto it has not been possible to do much more than make reasonable conjecture as to the possible outcome. But the development of modern computing machines has brought a numerical approach to such problems within compass provided that they can be simplified by suitable idealization while retaining the main features. In this way, although conclusions so derived must always be subject to some reserve, it may nevertheless be possible to take such questions at least one stage deeper than pure conjecture. The object of the

present paper is to describe the methods and results of such an investigation applied to well-known existing theories.

2. *The validity of the point-mass approximation.*—Although during an encounter of two stars or two liquid masses considerable deformations may occur when they are at and near their closest, that the relative motion can be regarded as the same as that of two points masses is likely to be a good approximation for two reasons. First there is the consideration that the greater part of the mass of a star is concentrated towards its central regions whereas we are concerned with collisions affecting only the surface material. But second, if at a point P the gravitational potential ϕ of a distribution is expanded in terms of distance r from its centre of mass O, then it always has the form

$$\phi(P)=\frac{M}{r}+\frac{A+B+C-3I}{2r^3}+O(r^{-4}),$$

where M is the total mass, and A, B, C are the principal moments of inertia at O, and I is the moment of inertia about OP. With the centre of mass as origin, the term in r^{-2} always disappears, while for any reasonably shaped distribution the quantity $A+B+C-3I$ is likely to be less than any of its terms. During most of the relative motion r will much exceed the dimensions of the bodies, but even when the values of r exceed the dimensions by only a small factor, the second and higher terms in $\phi(P)$ will amount to only a small proportion of the first term. The use of an inverse square law of force, which must more or less inevitably be adopted anyway, is therefore likely to provide a closer approximation for the relative motion of the bodies than might at first sight appear.

Moreover, for the same reasons, the motion of a particle of negligibly small mass moving between the two main bodies can with equally good approximation be investigated by regarding them as point masses at their mass-centres. The overall character of the whole motion of such a system can be expected not to be much influenced, as compared with the actual system, by the approximations involved in adopting point masses.

3. *The appropriate restricted three-body problem.*—In the tidal and collision theories, an amount of material far smaller in mass then either of the two stars involved is regarded as drawn out between the separating masses. It is this material that goes to form the primitive planets in the theories. We shall study its subsequent motion by treating it as a series of independent particles of negligible mass moving under the combined influence of the two main masses whose relative (hyperbolic) motion is taken as known. The motion of these particles will be followed out from the time of nearest approach of the two main masses, which instant will be taken as $t=0$, and it will be supposed that their initial velocities and positions are linearly in proportion with the initial relative velocity and position of the two particles representing the main masses. Thus, if the centre of mass of one of these latter is taken as origin, and if d denotes the closest distance apart of their centres of mass, while v_Δ is their relative speed at that instant, then a particle at distance λd from the fixed centre and $(1-\lambda)d$ from the other will be supposed to have initial speed λv_Δ perpendicular to the line of centres.

For equal masses of the main bodies, considerations of symmetry show that this assumption will be satisfied for $\lambda=\frac{1}{2}$ anyway. But it turns out that intermediate particles corresponding only to a minute range of values of λ are of interest, and hence that the assumption will closely hold for equal masses.

In the satellite problem, we shall similarly regard a single body as undergoing fission into two main masses while at the same time a stream of small droplets is formed between them and having initial speeds linearly distributed at the instant corresponding to closest separation of the two main masses.

We shall be concerned with determining for what values of λ intermediate particles can be captured by one of the main masses and go into an orbit round it of sufficient radial extent at all its parts to lie entirely outside the actual material body of this mass when its finite size is taken into account. We shall also investigate for what range of values of λ the intermediate particles escape from both component masses.

4. *The equations of motion.*—We replace the two main bodies by point masses m_1 and m_2, and denote by d the closest separation in their relative hyperbolic motion. At this instant $t=0$, when closest, their relative speed will be supposed given by

$$v_A=\sqrt{G(m_1+m_2)/d}\sqrt{e+1}=\sqrt{\frac{\mu(e+1)}{d}}=v_P\sqrt{\frac{e+1}{2}}, \tag{1}$$

where $\mu=G(m_1+m_2)$, and v_P is the parabolic speed corresponding to d, so that e is the eccentricity of the ensuing hyperbolic orbit, and $a=d/(e-1)$ is its semi-major axis. The final relative velocity of m_1 and m_2 when separated by great distance is accordingly given by

$$v_\infty=\sqrt{\frac{\mu}{a}}=\sqrt{\frac{\mu(e-1)}{d}}. \tag{2}$$

We denote by M a particle of insignificant mass that at $t=0$ is situated in line between m_1 and m_2, at distance λd from m_1 and moving at right angles to d with speed λv_A. We wish to determine the subsequent motion of M under the action of m_1 and m_2 in their known relative motion. By adjustment of units, the parameters of the problem can be reduced to three, namely m_1/m_2, e, and λ. The whole motion takes place in one plane, so that we can take rectangular axes OXY fixed in direction at $m_1(0, 0)$. Denoting the positions of m_2 and M also by these symbols, let

$$r=Om_2,\ r_1=MO,\ r_2=Mm_2.$$

Also, let the coordinates of M be denoted by (X, Y) and those of m_2 by (x_2, y_2). Then the equations of motion of M relative to these axes are readily found to be:

$$\left.\begin{aligned}\ddot{X}&=-\frac{Gm_1X}{r_1^3}-\frac{Gm_2x_2}{r^3}-\frac{Gm_2(X-x_2)}{r_2^3}\\ \ddot{Y}&=-\frac{Gm_1Y}{r_1^3}-\frac{Gm_2y_2}{r^3}-\frac{Gm_2(Y-y_2)}{r_2^3}\end{aligned}\right\}. \tag{3}$$

In these, x_2 and y_2 are known functions of the time determined by the adopted hyperbolic motion of m_2 relative to m_1. If the semi-axes of this hyperbola are denoted by A and B, and if also, as a matter of units, we take

$$d=1,\ m_1+m_2=1,\ \text{and}\ G=1, \tag{4}$$

thereby fixing the units of length, mass, and time, then we shall have

$$A=(e-1)^{-1},\quad B=(e+1)^{1/2}(e-1)^{-1/2}. \tag{5}$$

while the mean motion becomes

$$n=(e-1)^{3/2}. \tag{6}$$

Accordingly the coordinates of m_2 at any time t are given by

$$x_2=\frac{e-\cosh u}{e-1}, \quad y_2=\left(\frac{e+1}{e-1}\right)^{1/2}\sinh u, \tag{7}$$

where u is related to the time by Kepler's relation

$$(e-1)^{3/2}t=e\sinh u-u. \tag{8}$$

We also have

$$r=(x_2^2+y_2^2)^{1/2}=(e\cosh u-1)(e-1)^{-1}. \tag{9}$$

Equations (3), with these values for x_2, y_2, have then to be integrated with regard to the time for the values of X, Y. In accordance with the agreed assumptions, the appropriate starting values are:

$$(X, Y)=(\lambda, 0), \quad (\dot{X}, \dot{Y})=(0, \lambda\sqrt{e+1}). \tag{10}$$

The final energy per unit mass of M in its motion relative to m_1 will become constant if it is captured by m_1 or if it escapes from both m_1 and m_2. In the first case it will simply be equal to the total energy in the ultimate elliptic orbit about m_1 and will therefore be equal to $-m_1/2a$ where $2a$ is the major axis of the orbit in the adopted units. At other times this energy is given by

$$T=\tfrac{1}{2}(\dot{X}^2+\dot{Y}^2)-\frac{m_1}{r_1}, \tag{11}$$

and the calculation of this at every stage affords not only a test of accuracy of the work, in that in the above cases it will tend to a limit, but also indicates by its sign whether M is captured by m_1 or not. Moreover, that the energy has reached a constant value indicates that perturbations by the receding m_2 have become negligible, and the integration need be carried no further.

5. *Three collinear particles solution.*—Whatever the form of orbit in which m_1 and m_2 separate, there is always a unique value of λ, depending on the ratio m_1/m_2 only, for which the intermediate particle M remains not only collinear with m_1 and m_2 but describes a homothetically related orbit. The value of λ corresponding to this special case can be found by expressing the condition that $X=\lambda x_2$, $Y=\lambda y_2$ should be a solution of the equations of motion (3) for constant λ. This readily leads to the equation

$$\frac{m_1}{m_2}(\lambda-\lambda^{-2})=1-\lambda-(1-\lambda)^{-2}. \tag{12}$$

This is of course simply a particular case of Lagrange's collinear particles solution of the problem of three bodies with one of the three masses put equal to zero*.

This equation is readily soluble graphically, and for any given mass-ratio m_1/m_2 there is always just one value of λ in the range $0<\lambda<1$ (Fig. 1). For the parabolic separation of m_1 and m_2, for example, this root gives the position of the intermediate particle that can escape from both m_1 and m_2; for smaller values of λ the particle would be captured by m_1, and for larger values by m_2. It proves of considerable help in the investigation to know where this root comes, in that it

* Whittaker, E. T., *Analytical Dynamics*, p. 408, Cambridge 1927.

assists the selection of suitable values of λ for which to carry out integrations, and it also is some check on the resulting solutions.

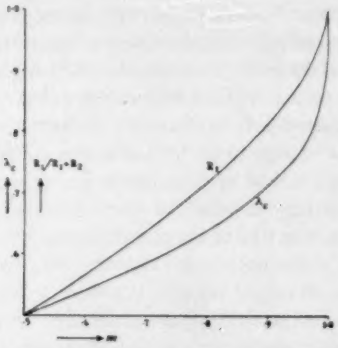

FIG. 1.—*The lower curve shows how the solution of* (12) *for the value of* λ_c *corresponding to the collinear particle solution changes with the mass-ratio* $m=m_1/m_1+m_2$) (*see Section* 5).
The upper curve shows how the radius R_1 *of the star* m_1 *increases withm, on the basis that* $R\propto m^{2/3}$ *for stars. It is seen that* $R_1>\lambda_c$ *except at* $m=0{\cdot}5$ *and* $1{\cdot}0$ (*see Section* 8).

6. *Quantities calculated.*

(i) The rectangular coordinates X, Y of the intermediate particle, for a series of suitable values of λ were calculated by step-by-step integration, the two second-order equations (3) in fact being replaced for this purpose by four first-order equations. The size of step taken averaged about 1 to 5 per degree of motion round m_1, and was adjusted to the circumstances of the motion at each stage.

(ii) The total energy per unit mass of M was calculated at each stage, and its limiting value determines the value of a for the undisturbed final motion of M.

(iii) From the preceding results, the final eccentricity of orbit of M is determined, and hence the angular momentum per unit mass of M in its ultimate motion about m_1 when it is captured, and also the distance of closest approach to m_1 in its subsequent motion, namely $a(1-e)$. (This must exceed the body-radius of m_1, when no longer regarded as a point mass, if M is to orbit about it.)

(iv) By plotting against λ the final energy of M, we can determine the range of values of λ for which intermediate particles escape from both m_1 and m_2.

7. *The collision and tidal hypotheses.*—In the collision theory, a second star passes so close to the sun that the surfaces actually come in contact, and a filament of material from the outer parts of the two stars is supposed to be drawn out between them as they separate. This filament is supposed capable of condensing into a few separate globules to give the primitive planets. Evidently the initial motions relative to the Sun of such bodies, once isolated from the stars in this way, will be closely in accordance with the dynamical theory here developed.

We assume to begin with that the mass of the approaching star is equal to that of the Sun and that in their relative motion the closest distance of their centres is $2R_\odot$. If their relative speed at great separation (after the collision) is v_∞, then the eccentricity of the orbit is given by

$$e-1=\frac{R_\odot v_\infty^2}{GM_\odot}=\frac{v_\infty^2}{v_e^2}, \qquad (13)$$

where v_c is the circular speed of a small particle at the Sun's surface. The value of this, 437 km sec^{-1}, is so great that values of e only slightly in excess of unity can be expected. Thus $e = 1{\cdot}01$ would be achieved for relative speed when at great distance of 43·7 km sec^{-1}, while $e = 1{\cdot}1$ requires 138 km sec^{-1}, and $e = 2$ would be attained only by a speed equal to the circular speed itself. Ordinary relative speeds of stars can therefore lead to values of e only slightly exceeding unity, but the possibility of higher values will not be entirely ruled out. In the integrations, the value of e refers of course only to the orbit of the two stars subsequent to their collision, and since some energy must be lost in the collision process, the original speed of relative approach would be even larger for a given eccentricity than these figures indicate. The energy needed for mere removal from the surface of the sun of a mass comparable with that of the planets corresponds to a speed of approach of the two stars of about 30 km sec^{-1}, and allowing for this loss a final speed of 43·7 km sec^{-1} would require an initial relative speed of 53 km sec^{-1}. The difference of speed would of course be less for higher values of e: thus a final speed of separation of 138 km sec^{-1} would require an initial approach speed of 142 km sec^{-1} in round figures.

Fig. 2 shows for $e = 1{\cdot}01$ the orbits of those intermediate particles that start at $\lambda = 0{\cdot}45$, 0·495, 0·498, 0·499, and 0·4995. Other cases were also computed but the paths have been omitted from the diagram to avoid confusion. Capture by m_1 is found to cease (final energy changes sign) at $\lambda = 0{\cdot}499\,999\,86$, so that only $2{\cdot}8 \times 10^{-7}$ of the whole range $0 < \lambda < 1$ corresponds to escape from both masses, a result of interest later. The remarkable feature of these orbits is that in every case they pass within distance $r_1 \doteqdot 0{\cdot}1$ of the point mass m_1 and that this closest distance is almost the same for every capture orbit starting at $\lambda \geqslant 0{\cdot}45$. (It is even less for ones starting closer in still, but these of course could scarcely be identified with planets formed in surface collision.)

This result is scarcely changed by raising the eccentricity to $e = 1{\cdot}1$ (for which value the corresponding curves are accordingly not shown), and there is only slight improvement in this respect if the eccentricity is raised even as high as $e = 2$, the curves for which are shown in Fig. 3. A number of interesting features common to each case emerge from the calculated values, and we therefore give these in the form of the following Table for the case $e = 2$ which is typical.

TABLE I

$e = 2 \quad m_1/m_2 = 1$

λ	a	e	$a(1-e)$	h
·45	·280	·537	·130	·446
·48	·375	·602	·149	·489
·49	·503	·710	·146	·500
·495	·739	·840	·118	·467
·498	1·55	·936	·099	·438
·500	...	2·0	...	·433

In compiling Table I the least value of λ taken was 0·45, as shown, since smaller values would correspond to planetoids commencing from levels deeper within the Sun than seems reasonable, but in any event the results show that smaller values of λ than this can be of little relevance anyway. For it is seen that the least value of r_1, that is $a(1-e)$, in the subsequent path has a *maximum* value of about 0·151, occurring at about $\lambda = 0{\cdot}486$. Since this can at the very most be

regarded as only about one-third the radius of the Sun, which must be at least 0·5, it follows that any planetoids formed in this way would describe orbits intersecting the solar surface and passing deep within it. Thus any material removed from the surface in such a collision and yet not escaping to infinity could be liberated only temporarily and must fall back onto the surface before completing even half a circuit of the Sun.

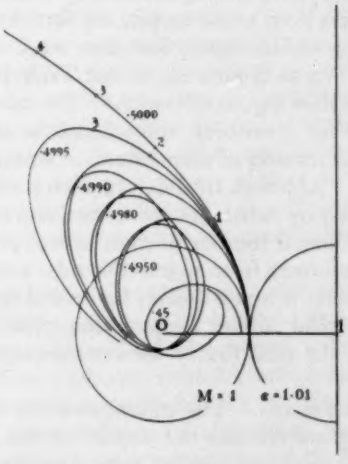

FIG. 2.

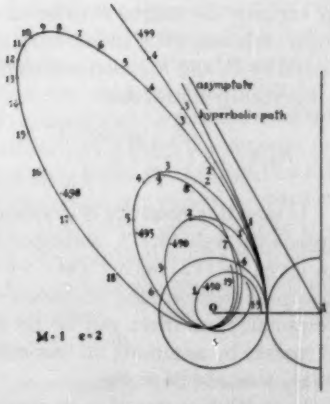

FIG. 3.

In the last column is shown the ultimate angular momentum that the planetoid would have regarding m_1 as a point mass. The value $h = 0{\cdot}433$ for $\lambda = 0{\cdot}5$ refers to the intermediate collinear particle, which describes a similar path to that of the passing star m_2 and so has exactly $\frac{1}{4}$ of its angular momentum per unit mass, which is 1·732 in the adopted units. It will be noticed that although initially the planetoids have angular momentum about m_1 increasing with distance as λ^2, the final

values have a maximum of 0·501 at about $\lambda = 0{\cdot}489$. This means that the greatest amount of angular momentum per unit mass that could result in planetoids formed in this way is distinctly less than one-third that of the passing star. It will be recalled that Russell* pointed out that in fact the average for the actual planets exceeds that of any reasonable passing star by a factor of 10 or more. The present investigation not only confirms the deficiency therefore, but shows that it is even greater than had been supposed and represented by a factor of 30 at the very least.

The tidal theory fares even worse despite the fact that in it the star passes at greater distance, coming within slightly less than $2{\cdot}2\,R_\odot$. This unit of distance gives the radius of the Sun as about 0·46, so that Table I covers this case equally well were it not for the following consideration. The calculations assume a transverse initial velocity of the planetoids, and whereas in collision this can be produced by direct material transfer of momentum, in tidal action no such sideways velocities would occur. Although tidal deformation travels across the surface, it would be achieved largely by radial motions inward and outward on the Sun, and would not involve any lateral transfer of mass except possibly to second order. Thus a primitive planet formed from an unstable tidal wave would have negligible initial angular momentum; it would quickly lag behind the passing star and would simply fall back to the solar surface almost if not quite where it was detached. This further defect of the tidal theory does not seem to have been generally noticed hitherto.

8. *Collision of unequal masses.*—The arguments so far are based on calculations for equal masses, but there remains the possibility that some of the difficulties might be reduced if the incoming star had mass considerably different from that of the Sun. In fact it turns out that the difficulties are even greater.

First, suppose the colliding star to have mass *less* than that of the Sun. For main series stars, we may suppose the radius R to be related to the mass roughly by $R \propto M^{2/3}$, or by a similar relation with index only slightly different. If the radii of m_1 and m_2 are denoted by R_1 and R_2, then collision requires that $R_1 + R_2 = 1$ in the present units, and it is readily found that

$$R_1 = \left\{1 + \left(\frac{1-m}{m}\right)^{2/3}\right\}^{-1}, \tag{14}$$

where $m = m_1/(m_1+m_2)$. If now this quantity is graphed against m (Fig. 1), it is found that R_1 always exceeds the value $\lambda = \lambda_c$ corresponding to the intermediate collinear particle solution given by (12) for $0{\cdot}5 < m < 1{\cdot}0$ which is the case we are considering. But all planetoids commencing at distance $\lambda > \lambda_c$ from m_1 certainly escape from this mass completely, so there can be no chance of improving the situation found for equal masses by assuming an incoming star of less mass than the Sun. In fact, the situation would be worse.

Second, the situation for a colliding star of mass *greater* than the Sun requires us to anticipate later discussion in the present paper in connection with the origin of satellites. In this case it is found that all planetoids captured by $m_2 (< m_1)$, m_2 for convenience now representing the Sun, describe orbits passing deeply through what would be the body of m_2 and so not capable of becoming satellites.

We may conclude therefore that as far as the present treatment of the problem goes not only would collisional or tidal action of another star upon the Sun fail by a

* Russell, H. N., *The Solar System and its Origin*, p. 114. Macmillan, New York, 1935.

large factor to endow the primitive planets with adequate amounts of angular momentum, but in fact that no planetoids whatever could be set into orbital motion round the Sun because of the finite size of that body.

9. *Encounter with a red-giant star.*—There is also the possibility that if the passing star were a red-giant of sufficiently large radius some easing of the angular momentum difficulty might result. For example, suppose the star had mass equal to the Sun but radius $9R_\odot$ for convenience, so that the unit of distance corresponding to closest separation of m_1 and m_2 would equal $10R_\odot$ in a grazing encounter. Even supposing an adequate quantity of material could be detached from the outer layers of the giant, the representing particles would begin at distance 0·3 to 0·4 at very most from m_1, the Sun, and so these would just about graze the surface at their first close approach, since the radius of the Sun is now 0·1 unit. Since the semi-parameter, $a(1-e^2)$, of an orbit must always be less than twice the closest distance, $a(1-e)$, it follows that any planets so formed could at best become rounded up into orbits of radius $2R_\odot$ even if they escaped reabsorption. But this has to be compared with the radius of Jupiter's orbit, at minimum, which is about $1000R_\odot$.

For a larger red-giant some slight increase in this maximum distance might well result, even say with everything in favour, by a factor of 10. But a mere encounter with the Sun, collisional or tidal, would seem entirely incapable of removing material in sufficient quantity from the outer layers, bearing in mind not only the total mass of the present planets but the fact that the composition of the outer layers of the giant must probably be regarded as almost entirely hydrogen. To obtain say 10^{32} g of material initially would require the outer 5 per cent or so in radius to be sheared off, supposing the material to come equally from all parts of the surface, which manifestly it would not. The Sun could extract material only from one locality where collision was occurring, and the requisite mass would mean going to far greater depth in a limited sector. The Sun would have to pass deep within the giant star, and then it would seem far more likely that the consequent energy loss would result in the capture of the Sun by the giant rather than a liberation of a quantity of material many times the total mass of the planets.

10. *The Binary Hypothesis.*—To meet this angular momentum difficulty, the idea was next introduced of material escaping from two other stars for some reason undergoing collision and separation in a region of space located at a distance from the Sun comparable with those of the great planets at present. The escaping material, not that captured by either star, would then be available to be captured in whole or in part by the Sun to give the initial planetary material appropriately endowed with angular momentum. There appear to be three possible ways in which such a situation could develop:

(i) collision of two stars originally independent of each other and of the Sun;

(ii) collision of an independent third star with a companion star to the Sun; and

(iii) rotational break-up into two main pieces of a companion star to the Sun.

The dynamics of such possibilities have earlier been discussed, but here we are concerned simply with the possibility that the separation may leave behind material not retained by either party to the collision and this material be captured by the Sun. In cases (i) and (ii), there would be no particular limitation on the mass-ratio

of the separating components, but in (iii) it seems certain that the two pieces must be of very different masses in a ratio exceeding 8 : 1 (if such break-up can occur for gaseous masses with strong central condensation at all).

For case (i), separation with anything like average stellar speed of two stars similar to the Sun, for example, will result, as has been seen, in a relative orbit differing only slightly from a parabola. Thus from equations (1) and (2) we have

$$\frac{v_\infty^2}{v_A^2} = \frac{e-1}{e+1} \doteqdot \tfrac{1}{2}(e-1), \quad \text{for} \quad e \doteqdot 1, \tag{15}$$

and for $v_A \sim 600\,\mathrm{km\,sec^{-1}}$ and $v_\infty \sim 60\,\mathrm{km\,sec^{-1}}$, the eccentricity of orbit is only 1·02 about. Now it turns out that only for values of e as high as 3 or more does the range of λ for which escape occurs from both m_1 and m_2 amount to as much as 1 per cent. But for stars similar to the Sun, this would require a relative velocity of approach (when at great separation) in excess of $400\,\mathrm{km\,sec^{-1}}$, which though perhaps not impossible would be very uncommon.

Table II shows the range of values of λ for which the intermediate particles can escape from both m_1 and m_2 calculated for the case $m_1 = m_2$ and for different values of the eccentricity of their relative motion.

TABLE II

Range of λ-values for escape in case $m_1 = m_2$

e	1	1·01	1·1	2·0	3·0	4·0
Range of λ	0	$2{\cdot}8 \times 10^{-7}$	$3{\cdot}6 \times 10^{-6}$	$1{\cdot}18 \times 10^{-3}$	$7{\cdot}4 \times 10^{-3}$	$2{\cdot}06 \times 10^{-2}$
v_∞/v_A	0	·0705	·218	·577	·707	·775

In the last line of Table II is shown the value of v_∞, the relative speed of m_1 and m_2 at great separation, in terms of v_A the speed at closest approach; this is related to the parabolic speed by (1).

Table II shows at once that for any reasonable speed of approach of the two stars, the range of λ for escape is less than 10^{-5} of the whole range $0 < \lambda < 1$. This strongly suggests that at very most only a corresponding fraction of the whole mass of the colliding stars could be liberated, whereas the formation of planets would require something like 10^{-3} at least of the combined mass of the two stars. An element of weakness enters the argument in supposing that the amount of mass escaping can be regarded as simply proportional to the range in λ, whereas self-gravitation of the intermediate material could conceivably operate to upset this and possibly increase the final amount of mass in the escape range. On the other hand, the whole mass of the two stars is by no means at any stage distributed uniformly from $\lambda = 0$ to $\lambda = 1$ but instead is concentrated almost entirely near the end values; only the intermediate small portion directly concerned in the collision is likely to be eligible for escape.

There are two ways in which an increase in the range for escape could come about. First there is that indicated directly by Table II, namely an increase in speed. But second, the same result can be achieved without actual increase of speed by supposing the colliding stars to be giants. Here however the hydrogen factor is still more adverse, and the small density in the outer layers would probably require a greater increase in the λ-range, to give the necessary amount of material, than can arise from the increase in e that red-giant stars would allow without increase in relative speed.

In so far as any conclusion can be reached, the present analysis strongly indicates that neither mechanism (i) nor (ii) is capable of releasing the necessary amount of material. This is reinforced by the consideration that ordinary stars are likely to contain a far higher proportion of hydrogen than does the planetary material.

11. *Rotational break-up of a star.*—There remains possibility (iii) to be considered. If the evolution of a rotating star with increasing average density follows in its general trend the kind of evolution established for a rotating liquid mass, then it has been shown that if initially the instability results in the mass dividing into two main pieces, these must be of very different masses, in a ratio exceeding 8 : 1, and that their relative motion is hyperbolic so that the two pieces escape from each other entirely. As the process would be closely similar to the rotational break-up of a primitive planet, which is discussed in detail in a later section of this paper concerned with the formation of satellites, we will here simply describe the main features of the disruption.

First, since the break-up is entirely intrinsic to the system, it is reasonable to expect a separation speed exceeding the parabolic speed by a substantial amount say 25 or even 50 per cent. For this first figure, $e=2$, and the final speed $v_\infty = \sqrt{\frac{1}{2}(e-1)}\,v_p$ after escape is therefore about 70 per cent of the parabolic speed. For a companion star for which the mass is 10⊙, for example, breaking up into two pieces of masses 9⊙ and 1⊙, the final relative speed of separation would be about 1000 km sec^{-1}. At a distance from the Sun comparable with that of the great planets, such a companion would have an orbital speed of about 20 to 30 km sec^{-1}, and so the speeds of both components relative to their common mass centre would easily exceed the escape value. But since they would separate in almost opposite directions relative to the Sun, any intermediate material could well have speed relative to the Sun of less than the escape value in part at least.

Now, in view of Table II, for $e=2$ the amount of material escaping both stars and available in part to be captured by the Sun might be of the order of 1 per cent the mass of the Sun, and so if containing a sufficient abundance of heavy elements could at least produce a primitive planetary system in so far as the amount of matter and initial angular momentum are concerned.

12. *Development of the primitive planetary filament.*—There remains the question whether a filament drawn out between two separating stars or fragments could form immediately into a string of individual gaseous planets, or whether owing to the high temperature it would expand out into a tenuous cloud round the Sun albeit at planetary distance. There can be little doubt that the material when in the stars must be regarded as at high temperature, of order 10^6 deg. K. The problem was taken up by Spitzer* some years ago who claimed to show that a filament of planetary mass initially possessing such a temperature would acquire escape velocity of expansion in a matter of minutes, and so would dissipate into space. This conclusion has often been quoted as disposing of collision theories and similar hypotheses. But the treatment fails to take account of the fact that within so short a time of formation of the filament, the parent stars would not have separated to any appreciable distance (separation by a radius requires a time of the order of 1 hour). They would therefore be on hand to exert restraining forces against the

* *Ap. J.*, 90, 675, 1939.

expansion in just the general directions needed and in strength suitable for controlling thermal speeds of stellar order. The question therefore remains an open one, and it is not our object to enter further into this difficult problem in the present paper.

The matter has some relation, however, to the question of the rapid rotations of the planets, but it turns out that whether planets could form in the filament at once or not, the rotations would seem to be explicable. For a in state of rotational break-up, a star of mean density 1 gm cm^{-3} would rotate in a period of a few hours, and all its elements would partake of some such rotation. Thus a planet formed from such material would when it contracted again to a density of order unity have a rotation period of the order required.

On the other hand, if the portion of filament captured by the Sun dispersed to form a cloud, the next stage is believed to be the solidification into small particles of this material, or such of it as could not continue to exist in gaseous form with cooling, and the gradual formation of a flat disk-shaped distribution of tiny particles each in independent orbital motion round the Sun. According to recent discussions of the development of this disk, aggregations would at first grow very gradually in it, and then at a later stage any reaching or exceeding a certain size would much more rapidly draw in the remainder of the disk of material in their locality, and thereby produce a few large aggregations—the planets. Now in the original disk, vorticity must be present with component perpendicular to the plane and in the same sense as the orbital rotations round the Sun. For if v is the circular orbital speed at distance r from the Sun, then $v \propto r^{-1/2}$, and the vorticity $r^{-1}\, d(rv)/dr$ is positive. A planet so forming would retain rotational momentum determined by this vorticity. Although the details of the mechanism have not yet received adequate analysis, it is in this way that the rotations of the planets are accounted for in the so-called disk theories.

13. *Break-up of a rotating planet.*—As a planet increases in mass by accretion, the range from which it can draw in material increases rapidly, and the rotatory effect of the added matter will also increase, and instability be approached. If planets were formed directly from released stellar material, there is little doubt that initially they would be large and gaseous, but would gradually cool and contract. The instability criterion is that $\omega^2/2\pi G\rho$ should be of order unity, and with increasing density this ratio increases much as $\rho^{1/3}$, so that a thousandfold increase of density could substantially affect stability. A large gaseous planet at low density could obviously be thoroughly stable and yet on cooling to liquid or solid state find itself endowed with more angular momentum than it could store.

But what concerns us here is that in either mode of formation rotational instability may come about. Indeed, in any theory that can account for the rapid rotations of the planets, there must be some mechanism by which a planet is able to rid itself of any excess of angular momentum in order to reach a final state of stability. It is here that the fission process enters to accomplish this very thing. An unstable planet would undergo division into two main pieces thrown apart with hyperbolic speed of separation. The mass-ratio of the components must be at least 8:1 in order that energy and angular momentum requirements can be met*. Fig. 4 shows the conjectural changes from the last stable Jacobi figure to two components separating hyperbolically.

* R. A. Lyttleton, *The Stability of Rotating Liquid Masses*, p. 139, Cambridge, 1953.

The nature of the initial motion of a Jacobi ellipsoid away from an unstable form has not yet been successfully investigated, but some indication of the speed involved can be obtained by comparing the quantities associated with the last stable ellipsoid with those for a stable binary system of mass-ratio of appropriate size. For the last stable Jacobi ellipsoid, the angular momentum is

$$H_E = 0{\cdot}390\, G^{1/2} M^{3/2} r^{1/2} \tag{16}$$

where $r^3 = abc = 1$, and its angular velocity is given by

$$\omega^2/2\pi G\rho = 0{\cdot}142. \tag{17}$$

These are to be compared with a stable binary system of the same total mass (and

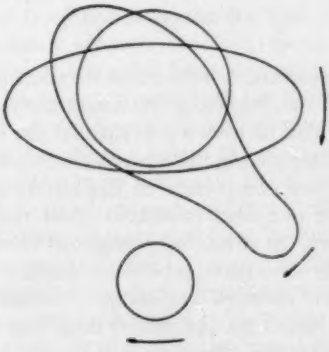

FIG. 4.

same density), with mass-ratio 10:1, in circular motion, for which the corresponding angular momentum is*

$$H_B = 0{\cdot}227\, G^{1/2} M^{3/2} r^{1/2}, \tag{18}$$

while the angular velocity is given by

$$\omega^2/2\pi G\rho = 0{\cdot}0444. \tag{19}$$

The Jacobi figure is seen to have about 1·8 times the angular velocity and 1·7 times the angular momentum of the double system, and it is the presence of these larger values that enables and indeed requires the detached smaller mass to be sent into hyperbolic motion.

Since, by (1), $\omega_A \propto (e+1)^{1/2}$, the above values as they stand would suggest an initial eccentricity of about 2·2, but such evidence as there is on how the Jacobi figure changes strongly indicates that the actual value is likely to exceed this because the moment of inertia of the system almost certainly decreases once instability sets

* *loc. cit.* p. 142.

in. It is known that for the equilibrium pear-shaped figures near the last stable ellipsoid*

$$\left.\begin{aligned} \omega^2/2\pi G\rho &= 0{\cdot}142\,(1+0{\cdot}0523f^2) \\ k^2 &= 0{\cdot}844\,(1-0{\cdot}0938f^2) \\ H\,(\text{pear}) &= H_E(1-0{\cdot}0677f^2) \end{aligned}\right\} \qquad (20)$$

where f is a numerical parameter measuring the departure of the pear from the ellipsoid, and of order unity for changes comparable with the dimensions of the ellipsoid itself. The terms given in (20) are of course simply the first terms of what must in fact be infinite series. The pear-shaped configuration has in fact *less* angular momentum and moment of inertia than the last stable ellipsoid, but if it were possible to give the pear the same angular momentum as the ellipsoid, then its angular velocity would be given by

$$\omega_P{}^2 = 0{\cdot}142\,(1+0{\cdot}19f^2). \qquad (21)$$

It seems reasonable to conjecture therefore that the eccentricity of orbit into which the escaping portion is thrown may be in the neighbourhood of $e=3$.

It is as a secondary result of such a process that the satellites may have their origin. For between the separating main pieces, a stream of material would form extending initially from one component to the other, but soon collecting into separate droplets to give incipient satellites. And this brings us again to a situation closely resembling the restricted problem of two separating point masses with particles of negligible mass moving between them.

14. *Subsequent motion of the main components.*—Considering first the two main pieces resulting from the fission, let us examine their final energy in relation to the Sun. The velocity of escape from the surface of Jupiter, for example, is at present about 60 km sec^{-1}, so if we regard Jupiter as the larger component from fission of a single mass, a relative velocity of this same order would result from an eccentricity of 3, by (1) and (2). Divided between the two masses in the ratio 1 : 9, the larger component would acquire a recoil of about 6 km sec^{-1} and the smaller one 54 km sec^{-1}. But the circular velocity at Jupiter's (present) distance is 13 km sec^{-1} and an increase of almost 6 km sec^{-1} in precisely the right direction would be needed to effect escape. So there would be no difficulty in envisaging conditions leading to the retention of the main mass by the Sun.

On the other hand, the smaller portion having only about 1/9 the original mass would take on about 54 km sec^{-1} recoil, and in whatever direction this chanced to be, it would result in complete escape from the solar system.

Exactly similar considerations apply to Saturn, Uranus, and Neptune, suggesting that they can each be regarded as the remaining larger portion of a single primitive planet broken up by rotational instability.

Clearly, these conclusions are not dependent on the precise value $e=3$ adopted above by way of illustration. Also, the values used for the escape and circular speeds refer to present-day orbits, whereas both the orbits and masses may have been considerably different in the early stages of the solar system, though not of course necessarily different in order of magnitude.

* Jeans, *Problems of Cosmogony*, p. 101, Cambridge, 1919.

The small orbital speed of each of the great planets in comparison with its surface escape speed is extremely striking, as Table III shows:

TABLE III

	Jupiter	Saturn	Uranus	Neptune
Orbital speed (km sec^{-1})	13	9·7	6·8	5·4
Surface escape speed	60	36	21	23

Equally striking, on the other hand, is the fact that for the terrestrial planets the situation is completely reversed and the escape speeds at their surfaces are considerably less than the orbital speeds, as Table IV shows:

TABLE IV

	Mercury	Venus	Earth	Mars
Orbital speed	48	35	30	24
Surface escape speed	3·8	10·2	11·2	5·0

Accordingly, if the terrestrial planets have resulted from fission of primitive larger planets, then on the present basis it would not be expected that the smaller components were ejected from the solar system, and it should be possible to identify appropriately related planets. In fact, these planets can be paired consistently with this. For the mass of Mars is 0·108 that of the Earth, and the greater orbital energy of Mars as compared with the Earth corresponds to a speed at the Earth's distance from the Sun of about 12 km sec^{-1}—a value close to the escape speed at the Earth's surface. Again, the mass of Mercury is about 1/15 that of Venus, and a similar energy difference exists between their two orbits. It is not of course possible to attach great significance to an argument resting on the present values of orbital elements, since we have no knowledge of the extent to which they may have changed since the first stages of the system. Even so, it is of some interest that the present values are remarkably consistent with a rotational mode of their formation. It may also be noted here that the foregoing numerical values indicate an eccentricity of orbit of separation of about 3.

15. *The origin of satellites.*—Assuming then that in order to attain internal stability a primitive planet eventually undergoes fission, with the further result that a stream of droplets of negligible mass is drawn out between the two separating components, then clearly the main masses may be able to retain some of the droplets in orbital motion to give satellites. The situation is again one that can be idealized to a restricted three-body problem, but here we shall have widely differing masses for the two controlling particles and also an eccentricity of their relative motion substantially exceeding unity. Detailed integrations have been carried out for the three cases

$$m_1 : m_2 = 9 : 1, \quad e = 2,\ 3,\ \text{and}\ 4,$$

for an adequate series of values of λ in each case.

As in the collision theory for a solar origin of planets, the restriction in producing satellites from droplets captured by either mass is the finite size of these bodies, which prevents satellites getting by at closest separation. But an essential difference now enters, for in the gradual development with increasing angular momentum along the Jacobi series, the angular velocity itself actually diminishes, and the increasing angular momentum is stored by means of the large moment of inertia implied by the elongation of figure. For the critical Jacobi ellipsoid, the ratios of the semi-axes are in fact

$$a : b : c : (abc)^{1/3} = 1{\cdot}886 : 0{\cdot}815 : 0{\cdot}651 : 1$$

so that the moment of inertia is 2·11 times that of the mass in spherical form. As

already seen in Section 13, it is to be expected that when stability is lost the elongation of figure increases. The smaller portion, containing about 0·1 of the mass would at first be pushed radially away from the larger mass, while a furrow develops and deepens rapidly as the mass undergoes fission. This radial motion may well persist until the division into two is complete. The subsequent motion may then be regarded as describable by that of two point masses separating hyperbolically. A certain amount of judgment has to be exercised to estimate the dimensions of the system at this stage. The system must contain total angular momentum equal to that of the last stable Jacobi figure, and calculation shows that if the separation of m_1 and m_2 at closest in their relative hyperbolic path is taken as unit of distance, (consistently with the units of the restricted three-body calculations), then the equatorial radii of the two components on the same scale would be about 0·4 and 0·2.

The excess angular momentum is got rid of as orbital angular momentum. Since the angular velocity has decreased along the Jacobi series, the resulting components can immediately revert to Maclaurin spheroids of moderate eccentricity and carry far less angular momentum than would render them unstable.

The question whether the subsequent motion of the intermediate particles is consistent with their going into satellite orbits can again be studied by means of a restricted three-body problem with the two separating main pieces represented by point masses moving in a hyperbolic relative orbit. The calculated orbits show similar general features to those earlier found for the case of equal masses, but the important difference appears in the present case that the component masses are now sufficiently smaller, in comparison with the initial separation of the centres, for some intermediate particles to go into orbit round the larger mass without intersecting its surface. For this to happen requires a value of e rather in excess of 2, but whatever the value of e no satellites can be captured in orbital motion by the smaller mass for the case $m_1/m_2 = 9$, and it is plain from the nature of the orbits that this must continue to hold for larger mass-ratios.

Even so, the resulting orbits subsequently come slightly inside the initial starting distance (measured by λ) and so pass near the surface of the body m_1 in later circuits. Many of the orbits are highly eccentric and possess such quantity of angular momentum that if rounded up to circular orbits (with no change of angular momentum, as might occur through dissipative effects) they would move at rather more than 2 radii distant from the centre of the main mass. Although this would mean that they would initially come within the formal Roche limit, it must be remembered that the value 0·4 for the radius of the larger mass is subject to some uncertainty and may well be smaller. Any increase of density towards the centre, which must occur for a large planet, would mean outer layers of density lower than the mean, and the impression one gets is that the resulting analogous Jacobi figure would be even more elongated before instability occurred, and this in turn would bring about an effectively smaller radius for the larger component mass. Equally important perhaps is the consideration that the theoretical Roche limit is based on the assumption that the rotatory and orbital periods of the satellites are identical, which would seem to be the arrangement most adverse to stability, whereas this would clearly not in general hold initially in any actual case. Non-resonance of these periods would certainly seem likely to increase the degree of stability of a satellite. Figs. 5 and 6 show some of the possible initial satellite orbits for the cases $e = 3$ and $e = 4$.

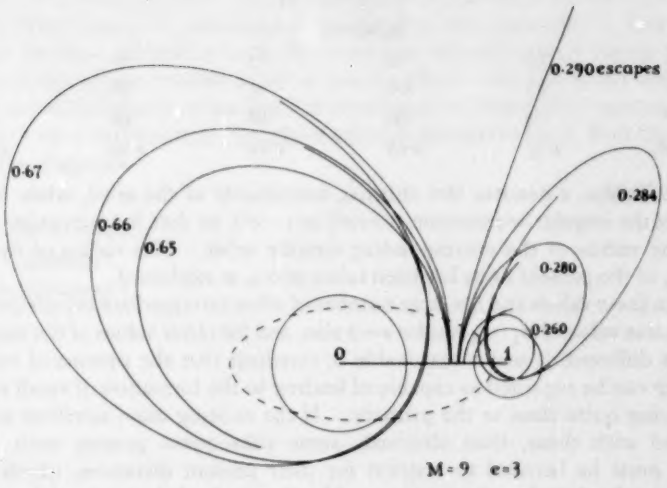

FIG. 5.

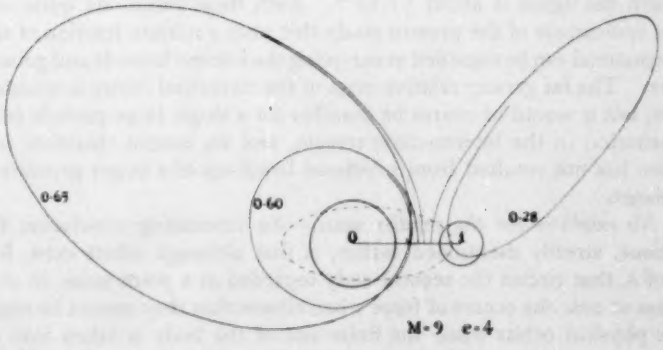

FIG. 6.

The following Tables show the relevant dimensions of resulting satellite orbits for a number of values of λ determining the starting point:

TABLE V

$m_1/m_2 = 9, \quad e = 3$

λ	·66	·67	·68	·69
e	·573	·678	·788	·934
h^2	·725	·742	·778	·754
r/R_1	1·81	1·86	1·94	1·88

TABLE VI

$m_1/m_2 = 9, \quad e = 4$

λ	·63	·64	·65	·66	·67
e	·54	·66	·74	·86	·97
h^2	·78	·82	·88	·90	·92
r/R_1	1·95	2·05	2·22	2·24	2·30

In these Tables, e denotes the ultimate eccentricity of the orbit, while h^2 is the square of the angular momentum, namely $a(1-e^2)$, so that in appropriate units h^2 gives the radius of the corresponding circular orbit. The radius of the larger mass R_1 in the present units has been taken as 0·4, as explained.

From these values and the large number of other intermediate calculations done for the same value of $m_1 : m_2$ and for $e = 2$ also, and for other values of the mass-ratio not very different, it seems reasonable to conclude that the process of rotational break-up can be regarded as capable of leading to the formation of small satellites but moving quite close to the primary. If the existing main satellites are to be identified with these, then obviously some subsequent process such as tidal friction must be invoked to account for their present distances, which exceed those arrived at here by a factor approaching ten for both Jupiter and Saturn, and also for Uranus. Neptune of course may be a special case anyway.

An interesting point that may be noted here is that the combined mass of the existing satellites of Jupiter is only about 2×10^{-4} that of Jupiter itself, while for Saturn the figure is about 3×10^{-4}. Both these values are quite consistent with the indications of the present study that only a minute fraction of the intermediate material can be regarded as surviving the various hazards and going to form satellites. The far greater relative mass of the terrestrial Moon is counter to this however, but it would of course be possible for a single large particle to form by self-gravitation in the intermediate stream, and we cannot therefore infer that the Moon has not resulted from rotational break-up of a larger primitive Earth-Mars planet.

16. *No satellites for the smaller mass.*—An interesting conclusion from the calculations, already mentioned earlier, is that although orbits exist, for larger values of λ, that circuit the second body regarded as a point mass, in every case these pass so near the centre of force when closest that they cannot be regarded as possible physical orbits when the finite size of the body is taken into account. For the case $m_1/m_2 = 9$, $e = 3$, the range of λ for which escape from both bodies occurs is

$$0{\cdot}6944 < \lambda < 0{\cdot}7131,$$

which is 1·87 per cent of the whole range. For the case $m_1/m_2 = 9$, $e = 4$, the corresponding range is

$$0{\cdot}6725 < \lambda < 0{\cdot}7170,$$

which is now 4·45 per cent of the whole range. The position of the collinear three particle solution is initially at $\lambda = 0{\cdot}709$ in both cases. The orbits about m_2 for values of λ greater than these upper limits are found to pass within less than 0·1 (considerably less in most cases) of the centre of m_2, whereas since in the present units the finite radius of this mass is about 0·2 this means that such captured particles will be reabsorbed into the body of m_2 at first return. Accordingly no satellites could result for the smaller mass.

17. *Acknowledgments.*—The author wishes to express his thanks to the Director of the Mathematical Laboratory at Cambridge and especially to Mrs Margaret Mutch for their assistance with the numerical calculations on which the whole investigation of the present paper is based. These calculations are not included in the text of the present paper but full details can be obtained by anyone interested on application to the author. Special thanks are also due to Dr A. Beer for assistance with the diagrams.

St John's College,
Cambridge:
1960 *September* 1.

ROCK CREEP: A CORRECTION

Harold Jeffreys and Stuart Crampin

(Received 1960 September 28)*

Summary

A mistake in the previous discussion of the modified Lomnitz law of creep is corrected. The index in the law is changed from 0·17 to 0·25. The other effects of creep are rediscussed and some are calculated that had not been calculated with the former index. The results are qualitatively similar to those found previously and no contradiction with the data is found.

1.—In a colloquium, Mr S. K. Banerjee called attention to the fact that in equation (10) (Jeffreys 1958 a) for the form of a pulse as modified by imperfection of elasticity of Lomnitz's type

$$\frac{1}{2}+\frac{1}{\pi}\tan^{-1}\frac{\beta t-cx}{sx}$$

there is a displacement at times before cx/β and therefore before x/β, since c is a cosine. Such anomalous behaviour has precedents, but none of the reasons why it has been found previously seemed relevant in this case. In fact the result rests on some rather dubious approximations, since (1) it is assumed that the whole effect of damping on a wave as it travels is expressed by the phase lag, irrespective of changes of amplitude; and (2), while for Lomnitz's original form it is a good approximation to take the lag as independent of the period, this is not true for the modified law. Incidentally (8) of the paper is a mistake in copying; it should be

$$\exp\{i\kappa(\beta t-x\,e^{-\frac{1}{2}i\eta})\},$$

and this has been used in deriving (9).

2.—The only satisfactory treatment is to return to (2)

$$\epsilon=\frac{P}{\mu}\left[1+\frac{q}{\alpha}\{(1+at)^{\alpha}-1\}\right], \tag{1}$$

giving

$$\epsilon=\frac{P}{\mu}\left[1+q\log(1+at)\right] \tag{2}$$

as an approximation when $\alpha\to 0$. The values of t may be divided into three ranges.

(i) at small. The law approximates to

$$\epsilon=\frac{P}{\mu}(1+qat), \tag{3}$$

which is the elasticoviscous law.

(ii) $at\gg 1$, $q(at)^{\alpha}/\alpha\ll 1$. The law approximates to

$$\epsilon=\frac{P}{\mu}\left[1+\frac{q}{\alpha}a^{\alpha}t^{\alpha}\right] \tag{4}$$

* Received in original form 1960 July 22.

or, as $\alpha \to 0$,

$$\epsilon = \frac{P}{\mu}[1 + q\log(at)]. \tag{5}$$

The creep is less than the initial strain.

(iii) $q(at)^\alpha/\alpha > 1$ or, as $\alpha \to 0$, $q\log(at) > 1$. The creep exceeds the initial strain.

In range (i) the solution is known (Jeffreys 1931). A pulse in a medium with these properties has a sharp beginning, travelling with velocity

$$\beta = (\mu/\rho)^{\frac{1}{2}}. \tag{6}$$

The initial displacement decreases exponentially as the pulse travels. But the indications of experiment are that a is of the order of $1000/1^s$ and q about $1/40$, and it appears absurd even to try to apply this rule to periods ranging from a few seconds to over a year. To make it consistent even with the existence of the Eulerian nutation qa would need to be of the order of $1/10^{\text{d}}$.

The applications to tidal friction and the Eulerian nutation already made belong to range (ii) and the resulting formulae are correct. The applications to the subsidence of surface inequalities belong to range (iii) and are also correct. The quantitative results, however, need revision. Some results found for exponential afterworking still need to be recalculated for the modified Lomnitz law.

What is in doubt is whether under these laws a pulse, though beginning with a very small amplitude, may increase rapidly to a much larger value and possibly become comparable in a few seconds with what it would be in the absence of creep. To discuss this it appears necessary to return to the exact form (1). In operational form we have for a stress $PH(t)$

$$\epsilon = \frac{P}{\mu}\left\{1 + \frac{q}{\alpha}f\left(\frac{p}{a}\right)\right\}H(t) \tag{7}$$

where

$$f\left(\frac{z}{a}\right) = z\int_0^\infty (1+at)^\alpha e^{-zt}\,dt - 1$$

$$= e^{z/a}\left\{a^\alpha \alpha! z^{-\alpha} - \sum_0^\infty \frac{(-1)^r z^{r+1}}{r!(\alpha+r+1)a^{r+1}}\right\} - 1 \tag{8}$$

$$\sim \sum_1^\infty \frac{\alpha!}{(\alpha-r)!}\frac{a^r}{z^r}. \tag{9}$$

The solutions for perfect elasticity can be adapted by replacing μ by the operator

$$\mu\left\{1 + \frac{q}{\alpha}f\left(\frac{p}{a}\right)\right\}^{-1}, \tag{10}$$

and the wave velocity β_0 by

$$\beta_0\left\{1 + \frac{q}{\alpha}f\left(\frac{p}{a}\right)\right\}^{-1/2}. \tag{11}$$

If the particle velocity at $x = 0$ is $H(t)$, that at general x will be

$$\exp\left[-\frac{px}{\beta_0}\left\{1 + \frac{q}{\alpha}f\left(\frac{p}{a}\right)\right\}^{1/2}\right]H(t). \tag{12}$$

The asymptotic form (9) gives

$$\exp\left[-\frac{px}{\beta_0}\left\{1 + \frac{qa}{2p} + \left(\frac{q(\alpha-1)}{2} - \tfrac{1}{8}q^2\right)\frac{a^2}{p^2} + \dots\right\}\right]H(t)$$

$$= e^{-qax/2\beta_0}\left\{1 + \frac{x}{\beta_0}\left(\frac{q(1-\alpha)}{2} + \tfrac{1}{8}q^2\right)a^2\left(t - \frac{x}{\beta_0}\right) + \dots\right\}H(t - x/\beta_0).$$

There is severe reduction of the initial velocity. If we take $q = 1/40$, $a = 6 \times 10^3/1^\alpha$, $x/\beta_0 = 20$ minutes, the exponent is about -180000. The damping of the variation of latitude effectively determines qa^α, and thus provides only one relation between q, a and α, namely

$$qa^\alpha = \frac{1}{40 \,.\, \frac{1}{2}\pi\alpha!}\left(\frac{2\pi}{430^\alpha}\right)^\alpha. \tag{14}$$

If $\alpha = 1$, qax/β_0 is of order $1/600000$ and there is no difficulty. But this is the elasticoviscous law and does not give enough tidal friction to account for the rotations.

But the term in $t - x/\beta_0$ increases rapidly if $\alpha < 1$, and the large factor a^2 is present. It is therefore possible that before $t - x/\beta_0$ has become large the velocity has become moderate. This requires a different expansion, since the first few terms of (13) are no longer a good approximation. We shall in fact be in range (2) where 1 can be neglected in comparison with at, and we can take

$$f(z/a) \doteqdot a^\alpha \alpha! z^{-\alpha}. \tag{15}$$

Then the velocity is

$$\exp\left[-\frac{px}{\beta_0}\left(1 + \frac{q(\alpha-1)!}{p^\alpha}a^\alpha\right)^{1/\alpha}\right] H(t). \tag{16}$$

Expansion in powers of $p^{-\alpha}$ would not be satisfactory, since it would again bring in positive powers of t. Instead we take only the first term and avoid the troublesome square root by expressing (16) directly as a complex integral

$$I = \frac{1}{2\pi i}\int_L \exp\left\{zt - \frac{zx}{\beta_0} - \frac{1}{2}\frac{qx}{\beta_0}(\alpha - 1)!\, a^\alpha z^{1-\alpha}\right\}\frac{dz}{z}. \tag{17}$$

This still vanishes for $t < x/\beta_0$. For $t > x/\beta_0$ we tried to use the method of steepest descents, but found that the exponent varied too slowly near the saddle-point to give a good approximation. We write the integral as

$$\frac{1}{2\pi i}\int_L \exp(\lambda z - \mu z^{1-\alpha})\frac{dz}{z}$$
$$= \frac{1}{2\pi i}\int_L \exp v\left(u - \frac{u^{1-\alpha}}{1-\alpha}\right)\frac{du}{u} \tag{18}$$

where

$$v = \mu^{1/\alpha}\lambda^{(\alpha-1)/\alpha}(1-\alpha)^{1/\alpha} \tag{19}$$

$$= \frac{\left\{\frac{1}{2}\frac{qx}{\beta_0}(\alpha-1)!\, a^\alpha\right\}^{1/\alpha}(1-\alpha)^{1-\alpha}}{(t - x/\beta_0)^{1/\alpha - 1}}. \tag{20}$$

A convergent series is

$$I = 1 - \sum_{r=1}^{\infty}\frac{\sin \pi r\alpha \,.\, \{r(1-\alpha)-1\}!\, v^{-r(1-\alpha)}}{\pi r!\,(1-\alpha)^r} \tag{21}$$

but this is also unsatisfactory when α is rather small, since the terms decrease slowly and several consecutive terms have the same sign. The integral can, however, be expressed in real form if we take a small semi-circle about the origin and put on the imaginary axis $u = \pm iv$ according as $I(u) \gtrless 0$. This gives

$$I = \frac{1}{2} + \frac{1}{\pi}\int_0^\infty \exp\left(-\frac{v}{1-\alpha}v^{1-\alpha}\sin\tfrac{1}{2}\pi\alpha\right)\sin\left(vv - \frac{v\cos\frac{1}{2}\pi\alpha}{1-\alpha}v^{1-\alpha}\right)\frac{dv}{v}. \tag{22}$$

Mr Swinnerton-Dyer makes the further transformation

$$w = \frac{\nu v^{1-\alpha}}{1-\alpha}; \tag{23}$$

then

$$I = \tfrac{1}{2} + \frac{1}{\pi(1-\alpha)} \int_0^\infty \exp(-w\sin\tfrac{1}{2}\pi\alpha)\sin w\left\{\left(\frac{w}{\nu}\right)^{\alpha/(1-\alpha)}(1-\alpha)^{1/(1-\alpha)} - \cos\tfrac{1}{2}\pi\alpha\right\}\frac{dw}{w} \tag{24}$$

which has the advantage that the integrand is bounded near the origin.

3. *Numerical values.*—From the damping of the Eulerian nutation, with a relaxation time of 15 years, we have from 2(14)

$$qa^n = \frac{1}{60\alpha!}(1{\cdot}2 \times 10^{-5}/1^s)^\alpha. \tag{1}$$

The expression for ν is (20) above.

An S pulse at 80° begins fairly sharply and attains something like half its final amplitude in about 2^s. Hence we consider a travel time of 20^m and

$$t - x/\beta_0 = 2^s.$$

Then

$$\nu = \frac{\left(10\dfrac{1-\alpha}{\alpha}\right)^{1/\alpha} 1{\cdot}2 \times 10^{-5}}{2^{1/\alpha}-1}, \tag{2}$$

where we have taken $\alpha! = 1$ for $0 \leqslant \alpha \leqslant 1$.

If the amplitude approaches the value for pure elasticity, 1, in 2^s we should take $I = \frac{1}{2}$ to give an equation for α. On the other hand there is some evidence of damping, and it may be better to take the limiting amplitude as $\frac{1}{2}$ and the amplitude after 2^s as 1/4.

Mr Swinnerton-Dyer evaluated I on EDSAC and found solutions

I	α	ν
$\frac{1}{2}$	0·256	0·446
$\frac{1}{4}$	0·236	1·684

α is appreciably larger than was found previously, the value in the previous paper being 0·17.

4. *Applications*

4.1. *The Moon's librations.*—In the course of this work three mistakes in copying were detected. In Jeffreys (1957 a), in 2(21) the first expression should read

$$n\left(1 + \frac{3\beta}{2(1+\kappa)} + 2\nu + \frac{9\kappa}{2(1+\kappa)}\right).$$

3(4) should read

$$\pm in(1 + \tfrac{3}{2}\beta) - \frac{17}{2}\frac{n^2\nu_0(\tau'-\tau)\tau'}{\tau(n^2\tau'^2+1)};$$

and 3(6) should be

$$+ in(3\gamma)^{1/2} - \frac{9}{2}\frac{n^2\nu_0(\tau'-\tau)\tau'}{\tau(3\gamma n^2\tau'^2+1)}.$$

ν_0 is the elasticity factor for short periods. Putting the new law into the expressions for the time factors we get for the three modes

$$\pm in(1+\tfrac{3}{2}\beta) - \frac{17}{2}n\nu_0 q(\alpha-1)!\frac{a^\alpha}{n^\alpha}\sin\tfrac{1}{2}\pi\alpha, \qquad (1)$$

$$\pm in(4\alpha_0\beta)^{1/2} - \left(\frac{1}{2\alpha_0}+\frac{2}{\beta}\right)2n\sqrt{(\alpha_0\beta)}\,\nu_0\frac{q(\alpha-1)!}{2\sqrt{(\alpha_0\beta)^\alpha}}\frac{a^\alpha}{n^\alpha}\sin\tfrac{1}{2}\pi\alpha, \qquad (2)$$

$$\pm in(3\gamma)^{1/2} - \frac{1}{2\gamma}q\frac{(\alpha-1)!}{(3\gamma)^{1/2(\alpha-1)}}\frac{a^\alpha}{n^\alpha}\sin\tfrac{1}{2}\pi\alpha, \qquad (3)$$

where α, the value of $(C_0-B_0)/A_0$ for the Moon, is written as α_0 to distinguish it. With

$$\alpha_0=4\times10^{-4},\ \beta=6\times10^{-4},\ \gamma=2\times10^{-4},$$
$$\nu_0=1{\cdot}5\times10^{-7},\ \ n=2\pi/28^d,\ \ \alpha=1/4,$$

we get for the relaxation times for the three modes.

$$7{\cdot}6\times10^5 \text{ years},\ 2{\cdot}5\times10^5 \text{ years},\ 4{\cdot}1\times10^4 \text{ years}. \qquad (4)$$

The damping is therefore enough to account for the smallness of the free librations.

4.2. *Tidal friction.*—The lags for different periods are as follows:

TABLE I

Period (days)	Lag ($\alpha=0{\cdot}25$)	Lag ($\alpha=0{\cdot}17$)
0·25	0·0036	0·0075
0·5	0·0044	0·0080
1	0·0053	0·0089
10	0·0095	0·0132
100	0·0172	0·0196
1000	0·0310	0·0289
10000	0·0559	0·0428
100000	0·1009	0·0634
1000000	0·1818	0·0939

The lag is smaller for periods up to 400^d, greater for longer periods. The ratio only just gets outside the range 0·5 to 2. The previous conclusion (Jeffreys 1957 b, 1958) that the law does not account for the secular accelerations of Phobos and Deimos still stands. (In the unnumbered equation in Jeffreys 1957 b, p. 587, line 5, $\tau'=1{\cdot}1\tau$ should be deleted.) The recession of the Moon now corresponds to

$$\frac{d\xi}{dt} = 0{\cdot}8\times10^{-19}/1^s,$$

about 0·08 of what is needed to account for the secular acceleration.

4.3. *Rotations of small bodies.*—Two corrections are needed to Section 5 of Jeffreys 1957 a. In (6) the factor π should be deleted. (10) is incorrect as the two angles subtracted are near $\frac{1}{2}\pi$, as in (3), and not small. The correct ratio of the values of $\dot{\omega}$ for rotation in 6 days and revolution in 12 days would be about 15, as shown by the table in Jeffreys 1958, p. 16. The main conclusion is somewhat

strengthened, namely that it is doubtful whether the long time scale for exponential afterworking can account for the rotation of the Moon and almost certain that it cannot account for that of Mercury. On the other hand it is less clear that the short time scale can.

In the more general form we have

$$\dot{\omega} = \frac{N}{C} = -\frac{45}{4}\frac{n^4\rho a^2 \sin 2\epsilon}{(1+\kappa)^2(19\mu + 2g\rho a)},$$

The treatment for Mercury is simpler than for the Moon, since n can be taken as constant. Then

$$\dot{\omega} = -8{\cdot}2 \times 10^{-20} \sin 2\epsilon/(1\ \text{sec})^2.$$

If Ω is the number of rotations per day we can write this as

$$\dot{\Omega} = -3{\cdot}5 \times 10^{-8} \sin 2\epsilon/\text{year}.$$

A rough numerical integration starting from a rotation period of 12 hours and using the lags in Table I gives the results in Table II.

TABLE II

Synodic rotation period (days)	Time interval (years)
0·5	
	7×10^9
1	
	$3{\cdot}0 \times 10^9$
2	
	$1{\cdot}7 \times 10^9$
20	
	$0{\cdot}1 \times 10^9$
200	

The time for the last interval really refers to the time needed to give a rotation period of

$$\left(\frac{1}{88} + \frac{1}{200}\right)^{-1} = 61^{\text{d}},$$

but the intervals shorten so rapidly that the further correction to give agreement between the periods of rotation and revolution is negligible.

It appears that if Mercury originally rotated in a day there has been time, on the present law, for the periods of rotation and revolution to have been brought into agreement. It is doubtful whether there has been time if the original rotation was much faster.

The effects of tidal friction on the Moon would be of the order of 100 times as fast on account of the factor n^4, and the law definitely accounts for the present rotation. The same holds for the satellites of Mars.

4.4. *Subsidence of a surface inequality.*—In (18) of Jeffreys (1958a) we get for $t = 10^8$ years

$$q(\alpha - 1)\,!\,(at)^\alpha = 9{\cdot}5$$

instead of 4. The changes of the Moon's ellipticities would be 10 per cent in 10^8 years and 17 per cent in 3×10^9 years.

The corresponding modification for the Earth suggests that the previous result will stand; perhaps half a harmonic of degree 2 would survive for 10^8 years and 0·2 for 3×10^9 years.

5. *Discussion.* The results of previous papers do not need any drastic change, but some comments on the uncertainty of the data are desirable. The time of relaxation of the free nutation of the Earth's axis has been taken as 15 years, but the original discussion indicated that this might be in error by a factor of 2 in either direction. Walker and Young (1955) in their first discussion got 3 ± 1 years. In their second (1957) after discussing several series of data they decided that there is " some evidence " that the relaxation time lies in the range 10 to 30 years. On the other hand Panckenho is reported as having found 90 years from variation of latitude observations at observatories other than the international ones. This paper is not yet published.

The estimate of 2^s for an S pulse at 80° to reach half its value for perfect elasticity is based on the sharpness of the beginning, but taking the growth to be to $\frac{1}{4}$ instead of $\frac{1}{2}$ the ideal value makes very little difference to α, and so, though the estimate is not much more than a guess, its inaccuracy is hardly likely to affect the results to any important extent. Also, judged by ratios, the periods concerned in problems of tidal friction are nearer to that of the Eulerian nutation than to those of earthquake waves. If the estimate of the relaxation time is altered by a factor of 2, none of the results found here would be affected to the extent of inviting some completely new interpretation of the data, except possibly that lengthening the time of relaxation might make it harder, and shortening it slightly easier, to understand the rotation of Mercury. On the other hand shortening the time of relaxation too much might lead to difficulties about the persistence of surface inequalities.

At the 1960 Helsinki meeting of the I.G.G.U. Lomnitz and J. R. Macdonald read a paper proposing a somewhat different modification of the law. Details have not yet been published.

160 Huntingdon Road,
Cambridge:
1960 *September* 27.

Department of Geodesy and Geophysics,
Madingley Rise,
Madingley Road,
Cambridge.

References

Jeffreys, H., 1931, *M.N. Geophys. Suppl.*, **2**, 321–2.
Jeffreys, H., 1957 a, *M.N.*, **117**, 506–15.
—— 1957 b, *M.N.*, **117**, 585–89.
—— 1958, *M.N.*, **118**, 14–17.
Walker, A. M., and Young, A., 1955, *M.N.*, **115**, 443–459.
—— 1957, *M.N.*, **117**, 119–141.

ERRATA

M.N., **119**, No. 6, pp. 657–664, 1959:

A. W. K. Metzner and P. Morrison, *The flow of information in cosmological models.*

The authors are very grateful to W. Davidson for kindly pointing out that the expression $dN = 4\pi l_s^2\, dl_s m$ for the steady-state model in line 13 on p. 659 is incorrect; it should read $4\pi m R^3(t_1) r^2\, dr$. Consequently (9*a*) becomes $N(Z)dZ = 4\pi m c^3 T^3 (Z-1)^2 Z^{-3}\, dZ$, and in each of (10*a*), (14), (15) the power of Z^{-1} should be one less, with corresponding changes in Table I. Most important, the total number of 'visible' sources, as calculated in Appendix 2, is now infinite in the steady-state model.

In spite of the infinite total *number* of sources, the authors' main point, that the information rate is finite, remains valid; there is an infinite sea of flickering 'dull-red' galaxies that contribute only negligibly to the power and information received.

M.N., **119**, No. 6, pp. 665–681, 1959:

W. Davidson, *Number count relations in observational cosmology.*

In (6.11), *for* 0·434 *read* the reciprocal 2·303.